

THE EFFECT OF ACUTE HYPOXIA ON
GLUCOSE, LACTATE, AND PYRUVATE
TRANSPORT FROM THE BRAIN
VENTRICLES OF THE DOG

Thesis for the Degree of Ph. D.
MICHIGAN STATE UNIVERSITY
DAVID KEITH MICHAEL
1972



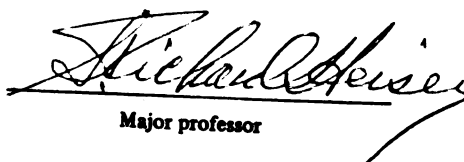
This is to certify that the
thesis entitled

THE EFFECT OF ACUTE HYPOXIA ON GLUCOSE,
LACTATE AND PYRUVATE TRANSPORT
FROM THE BRAIN VENTRICLES OF THE DOG
presented by

David Keith Michael

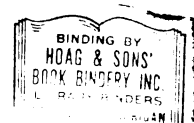
has been accepted towards fulfillment
of the requirements for

Ph.D. degree in Physiology


Major professor

Date 10/25/72

0-7639



ABSTRACT

THE EFFECT OF ACUTE HYPOXIA ON GLUCOSE, LACTATE, AND PYRUVATE TRANSPORT FROM THE BRAIN VENTRICLES OF THE DOG

By

David Keith Michael

The brain ventricular system of anesthetized adult dogs was perfused from the right cerebral ventricle to the cisterna magna with an artificial cerebrospinal fluid (CSF). In one series of experiments, dogs were ventilated with room-air (21% O₂) during the 240 minutes of ventriculo-cisternal perfusion. In another series, an initial 2 hour normoxic ($P_aO_2 = 97 \pm 1$ mm Hg) perfusion period was followed by a 2 hour period of ventilating the dogs with a 5-8% O₂ in N₂ mixture (hypoxia; $P_aO_2 = 39 \pm 2$ mm Hg). The perfusion inflow fluid contained inulin and trace quantities of radioactively labelled glucose or mannitol and lactate. The CSF concentrations of glucose, pyruvate, and lactate were lowered, unaltered, or elevated from their normal values by changing the concentrations in the perfusion inflow fluid. In certain experiments, mannitol was included in the perfusion inflow fluid in lieu of glucose. Steady-state measurements of inflow and outflow rates and concentrations

of the test molecules enabled the calculation of the rates at which each was removed from or entered the perfusion fluid.

Inulin clearance allowed estimation of CSF bulk absorption (\dot{V}_a) and formation (\dot{V}_f) rates. Inulin clearance increased ($p < 0.05$) with time ($6 \pm 2 \mu\text{l/min}$) and with hypoxia ($9 \pm 3 \mu\text{l/min}$). \dot{V}_f in normoxic dogs was $50 \pm 3 \mu\text{l/min}$. \dot{V}_f decreased ($p < 0.05$) with time ($7 \pm 2 \mu\text{l/min}$), but decreased more with hypoxia ($15 \pm 4 \mu\text{l/min}$).

Transependymal net glucose flux during both normoxia and hypoxia reflected the glucose concentration gradient between the CSF and plasma. The glucose outflux coefficient (K_o) demonstrated saturation kinetics implying carrier-mediated glucose efflux, whereas mannitol K_o ($16 \pm 3 \mu\text{l/min}$) was independent of concentration. Glucose K_o was less at normal CSF glucose concentration (5.0 mM) than at low concentration (0.0 mM), but its value ($78 \pm 8 \mu\text{l/min}$) was greater than that for mannitol, suggesting another glucose transport system of higher capacity. Glucose K_o like that of mannitol was unaffected by time, but in contrast to mannitol was reduced during hypoxia, suggesting an aerobic dependent glucose efflux.

There was a net lactate flux into CSF at CSF lactate concentrations ranging from 0.0 to 5.0 mM. Net lactate influx increased ($p < 0.05$) with time, but increased more ($p < 0.05$) during hypoxia. Carrier-mediated lactate

transport was indicated by the lack of a direct linear relationship between net lactate flux and CSF lactate concentrations. Lactate K_0 was concentration dependent and demonstrated saturation kinetics when lactate concentrations in the perfusion inflow fluid were normal (1.6 mM). K_0 was unaffected by perfusion time, but decreased with hypoxia when lactate concentration in the perfusion inflow was 0.0 mM.

There was always a net pyruvate flux into CSF even at CSF pyruvate concentrations of 3.0 mM. Carrier-mediated pyruvate transport was indicated by the lack of a direct linear relationship between net pyruvate flux and pyruvate concentrations in the CSF. Neither time nor hypoxia affected net pyruvate influx.

THE EFFECT OF ACUTE HYPOXIA ON GLUCOSE,
LACTATE, AND PYRUVATE TRANSPORT FROM
THE BRAIN VENTRICLES OF THE DOG

By

David Keith Michael

A THESIS

Submitted to
Michigan State University
in partial fulfillment of the requirements
for the degree of

DOCTOR OF PHILOSOPHY

Department of Physiology

1972

6-11-71

To my wife, Lynn,
whose understanding and support made this manuscript possible,
and to my children, Scott and Elizabeth.

ACKNOWLEDGMENTS

Many people have contributed significantly throughout the course of this study, and the author wishes to express his sincere gratitude to all.

The author wishes to thank his advisor, Dr. S. R. Heisey, for his constructive criticism, and financial support throughout this program, and to the other members of his academic advisory committee: Drs. T. Adams, W. D. Collings, J. R. Hoffert, and W. W. Wells for their guidance and support.

Recognition is given to Drs. C. Cress, T. A. Helmrath, J. R. Hoffert, B. H. Selleck, and W. W. Wells and to D. W. Bierer for their invaluable technical assistance, and to D. K. Anderson for assistance with the photography. I wish to express special thanks to Miss Nancy Turner for her conscientious efforts in the preliminary typing of this manuscript.

TABLE OF CONTENTS

	Page
LIST OF TABLES	vii
LIST OF FIGURES	ix
I. INTRODUCTION	1
II. LITERATURE REVIEW	5
2.1. Relationship of cerebrospinal fluid to blood and brain	5
2.2. Cerebrospinal fluid (CSF) formation	9
2.3. Cerebrospinal fluid (CSF) absorption	13
2.4. Quantitative measurement of molecular movement from the CSF	15
2.5. Glucose movement among blood, brain, and CSF	18
2.6. Lactate and pyruvate movement among blood, brain, and CSF	23
2.7. Hypoxia	28
III. STATEMENT OF PROBLEM	36
IV. METHODS AND MATERIALS	37
4.1. General operative and cannulation procedures	37
4.2. Brain ventricular and cisternal puncture	40
4.3. Experimental perfusion with test molecules	44
4.4. Experimental criteria	45
4.5. Sample collection and storage	45
4.6. Determination of normal CSF and plasma metabolite concentrations	46
4.7. Measurement of blood gas tensions and pH	46
4.8. Measurement of inflow and outflow rates and concentrations	47
4.9. Experimental design	48

	Page
4.9.1. Long duration brain ventricular perfusions in normoxic dogs	51
4.9.1.1. Elevated blood and low CSF inflow concentrations	51
4.9.1.2. Normal CSF inflow concentrations	52
4.9.1.3. Elevated CSF inflow concentrations	52
4.9.2. Brain ventricular perfusion during normoxia and hypoxia	53
4.9.2.1. Low CSF inflow concentrations	54
4.9.2.2. Elevated CSF inflow concentrations	54
4.9.2.3. Low CSF inflow concentrations with mannitol	55
4.9.2.4. Elevated CSF inflow concentrations with mannitol	55
4.10. Principles and calculations	56
4.10.1. Definition of symbols	56
4.10.2. Fluid balance	57
4.10.3. Bulk absorption rate, \dot{V}_a	57
4.10.4. CSF formation rate, \dot{V}_f	58
4.10.5. Derivation of net flux, J_x	58
4.10.6. Derivation of transepndymal outflux coefficient, K_o	59
4.11. Calculated parameters	60
4.12. Statistical methods	60
V. RESULTS	61
5.1. Arterial pH, PO_2 , PCO_2 , and rectal temperature	61
5.2. Cerebrospinal fluid bulk absorption and formation rates	62
5.3. Normal plasma and CSF concentrations of glucose, pyruvate, and lactate	62
5.4. Glucose flux from CSF	63
5.5. Lactate flux from CSF	65
5.6. Mannitol flux from CSF	67
5.7. Pyruvate flux from CSF	68
VI. DISCUSSION	79
6.1. CSF bulk absorption and formation rates	79
6.2. Glucose flux from CSF	81
6.3. Lactate flux from CSF	84
6.4. Pyruvate flux from CSF	86
VII. SUMMARY	88

APPENDICES	Page
A. COMPOSITION AND PREPARATION OF ARTIFICIAL DOG CEREBROSPINAL FLUID (CSF)	90
B. PREPARATION OF ANESTHETIC	92
C. DEPROTEINIZATION OF PLASMA AND CSF SAMPLES .	94
D. SPECTROPHOTOMETRIC DETERMINATION OF D- GLUCOSE	96
E. FLUOROMETRIC DETERMINATION OF PYRUVATE . . .	99
F. SPECTROPHOTOMETRIC DETERMINATION OF L- LACTATE	105
G. SPECTROPHOTOMETRIC DETERMINATION OF INULIN .	110
H. ISOLATION AND IDENTIFICATION OF RADIO- ACTIVELY LABELLED GLUCOSE	113
I. ISOLATION OF LABELLED LACTATE	120
J. LIQUID SCINTILLATION COUNTING	127
K. STATISTICAL FORMULAE	133
LIST OF REFERENCES	139

LIST OF TABLES

Table	Page
1. Arterial pH, PO ₂ , and PCO ₂ and rectal temperature in normoxic and hypoxic dogs during brain ventricular perfusion	69
2. Bulk absorption rate and CSF formation rate in normoxic and hypoxic dogs during brain ventricular perfusion	70
3. Glucose, lactate, and pyruvate concentrations in simultaneously obtained samples from arterial plasma and cisternal cerebrospinal fluid in twelve anesthetized dogs	71
4. D-glucose in the inflow fluid, outflow fluid, and arterial plasma in normoxic and hypoxic dogs during brain ventricular perfusion	72
5. Glucose transepndymal outflux coefficient and net flux rate at low, normal, and elevated perfusion inflow concentrations in normoxic and hypoxic dogs during brain ventricular perfusion	73
6. L-lactate concentration in the inflow fluid, outflow fluid, and arterial plasma in normoxic and hypoxic dogs during brain ventricular perfusion	74
7. Lactate transepndymal outflux coefficient and net flux rate at low, normal, and elevated perfusion inflow concentrations in normoxic and hypoxic dogs during brain ventricular perfusion	75
8. Mannitol transepndymal outflux coefficient at low and elevated perfusion inflow concentrations in normoxic and hypoxic dogs during brain ventricular perfusion	76

Table	Page
9. Mean pyruvate concentrations in the inflow fluid, outflow fluid, and arterial plasma in normoxic and hypoxic dogs during brain ventricular perfusion	77
10. Pyruvate net flux at low, normal, and elevated perfusion inflow concentrations in normoxic and hypoxic dogs during brain ventricular perfusion	78
H-1. Isolation and recovery of ^3H -glucose in the inflow and outflow fluids in dog Scl	119
I-1. Isolation of ^{14}C -lactate in ventricular perfusion effluent	126
K-1. Statistical block of glucose K_o data from 15 normoxic anesthetized dogs at different inflow fluid concentrations during two experimental brain ventricular perfusion periods	137
K-2. AOV table	138

LIST OF FIGURES

Figure	Page
1. Diagram of the experimental animal and equipment	39
2. Photograph of equipment used for ventriculocisternal perfusion in the anesthetized dog	43
3. Diagram showing the time of experimental manipulations and sample collections	50
I-1. Elution profile of CSF outflow sample containing ^3H -glucose and ^{14}C -lactate	125
J-1. ^{133}Ba external standard quench correction curves for differential counting of ^3H and ^{14}C samples	132

I. INTRODUCTION

The absence of any significant cerebral arterio-venous (A-V) plasma concentration differences for substrates other than glucose (Sokoloff, 1960) and a respiratory quotient (R.Q.) approximating 1 (Gibbs *et al.*, 1942) are convincing evidence that the brain derives its energy almost exclusively from glucose oxidation. Glucose is probably preferentially utilized by the adult mammalian brain, since the hypoglycemic effects on mammalian cortical electrical activity (E.E.G.) can be counteracted by iv glucose injections, but not by injections of fructose, galactose, hexose diphosphate, glyceric aldehyde, pyruvate, succinate, fumerate, or glutamate (Maddox *et al.*, 1939).

Glucose removed from blood is metabolized to pyruvate via the Embden-Myerhoff pathway within brain tissue. Pyruvate can be reduced to lactic acid, converted to acetyl coenzyme A by oxidative decarboxylation, carboxylated to form oxaloacetic or malic acids, or transaminated to form alanine. Ultimate conversion to carbon dioxide (CO_2) occurs via the tricarboxylic acid cycle and yields the high energy nucleotide triphosphates necessary for normal tissue function. When ^{14}C -glucose is perfused into blood, only 30-35%

of the ^{14}C -glucose taken up by brain is directly oxidized to $^{14}\text{CO}_2$ and H_2O and large amounts are converted into lipids, proteins, and other acid soluble components (Geiger, 1958). Only 1/3 of the glucose utilized by brain is for the direct formation of high energy molecules (i.e., adenosine triphosphate, ATP; phosphocreatine, PCr) and the remaining glucose (i.e., 65-70%) is metabolized for other purposes.

Glucose and glycogen content in the mammalian brain total 125-200 $\mu\text{moles}/100\text{ g}$ of brain and glucose consumption is 31 $\mu\text{moles}/100\text{ g}$ brain per minute (Sokoloff, 1960). Therefore, when cerebral blood flow (CBF) is diminished or arrested, cerebral function can only be maintained for a short time (i.e., 4-6 minutes) through utilization of its glucose and glycogen stores.

The large oxygen consumption (\dot{V}_{O_2}) of mammalian brain tissue (approximately 20% of total body \dot{V}_{O_2} at rest (Sokoloff, 1960)) coupled with low carbohydrate reserves accounts for the extreme sensitivity of the mammalian brain to anoxic, hypoxic, ischemic, and hypoglycemic conditions (Maddock *et al.*, 1939; Lowry *et al.*, 1964; Dahl and Balfour, 1964; White *et al.*, 1964). Ischemia results in the reduction of brain glucose and glycogen, as well as the reduction of high energy ATP and PCr, and an increase in lactic acid, inorganic phosphate, adenosine diphosphate (ADP), and creatine (Cr) (Lowry *et al.*, 1964; Gatfield *et al.*, 1966;

Folbergrova *et al.*, 1970) indicating an increase in anaerobic metabolism. Complete cessation of cerebral circulation in man results in unconsciousness within 10 seconds (Rossen *et al.*, 1943) the time interval required to use the estimated O_2 content in brain tissue (Kety, 1950). In the absence of O_2 , pyruvate is reduced to lactic acid. Lactic acid once formed cannot be used for energy production unless there is a transformation to pyruvic acid, an event associated with aerobic conditions (White *et al.*, 1964). It can be inferred that in the mammalian brain aerobic glucose utilization is not only a preferential pathway but an obligatory one.

Normal brain function depends upon the maintenance of a relatively constant ionic composition and adequate metabolite concentration in the interstitial fluid (ISF) bathing the neurons (Kerr and Ghantus, 1936; Merlis, 1960). There is substantial interest in solute exchanges between blood and brain tissue under various physiological conditions. The exchange of water and solutes can take place between blood plasma and brain ISF by two routes. A direct exchange may occur across blood capillaries into brain tissue, however, brain capillaries are much less permeable to solutes than blood capillaries in other tissues (Ferguson and Woodbury, 1969; Brooks *et al.*, 1970) and direct solute exchange between capillary blood and brain tissue is limited by this "blood brain" barrier. The brain is in communication

with another fluid in addition to the blood, the cerebrospinal fluid (CSF) (Truex and Carpenter, 1969), and an indirect solute exchange between blood and brain can occur via the CSF. Consequently, the manner in which brain ISF solute composition changes depends on the nature of transfer between blood and brain ISF, CSF and brain ISF, and blood and CSF.

Glucose moves from blood into brain and from blood into CSF by facilitated diffusion (Fishman, 1964; Crone, 1965; LeFevre and Peters, 1966), while pyruvate and lactate are hypothesized to move by simple diffusion (Siesjo *et al.*, 1968). Simultaneous rates of the movements of glucose, pyruvate, and lactate across the CSF-brain and/or CSF-blood barriers have not been measured. Knowing the flux rates and mode of transfer for these metabolites across the barriers separating CSF from blood and/or brain ISF during normoxia and hypoxia would aid in understanding brain metabolism and brain survival *in vivo*.

II. LITERATURE REVIEW

2.1. Relationship of cerebrospinal fluid to blood and brain

In the adult mammalian central nervous system (CNS) the cerebrospinal fluid (CSF) occupies two main compartments, the brain ventricles and the subarachnoid spaces. The brain ventricles consist of four interconnecting cavities: the two lateral ventricles, which connect by the intraventricular foramina of Monroe to the midline third ventricle, which communicates via the aqueduct of Sylvius with the fourth ventricle. The fourth ventricle connects with the subarachnoid spaces by the foramina of Luschka. The subarachnoid spaces are formed by the inner pial membrane, which follow the outer contours of the brain, and the arachnoid membrane, which is in apposition with the outermost dural membrane.

In the subarachnoid spaces, the CSF is separated from brain tissue by the pial membrane. As seen through the light microscope, the pia is a thin avascular membrane and the blood (pial) vessels supplying brain tissue lie on the surface of the membrane penetrating the pia to enter or to return from brain tissue (Millen and Woollam, 1961). Forbes (1928) studied these blood vessels *in vivo* and failed to

observe capillary loops, although he described small arterioles which permitted only a single column of erythrocytes to pass through them. Similar observations reported by Flexner (1933) and Hassin (1948) suggest that capillaries may be present in the subarachnoid spaces and would permit solute exchange between blood and CSF.

In four discrete regions, the pia is modified into highly vascular tissue. During fetal development, the pia and accompanying blood vessels invaginate and project into the brain ventricles, and with the neural epithelium (ependyma) lining the ventricles constitute the choroid plexuses (Arey, 1962; Davson, 1967). In these regions, i.e., the roofs of the third and fourth ventricles and the walls of the lateral ventricles, the membranes separating CSF from blood consists of two cell layers, the capillary endothelium and the ventricular ependyma (Davson, 1967).

Within the brain ventricles, CSF is separated from the surrounding neural tissue and brain extracellular fluid (ECF) by a single layer of ependymal cells, which comprise the walls of the ventricles. Some ependymal cells are close to cerebral blood vessels (Horstman, 1954) and may possess secretory functions (Fleischauer, 1964).

The relationship of CSF to brain ECF space and plasma has been demonstrated by Wallace and Brody (1937; 1939) and by Olsen and Rudolph (1955). Wallace and Brody (1937; 1939) administered salts of iodide, thiocyanate, and

bromide iv and after 24 hours determined the anion to chloride ratios present in the plasma and in various tissues of the dog. In all tissues examined except the brain, the anion to chloride ratio was the same as its ratio in the plasma, but in the brain the anion to chloride ratio was the same as in the CSF and lower than in the plasma. More recently, Olsen and Rudolph (1955) studied ^{24}Na and ^{82}Br transfer among blood, CSF, and brain tissue. They reported that following iv administration of these ions equilibration between the blood and the CSF required more than 16 hours, while equilibration between CSF and brain occurred in less than 30 minutes. Collectively, these data suggest that brain ECF equilibrates not with plasma but with CSF.

The first attempt to estimate the size of brain ECF space by placing ECF markers in the CSF was reported by Davson *et al.* (1961), who repeatedly replaced the CSF in rabbits with an artificial CSF containing a known sucrose concentration. The sucrose concentration in the subarachnoid spaces was maintained relatively constant for 2-3 hours by barbotage. The authors reported a spinal cord sucrose space of 12-14%. The brain sucrose space was 8-9% and this lower sucrose space was presumed to be due to inadequate mixing in CSF surrounding the brain surfaces.

Rall *et al.* (1962) measured brain ECF space by a different technique. They continuously perfused the dog's

brain ventricular system through a cannula in the lateral ventricle and collected fluid from another cannula in the cisterna magna, a technique first developed by Leusen (1948). The perfusion fluid contained ^{14}C -inulin as the ECF marker. After 3-5 hours of perfusion the dog was killed and the brain removed. Small coronal sections 5 mm thick were cut from select areas of the brain at successively greater distances from the ventricular surface and analyzed for ^{14}C activity. Activity was greatest in the brain sections immediately adjacent to the ventricular system and decreased progressively with each successive section, suggesting incomplete equilibration of the total ECF with CSF. The authors concluded that inulin penetration into brain ECF from CSF was slow; the inulin brain space was 12%. Recently, Levin *et al.* (1970) perfused the cerebral subarachnoid spaces in four different mammalian species and reported cerebral cortical ^{14}C -sucrose and ^3H -inulin spaces of 17-20%.

The brain ECF space estimated by the presentation of the ECF marker via the CSF is 12-20% of the total brain volume. Intravenous injection of ECF markers and the resultant 2-8% brain ECF space (Davson and Spaziani, 1959; Barlow *et al.*, 1961; Reed and Woodbury, 1963) has been suggested by Davson *et al.* (1961) to be due to the "sink action" of CSF, the brain ECF marker being continuously diluted by CSF production and CSF absorption into the blood.

This "sink-action," has been circumvented by combined presentation of the ECF marker via ventriculo-cisternal perfusion and infusion into the general circulation (Woodward *et al.*, 1967; Cutler *et al.*, 1969; Baethman *et al.*, 1970). These reports suggest a mammalian brain ECF space of 10-15%, a brain ECF space comparable to that obtained by perfusion of the CSF alone (Rall *et al.*, 1962).

2.2. Cerebrospinal fluid (CSF) formation

CSF is a colorless fluid containing ions which are also found in the blood, but unlike blood, contains no cells and only a very small amount of protein (Davson, 1967). In general, CSF has higher Cl^- and Mg^{++} concentrations than in a plasma dialysate (Kemeny *et al.*, 1962; Friedman *et al.*, 1963) while CSF concentrations of K^+ , Ca^{++} , and glucose are lower (Bito and Davson, 1966; Oppelt *et al.*, 1963b). Ultrafiltration of blood is not sufficient to explain CSF formation since an energy source other than blood hydrostatic pressure must be responsible for the observed ionic concentrations.

Some of the first studies on CSF formation were conducted by Dandy and Blackfan (1914) and Frazier and Peet (1914), who produced experimental hydrocephalus in the dog by plugging the aqueduct of Sylvius and proved beyond doubt that CSF is formed within the brain ventricles. Dandy (1919) showed the involvement of the choroid plexus by unilaterally

plexectomizing the dog while blocking both foramina of Monroe, which resulted in the development of a unilateral hydrocephalus in the nonplexectomized ventricle. Bering and Sato (1963) unilaterally plexectomized dogs but blocked the aqueduct of Sylvius or the cisterna magna with kaolin while leaving the foramina of Monroe open, and reported the development of an asymmetrical hydrocephalus.

More direct evidence bearing on the secretory activity of the choroid plexus has been provided by studies on the exposed choroid plexus (Welch, 1963; Ames *et al.*, 1965a). Welch (1963) cannulated the large vein draining most of the venous blood from the lateral ventricular choroid plexus in the rabbit and reported a venous to arterial hematocrit ratio of 1.15, and confirmed that fluid was lost from blood upon passage through the choroid plexus. Ames *et al.* (1965a) collected under oil and chemically analyzed the freshly secreted fluid from the exposed choroid plexus of the lateral ventricle of the cat. The concentrations of Na^+ , K^+ , Ca^{++} , Mg^{++} and Cl^- were sufficiently like those in CSF collected from the cisterna magna, and sufficiently different from a plasma filtrate to suggest that this fluid was a secreted CSF and not a pathological plasma exudate. Although such evidence favors the hypothesis that the choroid plexuses are sites of CSF formation, the ventricular ependyma within the aqueduct of Sylvius has also been reported by Pollay and Curl (1967) to be a source of CSF.

Bering (1959) reported a CSF formation rate (\dot{V}_f) of 0.050 ml/min in the anesthetized dog by collecting CSF outflow from a cannula placed in the cisterna magna. \dot{V}_f could be correlated with cerebral oxygen consumption (CMR_{O_2}) and with cerebral blood flow (CBF), but neither CMR_{O_2} nor CBF alone could account for the total CSF produced.

The first drug unequivocally shown to affect CSF production was the carbonic anhydrase inhibitor, acetazolamide (Diamox). Pollay and Davson (1963) reported approximately a 50% reduction in \dot{V}_f in the rabbit following either intravenous or intracisternal administration of the drug. Intravenous Diamox administration results in a 43% inhibition of \dot{V}_f in both the adult (Oppelt *et al.*, 1964) and newborn dog (Holloway *et al.*, 1972). Similarly, the rate of fluid formation by the exposed choroid plexuses is decreased following iv Diamox administration (Ames *et al.*, 1965b). This suggests that the formation and dissociation of carbonic acid (H_2CO_3) may be a necessary event in the metabolism of the cells responsible for CSF formation, and interference with this metabolism reduces the secretory processes.

Oppelt *et al.* (1963a) studied the effects of acidosis and alkalosis on \dot{V}_f in the dog. Acidosis, produced by either iv administration of HCl or 5-10% CO_2 inhalation had no consistent effect on \dot{V}_f . Alkalosis induced by iv bicarbonate administration caused a 23% reduction in \dot{V}_f ,

which could be further reduced to 45% by the simultaneous administration of Diamox. Respiratory alkalosis resulted in a 46% reduction in \dot{V}_f and the administration of Diamox during hypocapnia resulted in a 62% reduction of \dot{V}_f . Ames *et al.* (1965b) reported decreased fluid formation by the exposed choroid plexus following reduction of arterial CO_2 (P_aCO_2) by hyperventilation. These authors also reported an increased fluid formation when P_aCO_2 was increased by 10% CO_2 inhalation. It was observed that the P_aCO_2 effects were associated with vasomotion of the choroidal artery, so that the rate limiting factor in CSF formation by the choroid plexus may have been its blood supply. Since iv Diamox results in choroidal arterial constriction in the isolated perfused choroid plexus comparable with that produced by iv norepinephrine administration (Marci *et al.*, 1966), part of the Diamox effect on \dot{V}_f may be mediated via the vascular system.

\dot{V}_f is in part an active process as shown by studies using either dinitrophenol (DNP) or the cardiac glycoside, ouabain. DNP blocks the oxidative phosphorylation of ADP and in general abolishes the active transport of ions (e.g., the active extrusion of Na^+ from the squid's giant axon (Hodgkin and Keynes, 1955)). Davson and Pollay (1963) perfused the brain ventricles of the rabbit and reported \dot{V}_f was reduced 45% from control values when DNP (0.05 mM) was included in the perfusion fluid. Most secretory

processes involving the active transport of Na^+ and K^+ involve the enzyme ATPase, which is specifically inhibited by ouabain. Some early attempts to demonstrate inhibition of \dot{V}_f following iv administration of ouabain were not very successful (Davson and Pollay, 1963; Oppelt *et al.*, 1964). By contrast, Welch (1963) reported that CSF formation by the choroid plexus could be halved by 10^{-5} M ouabain iv, and 10^{-4} ouabain resulted in complete inhibition. Vates *et al.* (1964) have reported the *in vitro* Na-K ATPase activity of the excised cat choroid plexus was reduced about 75% when 10^{-5} M ouabain was included in the incubation media. \dot{V}_f was reduced significantly when ouabain was perfused through the ventricles of the cat (Vates *et al.*, 1964), the rabbit (Davson and Segal, 1970), and both the adult (Cserr, 1965) and newborn dog (Holloway *et al.*, 1972). The studies of drug effects on \dot{V}_f , particularly those of ouabain, imply that CSF production probably involves the active transport of Na^+ and K^+ across the choroidal epithelium. Such evidence indicates that CSF is a secretion, in the sense that active transport mechanisms are operative during its elaboration and metabolic energy is required.

2.3. Cerebrospinal fluid (CSF) absorption

Drainage of CSF from the ventricular system is via the foramina of Luschka into the subarachnoid space. CSF drainage from the subarachnoid space appears to be into

large endocranial venous sinuses, whose dural sheaths are perforated in certain places by numerous fingerlike evaginations (villi) of the arachnoid membrane projecting into the lumen of the sinus (Weed, 1923).

Welch and Friedman (1960) described the villi initially found by Weed as a series of interconnecting tubes. These investigators excised pieces of dural membrane containing villi and mounted the membrane so that it separated two fluid filled chambers. A hydrostatic pressure of about 10 mm H₂O was required to initiate fluid flow from the CSF side of the membrane to the blood side. Fluid flow was independent of colloidal osmotic pressure on the blood side and particulate suspensions up to 7 μ diameter placed on the CSF side passed through the villi without back filtering. They concluded that the arachnoid villi act as one way valves, through which both large and small molecules may exit from CSF into blood. Since large molecules, e.g., inulin or dextran, exit from the subarachnoid space (Rothman *et al.*, 1961; Davson *et al.*, 1962), smaller molecules and probably all the dissolved substances in CSF, whether naturally occurring or exogenously introduced will leave CSF by this mechanism of bulk absorption.

2.4. Quantitative measurement of molecular movement from the CSF

Molecules traverse membranes by simple diffusion and/or by carrier-mediated transport. Diffusion is the net movement of molecules from a region of greater concentration to a region of lesser concentration (Stein, 1967). In a carrier-mediated transport system the transported molecules or ions must attach themselves to a molecule present in the cell membrane in order to traverse the membrane. These carriers are assumed to be limited since when the concentration of the transported molecules on one side of the membrane is large all the carriers become occupied (i.e., saturated) and the transport rate across the membrane cannot be increased by further increases in the concentration of the transported molecule unless a non-carrier transport (e.g., diffusion) is also possible (Davson and Danielli, 1952). Among the criteria for identifying carrier-mediated transport are demonstrations of self-saturation of the carrier and/or competition for the carrier between structurally analogous compounds. Carrier-mediated transport along either an electrical or a chemical gradient is described as "passive" (e.g., facilitated diffusion) and carrier-mediated transport against an electrochemical gradient requires the expenditure of energy and is referred to as "active transport" (Stein, 1967).

Davson *et al.* (1962) have shown that when ^{24}Na , inulin, and p-aminohippurate (PAH) are simultaneously injected intracisternally in the rabbit, and their concentrations analyzed after one hour, the rate of molecular loss from CSF was always $^{24}\text{Na} > \text{PAH} > \text{inulin}$. These results imply that ^{24}Na and PAH leave the CSF by route(s) other than bulk absorption. Heisey *et al.* (1962) perfused the brain ventricles and estimated the rate of bulk absorption (\dot{V}_a) in the unanesthetized goat. Both flow rates and steady-state concentrations of inulin in the inflow and outflow fluids were measured and CSF clearance calculated using a formula analogous to that for calculating renal clearance. At intraventricular pressures below $-15 \text{ cm H}_2\text{O}$, all the inulin (M.W. = 5000) perfused into the ventricular system was recovered in the cisternal effluent, and inulin clearance was zero, indicating that inulin doesn't diffuse from the ventricles. When intraventricular pressure was raised above $-15 \text{ cm H}_2\text{O}$, inulin clearance increased linearly with pressure, indicating that inulin was removed from CSF mainly by bulk absorption distal to the fourth ventricle. Inulin clearance was considered an accurate estimate of \dot{V}_a . In addition to inulin, the CSF clearances of tritiated water (^3HOH ; M.W. = 20), urea (M.W. = 60), creatinine (M.W. = 113), and fructose (M.W. = 180) were estimated and their clearances from CSF always exceeded that of inulin. As intraventricular pressure increased the clearances of ^3HOH , urea,

creatinine, and fructose increased proportionally with the increase in inulin clearance. The clearance due to non-bulk absorptive processes (K_o) was estimated by subtracting from the total clearance the clearance due to \dot{V}_a , estimated by inulin clearance, and was found to be independent of intraventricular pressure.

Pappenheimer *et al.* (1961) reported that Diodrast was cleared from CSF approximately 3 times more rapidly than creatinine in goats whose brain ventricles were perfused with an artificial CSF. Considering only molecular size, creatinine (M.W. = 113) should leave CSF more rapidly than Diodrast (M.W. = 401). At elevated CSF Diodrast concentrations, they demonstrated saturation of the Diodrast K_o indicating carrier-mediated transport of Diodrast from the CSF. Diodrast transfer from CSF related to increasing perfusate concentrations was a 2 component curve: (1) a fast rate of transfer which was non-linear at Diodrast concentrations below 25 $\mu\text{g/ml}$ and (2) a slower, linear rise of transfer rate, with increasing Diodrast concentrations above 25 $\mu\text{g/ml}$. More recently, Bierer (1972) reported that PAH is transported from the perfused CSF system of the adult dog, as indicated by competitive inhibition of transport by another organic anion, Diodrast, and self-saturation.

2.5. Glucose movement among blood, brain, and CSF

Geiger *et al.* (1954) perfused the vasculature of the cat's brain with an artificial blood composed of ox erythrocytes, serum-albumin, and Ringer's solution, and reported that the brain was rapidly depleted of glucose despite the maintenance of a high glucose concentration in the perfusion fluid. Further experiments showed that glucose depletion was not the result of increased metabolism, but was primarily due to the failure of the brain to remove glucose from the blood. Addition of liver extract to the perfusion fluid, or the use of donor blood, abolished this effect suggesting that the blood-brain barrier to glucose was controlled by a substance(s) normally circulating in the blood. When a liver extract was included in the perfusion fluid, brain glucose concentration paralleled variations in the glucose concentration of the perfusion fluid. Elevations in perfusion fluid glucose concentration above 10 mM produced little or no increase in brain glucose concentrations, suggesting the possible involvement of a carrier-mediated transport of glucose from blood to brain.

More direct evidence of carrier-mediated transfer from blood to brain was presented by Crone (1965), who measured the amount of ^{14}C -glucose extracted from blood during a single circulation through the head. The technique consisted of giving a steady intracarotid infusion of test substances, whose permeability characteristics were to be

studied and withdrawing simultaneous blood samples from the carotid artery and the superior sagittal sinus. Analysis of the arterial and venous blood allowed measurement of solute loss to the brain. Dilution due to the blood entering brain from other sources was estimated by including in the injections T1824 (Evan's Blue dye) which was confined to the vascular system. Glucose extraction decreased as plasma glucose increased. The system was saturated at approximately 4 mM D-glucose. Fructose extraction, by comparison, was low, did not exhibit saturation, and was not carried by the same mechanism as glucose. This glucose carrier system has not shown to be responsive to iv insulin administration (Crone, 1965; Gilboe *et al.*, 1970). More recently, LeFevre and Peters (1966), Bidder (1968), and Buschiazzo *et al.* (1970) have presented evidence for carrier-mediated transport of hexose sugars from blood to brain in the rodent, as indicated by self-saturation and competition. Mayman *et al.* (1964) reported a brain glucose concentration range of 0.6-1.2 mmoles/kg H₂O, while blood glucose concentration was 5-8 mM in anesthetized mice; therefore, the glucose concentration gradient from blood to brain favors passive movement and suggests that glucose is transported across the blood-brain barrier via facilitated diffusion.

Fishman (1964) was the first to report the existence of a saturable blood to CSF glucose transport. In his study, blood glucose was raised and held steady by iv infusion, and

CSF glucose concentration determined at various times. CSF glucose concentration rose to a maximum of 11.6-13.3 mM independent of whether the plasma concentration was 16.7, 20.8, or 25.0 mM. Fructose was analyzed in a similar manner; its movement into CSF was slight and it did not show saturation when plasma concentration was raised. When 2-deoxyglucose was simultaneously infused with glucose, glucose penetration into CSF was competitively inhibited. Atkinson and Weiss (1970) repeated Fishman's work by analyzing glucose penetration over wider perturbations of plasma glucose concentrations. They reported a saturation of the glucose carrier at approximately 20 mM.

Evidence of carrier-mediated glucose transport from blood to CSF by the choroid plexus has been provided by Welch and co-workers (1970). The D-glucose concentration was measured in newly formed choroidal CSF and in arterial plasma samples collected simultaneously from adult rabbits. Plasma concentrations were systematically lowered by insulin or raised by iv glucose infusion. Glucose movement into CSF increased linearly with plasma concentrations up to 14 mM and CSF glucose maintained a level approximately 0.6 that of the plasma concentration. At plasma glucose concentrations between 14 and 20 mM choroidal CSF glucose concentration remained essentially constant (i.e., the system demonstrated self-saturation). When plasma glucose

concentration exceeded 20 mM, CSF glucose again increased linearly with plasma glucose concentration. These results imply the presence of at least one carrier which is operative at plasma glucose concentrations less than 14 mM and another inoperative at plasma glucose levels below 20 mM. Since glucose concentration in blood (6.3 mM) exceeds that in CSF (4.2 mM) (Bito and Davson, 1966), glucose probably moves from blood to CSF via facilitated diffusion.

The possibility of glucose transfer from CSF into adjacent neural tissue cannot be dismissed even though the functional activity of the isolated perfused cat spinal cord cannot be maintained by high glucose concentrations in the perfusion fluid (Wolff and Tschirgi, 1965). Bradbury and Davson (1964) compared glucose, creatinine, urea, and inulin clearance from ventriculocisternal perfusion fluid in anesthetized rabbits, and reported that glucose was cleared at the fastest rate. When solute concentrations were raised in the perfusion fluid, creatinine and urea outflux coefficients (K_o) were unaffected whereas that of glucose decreased approximately 48%, indicating saturation of glucose carrier-mediated efflux. Csaky and Rigor (1968) perfused the CSF ventricular system in the dog with an artificial CSF containing ^{14}C -glucose and reported that removing Na^+ or adding phlorizin or digitoxin in the perfusion fluid decreased the rate of ^{14}C -glucose disappearance from CSF. Bronsted (1970a and b) perfused the cerebral

ventricles of the cat and found that ^{14}C -glucose efflux from CSF was competitively inhibited by either xylose or mannose and was reduced when ouabain ($10^{-7} - 5 \times 10^{-5}\text{M}$) was included in the perfusion fluid. Such results imply a carrier-mediated transport for glucose from CSF and indicate that the transport system may be involved with active Na^+ transport.

The choroid plexus is capable of accumulating glucose and galactose *in vitro* (Csaky and Rigor, 1968). Glucose and galactose accumulation was inhibited by anoxia, ouabain, phlorizin, or DNP and by the absence of Na^+ in the incubation media. The complete inhibition of glucose and galactose accumulation by DNP or anoxia implies dependence on an aerobic utilization of energy. Although such results show accumulation is possible, they do not indicate whether this represents a tendency to remove glucose from CSF or to increase its CSF concentration. In vascular perfusions of the isolated horse choroid plexus, galactose transport from the incubation medium into the perfusate against a concentration gradient has been reported (Csaky and Rigor, 1968) and it has been inferred that the choroid plexus is similarly capable of actively transporting glucose from CSF to the blood. These *in vitro* results indicate the choroid plexus may be a site of active aerobic transport of glucose from CSF to blood, and that this transport system may be coupled with the movement of Na^+ .

2.6. Lactate and pyruvate movement among blood, brain, and CSF

McGinty (1929) attempted to correlate respiratory control in the anesthetized dog with brain lactate production as measured by arterial-jugular venous plasma lactate concentration differences. The author reported that when cerebral blood flow (CBF) was unimpaired, lactic acid was extracted from blood by the brain, but if CBF was impaired via ligation of the carotid arteries or if oxidative metabolism was inhibited by sodium cyanide iv, lactic acid was released from brain tissue. He concluded that excessive lactic acid production by brain resulted in an outward diffusion of lactic acid into venous blood. Jugular venous blood in the dog is not exclusively of cerebral origin and CBF measurements were not included in this study, making invalid McGinty's inferences regarding the production or uptake of lactic acid by the brain. Gurdjian *et al.* (1944) reported that the concentrations of lactate in the brain and in the blood vary independently and hypothesized that the blood-brain interchange of lactate must be slow. This hypothesis was subsequently supported by Klein and Olsen (1947) who increased blood lactate concentrations in the cat by iv injections and determined the lactate concentrations in arterial blood and in brain tissue at various times following the injections. They reported that although arterial plasma concentrations were increased 10-30 times

the preinjection concentration, brain lactate concentrations at 10 and 40 minutes following iv vascular injection did not differ significantly from brain lactate concentrations in cats not injected with lactate.

Alexander *et al.* (1962) reported no rise in CSF lactic acid concentration 30 minutes following iv lactic acid loading in dogs. Subsequent studies (Plum and Posner, 1967; Plum *et al.*, 1968) have shown that brain lactic acid concentration which is increased following hyperventilation correlates closely with CSF lactic acid concentration but not with sagittal sinus blood concentrations. These results suggest that CSF lactic acid concentration is not affected by blood lactate concentration but is probably a more accurate indicator of cerebral metabolism.

When tissue oxygenation is decreased, a metabolic shift occurs toward the reduced state of a metabolic system and pyruvate is reduced to lactate. However, lactate accumulation may result from nonhypoxic causes which increase glycolytic activity thereby increasing the concentrations of both pyruvate and lactate (Huckabee, 1958a). Huckabee claimed to identify nonhypoxic causes of increased lactate accumulation by simultaneously determining the pyruvate and lactate concentrations and calculating an "excess lactate": the lactate which was not due to increased pyruvate concentration. Since the ratio of lactate

pyruvate concentrations (L/P) reflect the oxidation-reduction state of cytoplasmic NADH/NAD^+ (Huckabee, 1958a) measurement of the L:P ratio of a tissue, and possibly the measurement of L:P ratio in plasma in equilibrium with the tissue could yield information on the presence of tissue hypoxia. When tissue O_2 supply is acutely decreased by hypoxia or anemia, the blood L:P ratio increases (Huckabee, 1958b; Cain, 1965) presumably due to tissue hypoxia. Sagittal sinus plasma lactate concentrations do not accurately reflect brain lactate concentrations (Plum *et al.*, 1968), but brain ECF concentrations at least with respect to Na^+ , Br^- , I^- , Cl^- , and SCN^- equilibrate with the CSF (Wallace and Brody, 1937, 1939; Olsen and Rudolph, 1955). Consequently, elevated L:P ratios of brain homogenates and of CSF have been used to indicate brain anaerobiosis (Kaasik *et al.*, 1970).

The relationship of the L:P ratios in brain homogenates and CSF have been studied by Granholm and Siesjo (1967, 1969) and Granholm *et al.* (1968). During normoxic normocapnia the CSF L:P ratio is less than that of homogenized brain tissue and is the result of an elevated CSF pyruvate concentration (Granholm and Siesjo, 1969). This suggests that pyruvate may diffuse from CSF into brain tissue down its concentration gradient to be metabolized. However, pyruvate concentration in arterial blood plasma is also less than that in CSF (Granholm and Siesjo, 1967)

implying that pyruvate movement into the CSF may involve more than simple diffusion.

Changes in pH influence the distribution of acids and bases between the ECF and intracellular fluid (ICF) (Milne *et al.*, 1958). If only the nonionized form is diffusible and if the compound exists in equal concentrations in the ECF and the ICF, the relation between the total concentrations of the acids and their anions will be determined by the hydrogen ion activity (pH) in these respective fluids. Both lactate (pK = 3.8) and pyruvate (pK = 2.5) are primarily ionized at body pH and should not rapidly traverse cell membranes.

Siesjo *et al.* (1968) have proposed a lactate-pyruvate transport system between brain ICF and the ECF (assumed in equilibrium with CSF) to explain the lower L:P ratio in the CSF. They hypothesized that lactate was converted to pyruvate simultaneously removing a proton (H^+) from the cell into the CSF. Such a system could continuously remove lactate from the cell and establish a pyruvic acid concentration gradient from CSF into the cell. Such a scheme is compatible with the observed brain tissue and CSF L:P ratios in the cat (Granholm and Siesjo, 1969), if it is assumed the conversion of lactate to pyruvate occurs faster than the diffusion of lactic acid from brain ICF and that of the diffusion of pyruvic acid in the opposite direction.

Prockop (1968) reported that lactic acid was cleared from CSF slower than that of a glucose analog, 3-0-methylglucose, and that lactic acid clearance exceeded the clearance of larger molecules such as creatinine and mannitol. Prockop suggested that since he observed no decrease in lactic acid clearance at different CSF lactate concentrations, lactic acid clearance could be explained solely by simple diffusion and bulk absorption. CSF lactate concentration in the dog is normally 1-2 mM (Prockop, 1968). Prockop's experiments were conducted at high CSF lactate concentrations (i.e., 5-10 mM) where lactate transport may be saturated, and limit inferences regarding the mode of lactic acid clearance from CSF.

Recently, Valenca *et al.* (1971) investigated CSF lactate clearance by intrathecal loading with either Na-lactate or lactic acid. He reported that most of the lactate injected into the CSF was recovered as an increase in brain lactate concentration. Similar increases in brain lactate concentration were found regardless of the form of lactate injected. It can be inferred that at high intrathecal concentrations (e.g., 10 mM) lactate can enter brain tissue but the mechanism of entrance cannot be deduced. Further studies are clearly necessary to define adequately the movements of lactate among the three extracellular fluid compartments of the brain.

2.7. Hypoxia

Hypoxia causes an increased brain glycolytic rate which results in increased lactate concentrations (Lowry *et al.*, 1964), increased cerebral blood flow (CBF) (Kety and Schmidt, 1948; Shimojyo *et al.*, 1968; Shapiro *et al.*, 1970; Fusjishma *et al.*, 1971), and alterations in the membranes of brain cells (Bakay and Lee, 1968). Membrane alterations may be responsible for the brain edema (Rall *et al.*, 1962; VanHarreveld *et al.*, 1965; Myers *et al.*, 1969; Bondareff *et al.*, 1970) often seen during hypoxia. Changes in CBF and/or membrane permeability could affect the amount of a substrate (e.g., glucose) removed from the blood by the brain, as well as the amount which enters the brain indirectly via the CSF. Likewise, the exit of lactate from brain either directly into the blood or into CSF could be affected.

In the spontaneously breathing animal, hypoxia causes hyerventilation resulting in a respiratory alkalosis (Kety and Schmidt, 1948; Shimojyo *et al.*, 1968; Shapiro *et al.*, 1970). Kety and Schmidt (1948) used the nitrous oxide technique to measure CBF in man and reported that CBF decreases during normoxic hypocapnia. This finding has been supported by Raichle *et al.* (1970), who reported decreased CBF following sustained hyperventilation in both dogs and man. In the dog, CBF decreased 60% within 30 minutes and declined an additional 6% during the subsequent five hours

of passive hyperventilation. Restoration of normocapnia returned the CBF to prehypocapnic control values. Similarly in men $P_a\text{CO}_2$ was decreased to 15-20 mm Hg by voluntary hyperventilation and within 30 minutes CBF decreased approximately 40%, and subsequent normocapnia restored CBF to prehypocapnic values.

Hypoxia increases CBF in man, which Kety and Schmidt (1948) attributed to cerebral vasodilation caused by the accumulation of metabolic products (i.e., CO_2 , H^+ , lactic acid). More recent studies in man report acute hypocapnic ($P_a\text{CO}_2 < 30$ mm Hg) hypoxia does not result in increased CBF unless $P_a\text{O}_2$ is decreased below 40 mm Hg (Shimojyo *et al.*, 1968; Shapiro *et al.*, 1970). Acute normocapnic hypoxia ($P_a\text{CO}_2 = 37$ mm Hg; $P_a\text{O}_2 = 40$ mm Hg) results in a 35% increase in CBF (Shapiro *et al.*, 1970), suggesting the vasoconstrictor effects of hypocapnia apparently counter the vasodilator response to hypoxia. Although total CBF increases during normocapnic hypoxia local CBF responses are variable (Fujishima *et al.*, 1971). Fujishima *et al.* (1971) studied hypoxic effects on local cortical CBF in the dog. Qualitative changes in CBF were recorded by a heated thermistor, flow probe placed either unilaterally or bilaterally in the parietal cortex. The heated thermistor probe placed in brain tissue was assumed to measure predominately changes in the capillary blood flow (Fujishima *et al.*, 1971).

Local CBF decreased in 33% of the dogs subjected to 6% O₂ in N₂ and increased in the other 67% of the dogs. The CBF of all dogs could be subsequently increased by normoxic hypercapnia. A local vasoconstrictor response to hypoxia may have occurred in areas of the cortex with a relatively low metabolic rate which shunted blood to more rapidly metabolizing tissue, and led to the variable CBF response to hypoxia found by Fujishima and co-workers. Hawegawa *et al.* (1968) have shown precapillary shunts in the cerebral cortex of the dog and direct A-V hunting in local areas could also be responsible for the variable hypoxic response.

Brain metabolism has been studied *in vivo* from the A-V differences of metabolites (Gibbs *et al.*, 1942; Solokoff, 1960). Brain metabolism can also be studied by decapitation, which converts the brain to a closed system, and measuring the rates of change in the concentrations of compounds capable of yielding energy under these conditions (Lowry *et al.*, 1964; Gatfield *et al.*, 1966; Folbergrova *et al.*, 1970). In the absence of oxygen (anoxic hypoxia), the major energy reserves are ATP, PCr, and the high energy phosphate bonds generated by the conversion of glucose and glycogen to lactate via glycolysis. Anoxic hypoxia, produced by ischemia results in a 4-7 fold increase in the rate of glycolysis and causes a decrease in the concentrations of brain glucose, glycogen, ATP, and PCr with a concomitant

increase in the concentration of lactate, ADP, inorganic phosphate and Cr (Lowry *et al.*, 1964).

Although these decapitation studies describe the general patterns of changes in brain energy metabolism, they cannot provide information concerning the metabolic events following reoxygenation. Recently, Kaasik *et al.* (1970) measured the lactate and pyruvate concentrations in blood, CSF and brain homogenates as well as the concentrations of brain ATP, ADP, AMP, and PCr during and after varying periods of asphyxia induced by respiratory arrest. They reported that during 3 minutes of asphyxia the brain tissue L:P ratio increased and the ATP:ADP and ATP:AMP ratios decreased. These changes were due to the rapid rise in lactate, ADP, and AMP concentrations and the rapid fall in ATP concentration. PCr concentration decreased but tissue pyruvate concentration did not change during asphyxia. In the restitution phase, ATP, ADP, AMP, and the ATP:ADP, ATP:AMP and the L:P ratios were normalized within two minutes. The normalization of the tissue L:P ratio was due to a rapid decrease in tissue lactate concentrations and a marked increase in pyruvate concentrations. These changes in the L:P ratio were interpreted as the very fast reoxidation of cytoplasmic NADH. However, the rephosphorylation of Cr was not complete and the tissue still showed a marked lactacidosis. In the CSF

there was a delayed increase in the lactate concentration and a delayed fall toward normal values. The highest lactate values were obtained after the resumption of normal breathing. Lactate values as well as the L:P ratios, were still elevated after 10 minutes. These changes were suggestive of a time lag in the movement of lactate and pyruvate from tissue into CSF, and the slow clearance of lactate from CSF. This study suggests that elevated lactate concentration in the CSF and the increased L:P ratio are important in indicating a hypoxic change in brain tissue.

Anoxic hypoxia results in a decreased brain ECF space (Rall *et al.*, 1962; VanHarreveld *et al.*, 1965). Rall *et al.* (1962) perfused the brain ventricular system of a dead dog and reported a brain inulin space less than that found in brain perfusions of live dogs. VanHarreveld *et al.* (1965) reported a 6% brain ECF space measured by electron microscopy in rat cortical tissue frozen 8 minutes after decapitation in contrast to a brain ECF space of 18-25% in rapidly frozen tissue. Both groups of investigators suggested the decreased brain ECF space was due to brain edema resulting from the absence of active aerobic metabolic processes, which maintained the osmotic equilibrium between brain ECF and ICF. Myers *et al.* (1969) produced hypoxia in fetal monkeys by inducing prolonged (i.e., 4-6 hours) maternal uterine contractions and measured hemoglobin saturation and pH in the carotid arterial blood in the

fetus. When hemoglobin saturation was reduced to less than 50% and pH reduced to 6.22-7.20, the brain became edematous. In a subsequent study, Bondareff *et al.* (1970) subjected fetal monkeys to a similarly produced hypoxia and measured the ECF space of the cerebral cortex from electron micrographs. They reported a 5% reduction in the ECF space in the hypoxic fetuses when compared to normal fetuses. In addition, mitochondria from hypoxic fetuses were swollen and characterized by the dissolution of the cristae. These data suggest that brain edema concomitant with hypoxia may have resulted in part from altered mitochondrial metabolism.

Eich and Wiemers (1950) were unable to demonstrate the breakdown of the blood-brain barrier to trypan blue during hypoxia. They concluded that the blood-brain barrier was at the capillary endothelium, since this tissue would be the last to suffer from hypoxia due to its close proximity to blood. Supportive evidence has been provided by Bakay and Lee (1968) and Goodale *et al.* (1970). Bakay and Lee (1968) subjected cats to prolonged hypoxia (3-5 hours) and studied the brain ultrastructure from electron micrographs. They reported no change in the capillary basement membrane which would indicate a change in capillary permeability. Recently, Goodale *et al.* (1970) perfused the isolated left canine lung and filled the alveoli with albumin -¹³¹I in Tyrode solution. They reported no change in the permeability of the alveolocapillary membrane during severe hypoxia

($P_aO_2 = 12$ mm Hg) as measured by the appearance rate of ^{131}I in the perfusion fluid.

Hypoxia appears to increase the permeability of the blood-CSF barrier to protein (Slobody *et al.*, 1957; Lending *et al.*, 1961). Radio-iodinated serum albumin (RISA; iv) appeared in the cisternal CSF of both immature (Lending *et al.*, 1961) and adult dogs (Slobody *et al.*, 1957; Lending *et al.*, 1961) more rapidly during hypoxia than during normoxia. In puppies but not adult dogs, hypercapnic hypoxia resulted in the faster appearance of RISA in cisternal CSF samples than when hypoxia alone was induced (Lending *et al.*, 1961), suggesting that age may affect the permeability of the blood-CSF barrier to protein during hypercapnic hypoxia. Bakay and Lee (1968) reported increased capillary permeability in the choroid plexus, which was indicated by increase in pinocytotic vesicles and a widening of the capillary basement membrane. The increased RISA permeability of the blood-CSF barrier during hypoxia may be due to increased membrane permeability in the choroid plexuses.

CSF is a secretion. Active transport mechanisms operate in its elaboration from blood, and metabolic energy is required (see section 2.2). Bering (1959) reported that \dot{V}_f in anesthetized dogs was correlated with cerebral oxygen consumption. The effects of ouabain on \dot{V}_f have been reviewed (see section 2.2) and suggest active transport of Na^+ and K^+ contribute to CSF formation. In both the

newborn (Holloway *et al.*, 1972) and adult dog (Michael *et al.*, 1972) \dot{V}_f determined by the ventriculocisternal perfusion technique, was reduced during hypoxia. This suggests that CSF formation is in part an aerobic metabolic process.

Recently, Michael *et al.* (1971) reported increases in both RISA and creatinine clearance from the perfused brain ventricular system of the rabbit during hypoxia and suggested that hypoxia increased the permeability of the CSF-blood and/or CSF-brain barrier(s).

III. STATEMENT OF PROBLEM

The purpose of the present study is to determine the flux rates and mode of transfer of glucose, lactate, and pyruvate from cerebrospinal fluid (CSF) of the anesthetized dog. The simultaneous fluxes of these molecules will be determined during both normoxia and hypoxia. Using a ventriculocisternal perfusion technique CSF concentrations of glucose, pyruvate, and lactate can be changed from their normal values and net transependymal flux rate (J_x) can be calculated. The simultaneous calculation of the transependymal outflux coefficient (K_o) for radioactively labelled glucose and lactate will define their efflux rate from the CSF. Both CSF formation (\dot{V}_f) and bulk absorption (\dot{V}_a) rates will be calculated under all experimental conditions, since their values must be known to estimate J_x and K_o .

IV. METHODS AND MATERIALS

4.1. General operative and cannulation procedures

Adult mongrel dogs (3-11 kg) of either sex obtained from Michigan State University Center for Laboratory Animal Resources (C.L.A.R.) were anesthetized with Dial and urethane solution (Appendix B; 0.6 ml/kg; ip) and tracheotomized. A diagram of the experimental equipment arrangement is shown in Figure 1. The animal's ventilation was controlled throughout the experiment by means of a positive pressure respirator (Model 607; Harvard Apparatus Co., Dover, Mass.) connected to a plastic "T" tube in the trachea; lung inflation was controlled by adjusting a clamp fitted on the side arm which was open to atmosphere. The respiratory pump was set to cycle 8-12 times/min with a stroke volume of 160-220 ml.

The femoral artery was cannulated (Figure 1) to collect anaerobic blood samples and to monitor arterial pressure with a pressure transducer (Model P23D; Grass Instruments, Quincy, Mass.) and a polygraph (Model 5P; Grass Instruments). The arterial pressure transducer was calibrated using a mercury manometer; the pressure response was linear over a range of 0 to 200 mm Hg. The cannula was

Figure 1. Diagram of the experimental animal and equipment. The anesthetized dog was placed in a prone position with the head secured in a stereotaxic frame (not shown). The tracheotomy tube was connected to a respirator which pumped either room-air (21% O₂; normoxia) or to a low O₂ mixture (5-8% O₂ in N₂; hypoxia). A femoral arterial cannula allowed monitoring of blood pressure via a pressure transducer connected to a polygraph as well as the collection of anaerobic blood samples for determining pH_a, P_aCO₂, P_aO₂ and plasma glucose, pyruvate, and lactate concentrations. A thermometer inserted (2-3 cm) beyond the rectal sphincter enabled the monitoring of body temperature (T_{re}). T_{re} was maintained ($\pm 0.3^{\circ}\text{C}$) by intermittent use of a heating pad on the dog's ventral surface and an infrared lamp (not shown) directed at the dorsal surface. Artificial CSF containing the test molecules (see 4.9) was pumped through the ventricular needle into the right lateral ventricle and collected from the cisternal cannula, which was connected to a drop recorder with an adjustable outflow height. Intraventricular pressure was monitored by a pressure transducer connected to a polygraph. The outflow height was adjusted to obtain a perfusion pressure of 2-4 cm H₂O.

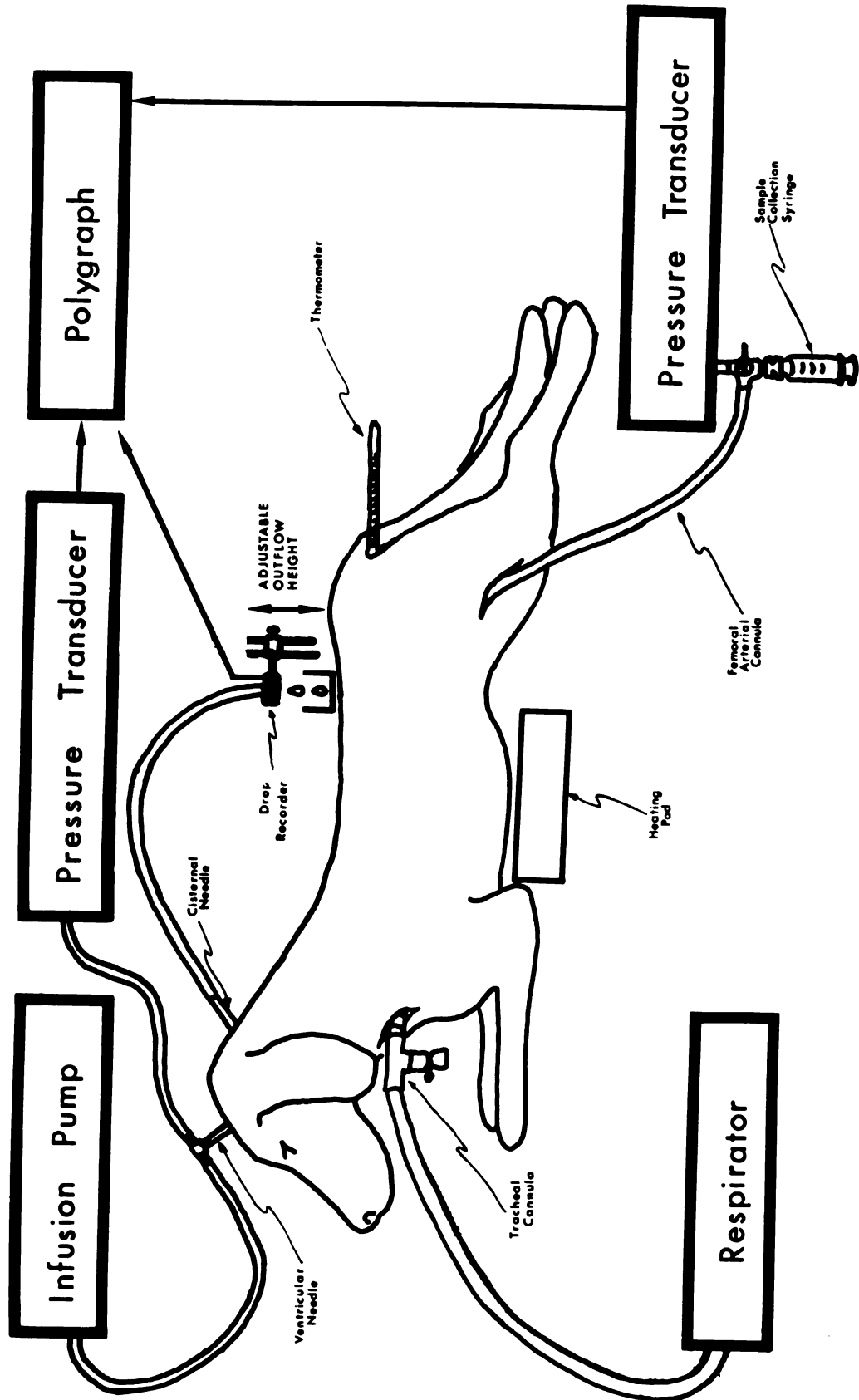


Figure 1

maintained patent by flushing with a heparin-NaCl solution (1 I.U. sodium heparin/ml 0.9% NaCl).

The animal was placed in a prone position and the head secured in a stereotaxic frame (Model 1504; David Kopf Instrument Co., Tujunga, Cal.) by a snout clamp and ear-bars inserted into the external auditory meatus. The stereotaxic frame was tilted 45° from the horizontal plane to elevate the animal's head and flex the neck, thereby maximizing the area between the atlas and the base of the skull. The skull and atlanto-occipital (A-O) membrane were exposed by means of a midline skin incision extending from the orbital sockets caudally to the 4th cervical vertebra, and muscle retraction with cauterization. A 6 mm diameter hole was trephined in the right parietal bone (5.0 mm lateral and 5.0 mm caudal from the intercept of the central saggital and coronal sutures) to expose the dura over the right cerebral hemisphere.

4.2. Brain ventricular and cisternal puncture

The ventricular probe needle (20 ga.; 2" length; short bevel) was placed in a micromanipulator electrode carrier (Model 1460; David Kopf Instrument Co.) and stereotaxically placed with the tip on the dura at a point 5.0 mm lateral and 5.0 mm caudal to the intercept of the central saggital and coronal sutures and perpendicular to the plane of the stereotaxic frame. Artificial cerebrospinal fluid, CSF, (Appendix A) was pumped from a 50 ml

disposable polyethylene syringe by an infusion pump (Model 975; Harvard Apparatus Co.) through a length of P.E. 50 tubing connected to a male needle adaptor on the ventricular probe needle (Figures 1 and 2). A second outlet on the adaptor was connected via P.E. 50 tubing to a low pressure (0-5 mm Hg) transducer (Model P23BC; Grass Instruments Co.), which enabled continuous monitoring of perfusion pressure. The transducer was calibrated using a water reservoir; output was linear over a range of 0 to 40 cm H₂O. The level of the external auditory meatus (i.e., stereotaxic ear bars; Figure 2) was defined as a point at which zero cm H₂O perfusion pressure would be measured. The perfusion pressure at ear-bar height was subtracted from the recorded experimental perfusion pressure to obtain the intraventricular pressure.

The perfusion pressure with the ventricular probe needle tip touching the dura was noted and the needle was lowered to puncture the dura. As the needle was lowered into brain tissue, perfusion pressure rose, and when the right lateral ventricle was punctured perfusion pressure dropped immediately to 10-20 cm H₂O, and cardiac and respiratory pulsations were evident in the pressure recording. The depth of the ventricular penetration ranged 0.6-1.1 cm below the dura.

The cisternal needle (20 ga.; 2" tube; short bevel), held bevel up in a micromanipulator (Model MM-3; Eric

Figure 2. Photograph of equipment used for ventriculocisternal perfusion in the anesthetized dog. The head of the dog was placed in a stereotaxic frame (A) and secured by a snout clamp (not shown) and ear bars (B). The ventricular probe needle (C), stereotaxically positioned in the right lateral ventricle by a standard stereotaxic electric holder (D), was connected to a syringe drive pump (not shown) and a pressure transducer (E) connected to a polygraph (not shown) for monitoring perfusion pressure. The neck muscles were sectioned and retracted and the outflow needle (F) positioned in the cisterna magna via micromanipulator (G). The outflow needle was connected to a photoelectric drop-counter (H) by means of P.E. tubing (I).

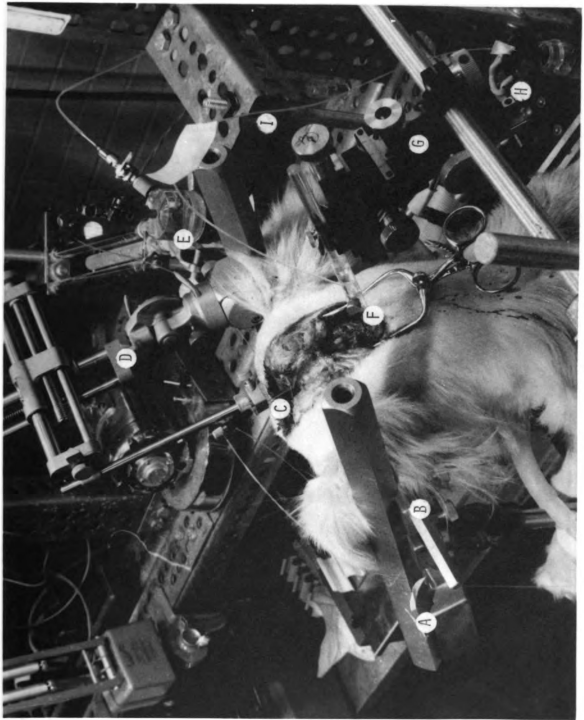


Figure 2

Sobotka Co., Inc., Farmingdale, N.Y.), was directed rostrally and positioned with the point on the A-O membrane at the midline, midway between the atlas and the base of the skull and in a plane parallel to the stereotaxic frame. A 50 cm length of P.E. 90 tubing was connected to the needle as the outflow cannula (Figures 1 and 2). The cisternal needle was lowered to puncture the A-O and dural membranes and movement of CSF into the outflow cannula and a further drop in perfusion pressure indicated a connection with the ventricular needle. The depth of the cisternal penetration ranged 0.3-0.6 cm below the A-O membrane. The outflow cannula was positioned in a photocell drop-counter (Model PTT1; Grass Instruments Co.) and the height of the drop counter adjusted to obtain a net intraventricular pressure of 2-4 cm H₂O.

4.3. Experimental perfusion with test molecules

After determining that the perfusion circuit had a steady outflow rate (\dot{V}_O), and a low, stable intraventricular pressure (4.2), a disposable syringe containing approximately 60 ml of artificial CSF and the dissolved test molecules (see section 4.9) was placed in the perfusion circuit. This interchange was accomplished by interchanging the inflow tubing from the respective syringes at the male needle adaptor. The introduction of air into the perfusion circuit was prevented by maintaining a hydrostatic head (approximately 40 cm H₂O) from the calibration reservoir through the

pressure transducer. After the inflow tubing interchange, the hydrostatic head was removed and if necessary, intraventricular pressure again set at 2-4 cm H₂O by adjusting the outflow height.

4.4. Experimental criteria

Data from experiments in which intraventricular pressure did not remain stable (i.e., varied by more than 2 cm H₂O) or where \dot{V}_O was highly variable within the experimental periods (4.9) were not used in this study. Blood in any CSF outflow sample precluded using that sample. Following the 240 minutes of the experimental perfusion, an artificial CSF (Appendix A) containing methylene blue was perfused for 60 minutes. The animal was killed by injecting 10 ml of a saturated KCl solution iv, after which the skull and brain were removed. Appearance of stain (methylene blue) was used to confirm needle placement; staining outside the ventriculocisternal system precluded using data from that specific experiment.

4.5. Sample collection and storage

Following flushing of cannula dead space four ml arterial blood samples were drawn in a heparinized syringe, and immediately centrifuged (1000 x g; 0°C; 10 minutes) in a refrigerated centrifuge (Model PR-2; International Equipment Co., Needham, Mass.). Plasma was decanted into vials,

capped, frozen, and stored at -20°C . CSF samples were collected into 20 gm vials, capped, weighed, frozen, and stored not longer than 40 hours at -20°C .

Anaerobic arterial blood samples (0.5-1.0 ml) were drawn in a heparinized syringe immediately after each 4 ml sample. The syringe was capped with a Hg-filled female syringe adaptor and kept in ice water (0°C) for a maximum of one hour prior to $P_a\text{O}_2$, $P_a\text{CO}_2$, and pH measurements (4.7).

4.6. Determination of normal CSF and plasma metabolic concentrations

CSF and plasma samples were obtained from 12 dogs by puncturing the dura over the cisterna magna (4.2) and allowing 1-2 ml of CSF to flow into a vial, while simultaneously obtaining a femoral arterial blood sample (4.1; 4.5). These samples were used to determine the normal concentrations of glucose, pyruvate, and lactate in CSF and plasma (4.8). The volume of CSF removed was replaced by 2-4 ml of artificial CSF (Appendix A) prior to the ventricular puncture (4.2).

4.7. Measurement of blood gas tensions and pH

$P_a\text{CO}_2$, $P_a\text{O}_2$ and arterial pH (4.5) were measured using thermostated (38°C) Types E5036, E5046, and E5021 Radiometer electrodes (The London Co., Westlake, Ohio), respectively, in conjunction with a Radiometer pH meter containing pH, PO_2 , and PCO_2 scales (Model PHM27; The London Co.). $P_a\text{CO}_2$ and $P_a\text{O}_2$ electrodes were calibrated using gas

mixtures verified by a Haldane-Bailey gas analyzer (Arthur H. Thomas, Philadelphia, Pa.). The O_2 mixtures were also used to calibrate the O_2 analyzer (Model C2; Beckman Instruments, Inc., Fullerton, Cal.) which enabled the rapid determination of the O_2 - N_2 mixtures used to induce hypoxia. The pH electrode was standardized with commercial buffers (pH = 6.84; pH = 7.384; Scientific Products Inc., Allen Park, Mich.) P_aO_2 , P_aCO_2 , and pH measurements were corrected to rectal temperature with a Radiometer Blood-Gas Calculator (The London Co.).

4.8. Measurement of inflow and outflow rates and concentrations

Inflow and outflow rates (\dot{V}_i and \dot{V}_o) were determined gravimetrically (± 0.1 mg; Mettler Instrument Corp., Highstown, N.J.) using tared vials referenced to sample time (± 0.1 min., Precision timer, Arthur H. Thomas). \dot{V}_i was determined by collecting fluid from the perfusion syringe at the beginning and at the conclusion of the experiment. For this study 1 mg of fluid was assumed to occupy a volume of 1 μ l. Inflow and outflow concentrations (c_i and c_o) of D-glucose (Appendix D), L-lactate (Appendix F), and inulin (Appendix G) were determined spectrophotometrically. Pyruvate concentrations were determined fluorometrically (Appendix E). 3H -glucose and ^{14}C -lactate were isolated (Appendices H and I) and their radioactivity counted using

standard liquid scintillation procedures (Appendix J). In some experiments ^3H -mannitol was used in lieu of ^3H -glucose, and the radioactivity counted using liquid scintillation procedures.

4.9. Experimental Design

Each experiment lasted 4 hours (Figure 3). Supplemental doses of Dial and urethane solution (0.4 ml/kg; ip) were administered at zero time and after 120 minutes of perfusion. Perfusion for 60 minutes prior to initial sampling enabled the outflow concentrations (c_o) of the test molecules (see below) to attain steady levels. Three 19-21 minute steady-state CSF outflow samples were obtained between 60-120 minutes of the experimental perfusion (P_1). Arterial blood samples were drawn midway in outflow sample collection (i.e., at 70, 90, and 110 minutes). Another 60 minute equilibration period was begun at 120 minutes and was followed by three 19-21 minute CSF outflow sample collection periods with their corresponding blood samples (P_2). In one series of experiments (4.9.1) the dogs were maintained normoxic ($P_a\text{O}_2 \geq 85$ mm Hg) during the 240 minutes of ventricular perfusion; in the other series (4.9.2) hypoxia ($P_a\text{O}_2 \leq 50$ mm Hg) was produced at 120 minutes by ventilating the animal with 5-8% O_2 in N_2 and continued through P_2 .

Figure 3. Diagram showing the time (abscissa; minutes) of experimental manipulations and sample collections. The dog was anesthetized (D_o) and surgical procedures performed. At time 0, ventricular perfusion was begun and continued for 240 minutes. Supplemental doses of anesthetic (D_s) were administered at 0 and 120 minutes of perfusion. Three 20 minute CSF outflow samples were collected between 60-120 minutes (P_1) and between 180-240 minutes (P_2). CSF outflow concentrations and perfusion outflow rates were determined from the CSF samples (4.8). Arterial blood samples (numbered arrows) were collected midway through each CSF outflow collection period, enabling the measurement of pH, PO_2 , PCO_2 and plasma concentrations of glucose, pyruvate, and lactate. In one series of experiments (4.9.1.) the dogs were maintained normoxic ($P_aO_2 > 85$ mm Hg) during the 240 minutes of ventricular perfusion. In the other series (4.9.2.) hypoxia ($P_aO_2 \leq 50$ mm Hg) was produced at 120 minutes and continued through P_2 by ventilating the animal with 5-8% O_2 in N_2 .

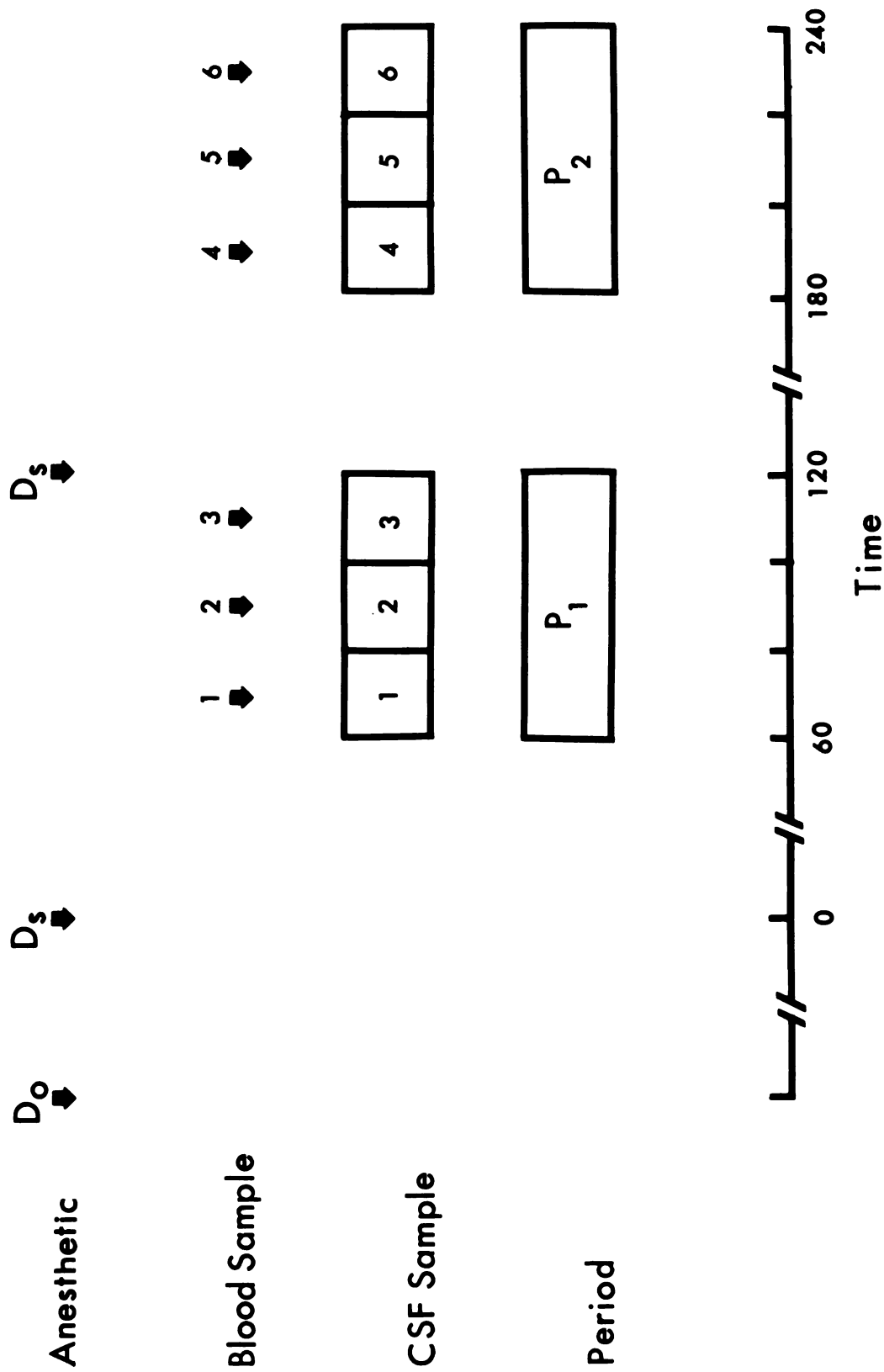


Figure 3

4.9.1 Long duration brain ventricular perfusions in normoxic dogs

All animals were ventilated with room air (normoxia; $P_aO_2 = 85 - 110$ mm Hg) for the entire 240 minutes (see Figure 3) of brain ventricular perfusion. These experiments were conducted: (a) to examine the effect of 4 hours of brain ventricular perfusion in normoxic animals on the bulk absorption rate (\dot{V}_a), CSF formation rate (\dot{V}_f), the transepithelial flux rates (K_o) of D-glucose and L-lactate, and the net flux rates (J_x) of D-glucose, pyruvate, and lactate, and (b) to examine the effects of blood and CSF concentrations of D-glucose, pyruvate, and lactate on their respective movements (i.e., flux rates) across membranes separating CSF from blood and/or brain.

4.9.1.1. Elevated blood and low CSF inflow concentrations

Glucose, pyruvate, and lactate flux into CSF was induced in 6 dogs by decreasing CSF inflow concentrations while blood concentrations were elevated for these metabolites. The perfusion fluid contained 1 mg/ml inulin, and trace quantities of 3H -glucose (0.5 μ C/ml; D-glucose-2- 3H ; New England Nuclear, Boston, Mass.) and ^{14}C -lactate (0.05 μ C/ml; Na-L-lactate-3- ^{14}C ; New England Nuclear). Inflow fluid osmolality was 307 ± 2 mOsmol/l. Blood glucose, pyruvate, and lactate concentrations were increased by injecting a priming dose (1 ml/kg) of 2.7 M D-glucose, 1.2 M Na-pyruvate, and 2.7 M Na-lactate into the brachial

vein, followed by a constant infusion (0.01 ml/min per kg) of a solution containing 8.9 M D-glucose, 25 mM Na-pyruvate, and 4.4 M Na-lactate pumped by a syringe drive pump (Model 975; Harvard Apparatus Co.).

4.9.1.2. Normal CSF inflow concentrations

In 4 dogs the perfusion fluid contained normal CSF concentrations of D-glucose, pyruvate, and lactate; no attempt was made to alter blood concentrations for these metabolites. The perfusion fluid contained 1 mg/ml inulin, 4.3-4.7 mM D-glucose, 0.09-0.19 mM Na-pyruvate, 1.2-1.7 mM Na-lactate, and trace quantities of ^3H -glucose (0.5 $\mu\text{c}/\text{ml}$; D-glucose-2- ^3H ; New England Nuclear) and ^{14}C -lactate (0.05 $\mu\text{c}/\text{ml}$; Na-L-lactate-3- ^{14}C ; New England Nuclear). The NaCl concentration in the artificial CSF (Appendix A) was decreased from 141.2 mEq/l to 133.0 mEq/l to adjust perfusion fluid osmolality to 307 ± 2 mOsmol/l.

4.9.1.3. Elevated CSF inflow concentrations

In 5 dogs D-glucose, pyruvate, and lactate concentrations in the perfusion fluid were increased to 2-6 times that of normal CSF concentrations. No attempt was made to alter blood concentrations of glucose, pyruvate, or lactate. The perfusion fluid contained 1 mg/ml inulin, 15.7-17.9 mM D-glucose, 0.28-0.33 mM Na-pyruvate, 4.3-5.9 mM Na-lactate, and trace quantities of ^3H -glucose (0.5 $\mu\text{c}/\text{ml}$; D-glucose-2- ^3H ; New England Nuclear) and ^{14}C -lactate (0.05 $\mu\text{c}/\text{ml}$;

Na-L-lactate-3-¹⁴C; New England Nuclear). NaCl concentration in artificial CSF (Appendix A) was decreased to 114.4 mEq/l to obtain a perfusion fluid osmolality of 309 ± 3 mOsmol/l.

4.9.2. Brain ventricular perfusion during normoxia and hypoxia

These experiments were designed to examine the effects of hypoxia on: bulk absorption rate (\dot{V}_a), CSF formation rate (\dot{V}_f), the transependymal outflux rates (K_o) of glucose and lactate, and the net transependymal flux rates (J_x) of glucose, pyruvate, and lactate at low and high CSF concentrations for these metabolites. Dogs were ventilated with room air (normoxia; $P_aO_2 = 85 - 110$ mm Hg) during P_1 (see Figure 3). After 120 minutes of perfusion hypoxia ($P_aO_2 \leq 50$ mm Hg) was induced by connecting the respirator to a 150 liter Douglas bag (Warren E. Collins, Inc., Boston, Mass.) filled from a high pressure gas cylinder which contained 5-8% O_2 in N_2 . Hypoxia was maintained through P_2 .

Since both glucose and lactate K_o 's reported for experiments described in 4.9.1 appeared to exhibit saturation kinetics (indicating the presence of carrier-mediated transport from CSF), ³H-mannitol (considered to be a passively diffusing molecule; Prockop, 1969; Bronsted, 1970a; Bierer, 1972), was included in the perfusion fluid in lieu of ³H-glucose in some experiments. Comparison of mannitol K_o 's at low and high CSF mannitol concentrations with those

of lactate would provide evidence regarding a saturable lactate carrier (Stein, 1967).

4.9.2.1. Low CSF inflow concentrations

In 3 dogs glucose, pyruvate, and lactate flux into CSF was induced by decreasing CSF concentrations for these metabolites. No attempt was made to alter blood concentrations of glucose, pyruvate, and lactate. The perfusion fluid contained 1 mg/ml inulin, and trace quantities of ^3H -glucose (0.5 $\mu\text{C}/\text{ml}$; D-glucose-2- ^3H ; New England Nuclear) and ^{14}C -lactate (0.05 $\mu\text{C}/\text{ml}$; Na-L-lactate-3- ^{14}C ; New England Nuclear). Perfusate osmolality was 306 ± 2 mOsmols/l.

4.9.2.2. Elevated CSF inflow concentrations

In 3 dogs glucose, pyruvate, and lactate concentrations were increased 2-5 times that of their normal CSF concentrations; no attempt was made to alter blood metabolite concentrations. The perfusion fluid contained 1 mg/ml inulin, 11.1-11.2 mM D-glucose, 0.22-0.24 mM Na-pyruvate, 3.7-4.4 mM Na-lactate, and trace quantities of ^3H -glucose (0.5 $\mu\text{C}/\text{ml}$; D-glucose-2- ^3H ; New England Nuclear) and ^{14}C -lactate (0.05 $\mu\text{C}/\text{ml}$; Na-L-lactate-3- ^{14}C ; New England Nuclear). NaCl concentration in artificial CSF (Appendix A) was decreased to 114.4 mEq/l to obtain a perfusion fluid osmolality of 304 ± 2 mOsmol/l.

4.9.2.3. Low CSF inflow concentrations with mannitol

In 3 dogs glucose, pyruvate, and lactate flux was induced by decreasing CSF concentrations for these metabolites; no attempt was made to alter blood concentrations of these metabolites. Trace quantities of ^3H -mannitol were included in the perfusion fluid in lieu of ^3H -glucose to allow the calculation of mannitol K_o at low CSF inflow concentrations. The perfusion fluid contained 1 mg/ml inulin, and trace quantities of ^3H -mannitol (0.5 $\mu\text{C}/\text{ml}$; D-mannitol-1- ^3H ; New England Nuclear) and ^{14}C -lactate (0.05 $\mu\text{C}/\text{ml}$; Na-L-lactate-3- ^{14}C ; New England Nuclear). Perfusion fluid osmolality was 305 ± 2 mOsmol/l.

4.9.2.4. Elevated CSF inflow concentrations with mannitol

In 3 dogs pyruvate and lactate concentrations in the CSF perfusion fluid were 2-6 times their normal CSF concentrations and CSF glucose concentration was 0 mM to induce glucose influx. D-mannitol concentration in the perfusion fluid was increased in an attempt to demonstrate saturation of mannitol K_o . No attempt was made to alter blood glucose, pyruvate, or lactate concentrations. The perfusion fluid contained 1 mg/ml inulin, 16.0-16.5 mM D-mannitol, 0.26-0.28 mM Na-pyruvate, 4.0-5.8 mM Na-lactate, and trace quantities of ^3H mannitol (0.5 $\mu\text{C}/\text{ml}$; D-mannitol-1- ^3H ; New England Nuclear) and ^{14}C -lactate (0.05 $\mu\text{C}/\text{ml}$; Na-L-lactate-3- ^{14}C ; New England Nuclear). NaCl concentration

in artificial CSF (Appendix A) was decreased to 114.4 mEq/l to obtain a perfusion fluid osmolality of 309 ± 3 mOsmol/l.

4.10 Principles and calculations

Principles and equations used in the calculation of bulk absorption rate, CSF formation rate, net flux rate, and the transepithelial outflux rate have been previously described (Pappenheimer *et al.*, 1961; Heisey *et al.*, 1962; Pappenheimer *et al.*, 1965) and are presented below.

4.10.1. Definition of symbols

\dot{V} = flow rate ($\mu\text{l}/\text{min}$).

i,o,p = subscripts referring to inflow, outflow, and plasma respectively.

f,a = subscripts referring to formation and bulk absorption of fluid.

c = concentration (quantity/ μl).

\bar{c} = estimated mean concentration in the ventricular system.

$$= \frac{c_i - c_o}{\ln c_i / c_o} \quad (\text{quantity}/\mu\text{l})$$

when $c_i = 0$, the function above is undefined

and \bar{c} was estimated by: $\bar{c} = c_o + 0.37 (c_i - c_o)$

(Pappenheimer *et al.*, 1961).

\dot{n}_x = steady state movement of any substance, x, from or into CSF perfusion.

$$= \dot{V}_i c_i - \dot{V}_o c_o \quad (\text{quantity}/\text{min}).$$

C_x = clearance of x.

$$= \dot{n}_x / c \quad (\mu\text{l}/\text{min}).$$

c may be \bar{c} or c_o depending on whether the substance is cleared from ventricular fluid or from fluid reabsorbed distal to the fourth ventricle.

4.10.2. Fluid balance

In the perfused brain ventricular system, fluid is added to the system by the perfusion syringe (inflow fluid; \dot{V}_i) and by the amount of CSF formed by the animal (\dot{V}_f). Fluid is lost from the perfusion system via the outflow cannula (outflow fluid; \dot{V}_o), and by the amount of fluid absorbed in bulk through large exit routes such as the arachnoid villi (\dot{V}_a). In the steady-state the total fluid inflow equals the total fluid outflow. In summary:

$$\dot{V}_i + \dot{V}_f = \dot{V}_o + \dot{V}_a \quad (\text{Eq. 1})$$

4.10.3. Bulk absorption rate, \dot{V}_a

Heisey *et al.* (1962) reported that diffusion of the polysaccharide inulin (In) from the ventricular system into brain tissue was insignificant; the inulin lost from CSF could be accounted for by bulk absorption distal to the fourth ventricle. Inulin is removed from the subarachnoid spaces by bulk absorption at a rate which varies linearly

and directly with CSF hydrostatic perfusion pressure (Heisey *et al.*, 1962, Bering and Sato, 1963). Bulk absorption can then be expressed as:

$$\dot{V}_a = \frac{\dot{V}_i c_i - \dot{V}_o c_o}{c_o} = \text{clearance of inulin, } C_{In} \quad (\text{Eq. 2})$$

where c 's are inulin concentrations.

4.10.4. CSF formation rate, \dot{V}_f

CSF formation rate, \dot{V}_f , can be estimated by substituting equation 2 in equation 1 to obtain:

$$\dot{V}_f = \dot{V}_o - \dot{V}_i + C_{In} \quad (\text{Eq. 3})$$

4.10.5 Derivation of net flux, J_x

Ions or metabolites can enter the ventricular system in freshly formed CSF or by exchange (active or passive) with blood or brain through tissues lining the ventricular system (transependymal exchange). Similarly, ions or metabolites can leave the ventricular system by absorption in bulk from the subarachnoid spaces or by transependymal exchange. Under the experimental conditions of ventriculocisternal perfusion, substances can also enter or leave the ventricles with the perfusion inflow and outflow fluids. The net transependymal flux rate (J_x , $\mu\text{moles/min}$) of any molecule, x , during the steady-state is

$$J_x = \dot{V}_i c_i - \dot{V}_o c_o + \dot{V}_f c_f - \dot{V}_a c_o \quad (\text{Eq. 4})$$

Substituting equations 2 and 4 in equation 5 and rearranging terms:

$$J_x = \dot{V}_i (c_i - c_f) - (\dot{V}_o + C_{In}) (c_o - c_f) \quad (\text{Eq. 5})$$

All quantities except c_f are measureable; c_f must be estimated.

4.10.6. Derivation of transependymal outflux coefficient, K_o

In the case where a test molecule not present in either plasma or CSF is added to the perfusion fluid, c_p and c_f are zero and equation 6 reduces to

$$J_x = \dot{V}_i c_i - (\dot{V}_o + C_{In}) c_o \quad (\text{Eq. 6})$$

J_x in equation 6 is an outflux, J_{x_o} . J_{x_o} is determined by the characteristics of the transependymal membranes limiting the movement of the test molecule from the ventricular system (outflux coefficient, K_o) and the ventricular concentration of the test molecule, \bar{c} .

$$J_{x_o} = K_o \bar{c} \quad (\text{Eq. 7})$$

Substituting equation 7 into 6 and rearranging

$$K_o = \frac{\dot{V}_i c_i - (\dot{V}_o + C_{In}) c_o}{\bar{c}} \quad (\text{Eq. 8})$$

For test substances normally present in plasma or brain, K_o , may be determined using equation 8 if an isotope of the test substance is added to the perfusate.

4.11. Calculated parameters

Bulk absorption (\dot{V}_a) was estimated by inulin clearance (C_{In} ; Equation 2); CSF formation rate (\dot{V}_f) was calculated using Equation 3. The net flux (J_x) for glucose (g), pyruvate (py) and lactate (l) were calculated using equation 5 and the chemical concentrations for these metabolites (4.8). The calculation of J_g' ; the glucose concentration in newly formed CSF (c_f) was assumed to be 0.6 that of the plasma concentration (c_p) (Welch *et al.*, 1970); for the calculation of J_g , c_f was assumed = 0. For the calculation of both J_l and J_{py} , c_f was assumed to be zero; for J_l' and J_{py}' , c_f was assumed equal to c_p . The transepithelial outflux coefficient (K_o) for glucose, lactate, and mannitol was calculated using equation 8 and radioactively labelled molecules.

4.12. Statistical methods

Individual means (\bar{x}) were calculated for each parameter (4.11) from 3 values obtained during each period of an experiment (4.9). In some instances the grand means (\bar{X}) and the standard error of the grand mean (S.E.) was calculated (Appendix K) for all individual \bar{x} during a given perfusion period at a given inflow concentration (4.9).

Data was analyzed for significant differences using a split-plot design analysis of variance (AOV, see Appendix K) and critical values for Student's t distribution ($P < 0.05$).

V. RESULTS

5.1. Arterial pH, PO₂, PCO₂ and rectal temperature

Prefatory studies indicated that body temperature, P_aCO₂ and anesthesia affect CSF production and molecular flux from CSF, possibly related to effects on cerebral blood flow and/or cerebral metabolism. In the present study changes in rectal temperature (T_{re}) were minimized by intermittent external heating and those in P_aCO₂ by artificially ventilating the dogs at a constant rate and depth (see section 4.1). Anesthetic was administered at the same time during experiments to minimize its variability as an operant factor.

Ventriculocisternal perfusions were performed on 27 dogs. Fifteen were ventilated with room-air (normoxia); 12 were normoxic only for the initial 2 hours and were then ventilated with 5-8% O₂ in N₂ (hypoxia) for the remaining 2 hours (see section 4.9). Mean values of pH_a, P_aCO₂, P_aO₂, and T_{re} for each dog were calculated from 3 measurements between 60-120 minutes (P₁) and between 180-240 minutes (P₂) of the perfusion (Figure 3; section 4.12). Data reporting mean pH_a, P_aCO₂, P_aO₂, and T_{re} for all normoxic and hypoxic dogs are summarized in Table 1. T_{re} (approximately 38°C)

and $P_a\text{CO}_2$ (approximately 38 mm Hg) were considered to be normal in both normoxic and hypoxic dogs. There was no difference ($p > 0.05$) in $P_a\text{O}_2$ among normoxic perfusion periods (A- P_1 and P_2 ; B- P_1) and $P_a\text{O}_2$ was decreased ($p < 0.05$) during hypoxia (B- P_2) producing normocapnic hypoxia. Arterial pH was not different ($p > 0.05$) among normoxic perfusion periods. During hypoxia, pH_a decreased ($p < 0.05$), suggesting the release of metabolic acids from hypoxic tissue into the blood.

5.2. Cerebrospinal fluid bulk absorption and formation rates

Data for CSF bulk absorption rate (\dot{V}_a) and formation rate (\dot{V}_f) in normoxic and hypoxic dogs during brain ventricular perfusions are summarized in Table 2. \dot{V}_a during the initial 2 hours of perfusion (P_1 ; Conditions A and B) was the same. \dot{V}_a increased similarly ($p < 0.05$) during P_2 in both normoxic and hypoxic dogs. \dot{V}_f decreased ($p < 0.05$) during P_2 in both normoxic (Condition A) and hypoxic (Condition B) dogs.

5.3. Normal plasma and CSF concentrations of glucose, pyruvate, and lactate

Table 3 contains data for D-glucose, pyruvate, and L-lactate concentrations in arterial plasma and cisternal CSF samples obtained simultaneously from normoxic dogs prior to ventriculocisternal perfusion. Plasma glucose concentration was greater ($p < 0.05$) than CSF glucose concentration.

The plasma and CSF concentrations of either lactate or pyruvate were not different ($p > 0.05$).

5.4. Glucose flux from CSF

The effect of different D-glucose concentrations in the perfusion inflow fluid (c_i) and plasma (c_p) on outflow concentrations (c_o) is shown by data summarized in Table 4. When c_i was less than c_p (i.e., $c_i = 0.0$ and 4.5 mM), c_o exceeded c_i , indicating that glucose moved into the perfusion fluid. At elevated c_i (i.e., 16.9 and 11.1 mM), c_i exceeded c_o showing that glucose moved out of the perfusion fluid. In one group of dogs (Condition A; $c_i = 0.0$ mM) both c_o and c_p were less ($p < 0.05$) during P_2 compared with P_1 , suggesting that alterations in c_p affected c_o .

In 5 dogs (Condition A), elevation of glucose c_i resulted in a glucose extraction from the perfusion fluid of 35% (percent extraction = $100 (c_i - c_o)/c_i$) during both P_1 and P_2 . In 3 dogs with elevated c_i (Condition B), glucose extraction was increased during P_2 to twice the P_1 value. These data suggest an increase in transependymal outflux during hypoxia possibly due to increased glycolysis in brain tissue.

Glucose K_o 's when glucose c_i 's were low (c_1), normal (c_2) and elevated (c_3 , c_4) are summarized in Table 5. K_o was independent of time at all c_i 's under normoxic conditions (A- P_1 and P_2). K_o at c_1 was greater ($p < 0.05$) than

at either c_2 , c_3 , or c_4 , and K_O 's at c_2 , c_3 , and c_4 were not different ($p > 0.05$) from each other during normoxia (A-P₁ and P₂; B-P₁). Hypoxia reduced ($p < 0.05$) K_O at both low and elevated c_i 's, suggesting that hypoxia may affect metabolic processes responsible for glucose movement from CSF.

Net glucose transependymal flux rates, summarized in Table 5, were calculated assuming that $c_f = 0.0$ mM (J_g) and that $c_f = 0.6 c_p$ (J'_g ; Welch *et al.*, 1970). The difference between J_g and J'_g at comparable c_i 's represents glucose influx which could be attributed to that entering in CSF produced by the animal and is a function of \dot{V}_f (which was measured) and c_f (which could not be measured). Since J_g and J'_g represent glucose movement only by diffusion or carrier-mediated transport, a glucose influx will be larger when c_f is assumed equal to 0.0 mM (J_g) than when $c_f = 0.6 c_p$. Both J_g and J'_g were highly variable among dogs, but were constant during normoxia in individual animals. When perfusion inflow concentrations were low (c_1) or normal (c_2) glucose net flux rates were negative indicating a net flux into CSF. At elevated c_i (c_3 , c_4), both J_g and J'_g were positive, indicating a net glucose outflux. These data corroborate the changes in glucose concentration. There was no change ($p > 0.05$) in J'_g with time during normoxia (i.e., A-P₁ and P₂). The change ($p < 0.05$) in J_g at c_1 cannot be explained. In condition B-P₁ at c_1 and c_4 glucose

flux (J_g and J'_g) was less than that in A-P (c_1 and c_3 , respectively) and probably reflect different c_i 's and c_p 's in the two conditions (see Table 4). During hypoxia (B-P₂) there was an increase ($p < 0.05$) in net glucose influx at c_1 . Glucose (J_g and J'_g) at c_4 did not increase ($p > 0.05$) during hypoxia even though glucose extraction from the perfusion fluid doubled (Table 4). Changes in J_g were similar to those of J'_g except that flux rates did not change ($p > 0.05$) during hypoxia at c_1 .

5.5. Lactate flux from CSF

Data reporting the effect of different L-lactate c_i 's and c_p 's on c_o are summarized in Table 6. At low (0.0 mM) and normal (1.5 mM) c_i 's, c_o always exceeded c_i indicating lactate movement into CSF from blood or brain. At low and normal c_i 's, c_o increased ($p < 0.05$) with time although c_p did not change ($p > 0.05$), suggesting that the lactate came from brain. During hypoxia, at low c_i 's, c_o also increased ($p < 0.05$) but was accompanied by an increase ($p < 0.05$) in c_p .

At elevated c_i 's (5.2 and 4.5 mM), c_o was the same as c_i during normoxia (A-P₁ and P₂) and always exceeded c_p . These data indicate that lactate movement from CSF is slow. During hypoxia (B-P₂), both c_o and c_p increased ($p < 0.05$), but the increase in c_o could result from lactate diffusion from plasma.

Lactate K_O (^{14}C -lactate) at low (c_1), normal (c_2), and elevated (c_3 , c_4) c_i 's are summarized in Table 7. During normoxia K_O values did not change ($p > 0.05$) with time (A- P_1 and P_2). K_O at c_1 was greater ($p < 0.05$) than at either c_2 or c_3 and the K_O 's at c_2 and c_3 were not different ($p > 0.05$). During hypoxia (B- P_2) K_O decreased ($p < 0.05$) at c_1 , but did not change ($p > 0.05$) at c_4 .

The net lactate transependymal flux rates, reflected by data reported in Table 7, were calculated: assuming $c_f = 0.0$ mM (J_1) and $c_f = c_p$ (J_1'). The difference between J_1 and J_1' at comparable c_i 's (range = 80-230 nmoles/min) represents the maximum effect which changes in plasma lactate concentration and/or \dot{V}_f could have on net lactate flux. The first assumption may be more nearly correct since data in Table 6 suggest that CSF lactate concentration is independent of that in plasma. J_1 and J_1' were negative at all c_i 's indicating a net transependymal influx of lactate. During P_1 (Condition A) lactate influx at c_1 was greater ($p < 0.05$) than at either c_2 or c_3 , while there was no difference ($p > 0.05$) between net influx at c_2 and c_3 . During normoxia, net lactate influx increased ($p < 0.05$) with time at all c_i 's. Since c_p was unchanged (Table 6), this suggests lactate movement from brain during P_2 . At c_1 , lactate influx was greater ($p < 0.05$) during A- P_1 than during B- P_1 . During A- P_1 , plasma glucose, pyruvate, and lactate were increased (section 4.9.1.1) and may have increased brain

lactate production. At c_3 and c_4 blood metabolite concentrations were not elevated and lactate influx in these dogs were not different ($p > 0.05$). Lactate diffusion from plasma cannot explain net lactate influx, since at c_3 and c_4 , during P_1 , c_i exceeds c_p (Table 6). During hypoxia ($B-P_2$), net lactate influx was greater than during $B-P_1$ ($p < 0.05$) at both c_1 and c_4 and the increase at c_4 was greater ($p < 0.05$) than the increase during normoxia ($A-P_2$; c_3).

5.6. Mannitol flux from CSF

Both glucose and lactate K_o 's appear to demonstrate saturation kinetics (Tables 5 and 7) suggesting carrier-mediated transport for these materials from CSF. 3H -mannitol, considered to be a passively diffusing molecule (Prockop, 1968; Bronsted, 1970a; Bierer, 1972), was included in the perfusion fluid in lieu of 3H -glucose (sections 4.9.2.3 and 4.9.2.4). D-mannitol K_o 's at low (c_1) and elevated (c_2) c_i 's are summarized in Table 8. During normoxia (P_1) and hypoxia (P_2), K_o was independent of concentration, supporting the hypothesis that D-mannitol leaves the CSF only by bulk absorption and simple diffusion (Prockop, 1968; Bronsted, 1970a; Bierer, 1972). K_o 's for mannitol, unlike those for glucose and lactate (Tables 5 and 7), were not different ($p > 0.05$) during hypoxia.

5.7. Pyruvate flux from CSF

The effects of pyruvate c_i and c_p on c_o are shown by data reported in Table 9. Neither time (Condition A) nor hypoxia (Condition B) affected c_o . When c_p was elevated (Condition A; $c_i = 0.00$ mM), c_o reflected c_p and was higher than when c_p was normal (Condition B; $c_i = 0.00$ mM), indicating pyruvate may diffuse from plasma into CSF. When c_i was normal (0.12 mM) or elevated (0.24 and 0.29 mM), c_o was the same as c_i and always greater ($p < 0.05$) than c_p . These data indicate that pyruvate moves into more readily than it moves out of the CSF.

The net pyruvate transependymal flux rates, summarized through data reported in Table 10, were calculated: assuming $c_f = 0.00$ mM (J_{py}) and that $c_f = c_p$ (J'_{py}). The difference between J_{py} and J'_{py} at comparable c_i 's (range = 2-12 nmoles/min) represents the maximum effect which changes in c_f and/or \dot{V}_f could have on net pyruvate flux. Net pyruvate flux (J_{py} and J'_{py}) was negative at all c_i 's indicating a net transependymal influx. Net influx was not different ($p > 0.05$) during P_2 at any c_i , and indicates that neither time (A- P_1 and P_2) nor hypoxia (B- P_2) affected pyruvate influx. During A- P_1 , net influx at low c_i (c_1) was greater ($p < 0.05$) than at either normal (c_2) or elevated (c_3) c_i 's. There was no difference ($p > 0.05$) in net influx at c_2 and c_3 . The greater ($p < 0.05$) net influx of pyruvate at c_1 in A- P_1 when compared with B- P_1 could be due to the elevated c_p in the former (see Table 9).

Table 1. Arterial pH, PO₂, and PCO₂ and rectal temperature (T_{re}) in normoxic and hypoxic dogs during brain ventricular perfusion

Condition	pH _a	P _a O ₂ (mm Hg)	P _a CO ₂ (mm Hg)	T _{re} (°C)
A. Long Duration Normoxia				
P ₁				
$\bar{X} \pm SE$	7.34 ± 0.02 (15)	100 ± 2 (15)	38 ± 1 (15)	38.4 ± 0.3 (15)
P ₂				
$\bar{X} \pm SE$	7.33 ± 0.02	100 ± 2	38 ± 1	38.6 ± 0.3
$\Delta\bar{x} \pm SE$	-0.01 ± 0.01	-1 ± 1	0 ± 1	0.1 ± 0.1
B. Normoxia-Hypoxia				
P ₁				
$\bar{X} \pm SE$	7.35 ± 0.02 (12)	97 ± 1 (12)	38 ± 1 (12)	38.0 ± 0.3 (12)
P ₂				
$\bar{X} \pm SE$	7.27 ± 0.03	39 ± 2	37 ± 1	38.1 ± 0.3
$\Delta\bar{x} \pm SE$	-0.08 ± 0.01*	58 ± 1*	-1 ± 1	0.1 ± 0.0

Number of dogs in parentheses.

* $p < 0.05$; $P_1 \neq P_2$.

Table 2. Bulk absorption rate (\dot{V}_a) and CSF formation rate (\dot{V}_f) in normoxic and hypoxic dogs during brain ventriculation perfusion

Condition	\dot{V}_a ($\mu\text{l}/\text{min}$)	\dot{V}_f ($\mu\text{l}/\text{min}$)
A. Long Duration		
Normoxia		
P_1 $\bar{X} \pm \text{SE}$	24 ± 2 (15)	52 ± 4 (15)
P_2 $\bar{X} \pm \text{SE}$	30 ± 3	45 ± 3
$\Delta\bar{X} \pm \text{SE}$	$6 \pm 2^*$	$-7 \pm 2^*$
B. Normoxia-Hypoxia		
P_1 $\bar{X} \pm \text{SE}$	23 ± 3 (12)	45 ± 3 (12)
P_2 $\bar{X} \pm \text{SE}$	32 ± 5	$30 \pm 4^*$
$\Delta\bar{X} \pm \text{SE}$	$9 \pm 3^*$	$-15 \pm 4^{*\dagger}$

Number of dogs in parentheses.

* $p < 0.05$; $P_1 \neq P_2$.

$^\dagger p < 0.05$; A \neq B.

Table 3. Glucose, lactate, and pyruvate concentrations in simultaneously obtained samples from arterial plasma and cisternal cerebrospinal fluid (CSF) in twelve anesthetized dogs

Sample	Glucose (mM)	Lactate (mM)	Pyruvate (mM)
Plasma	7.0 ± 0.8	1.6 ± 0.3	0.12 ± 0.02
CSF	$5.0 \pm 0.2^*$	2.0 ± 0.4	0.13 ± 0.01

Data expressed as mean \pm SE.

* $p < 0.05$, plasma \neq CSF.

Table 4. D-glucose concentration in the inflow fluid (c_i), outflow fluid (c_o), and arterial plasma (c_p) in normoxic and hypoxic dogs during brain ventricular perfusion

Condition	D-Glucose Concentration mM					
	c_i	c_o	c_p	c_i	c_o	c_p
A. Long Duration Normoxia						
P_1	(6)	(6)	(6)	(4)	(4)	(5)
$\bar{X} \pm SE$	0.0	3.4 ± 0.6	$11.4 \pm 1.0^{\dagger}$	4.5 ± 0.2	6.3 ± 1.2	11.1 ± 1.3
P_2						
$\bar{X} \pm SE$		2.8 ± 0.6	$9.2 \pm 0.5^{\dagger}$		6.5 ± 1.5	11.0 ± 1.6
$\Delta X \pm SE$		$-0.6 \pm 0.2^*$	$2.2 \pm 0.8^*$		0.2 ± 0.3	-0.1 ± 0.5
B. Normoxia-Hypoxia						
P_1	(9)	(9)	(9)	(3)	(3)	(3)
$\bar{X} \pm SE$	0.0	2.0 ± 0.2	8.8 ± 0.5	11.1 ± 0.1	9.6 ± 0.4	5.9 ± 0.2
P_2						
$\bar{X} \pm SE$		2.8 ± 0.5	9.1 ± 1.2		8.0 ± 1.2	5.7 ± 0.4
$\bar{X} \pm SE$		0.7 ± 0.4	0.3 ± 1.1		-1.6 ± 1.2	-0.2 ± 0.6

Number of dogs in parentheses.

* $p < 0.05$; $P_1 \neq P_2$.

$^{\dagger}c_p$ elevated by iv infusion (see section 4.9.1.1).

Table 5. Glucose transepndymal outflux coefficient (K_O) and net flux rate (J_g ; J'_g) at low (c_1), normal (c_2) and elevated (c_3 ; c_4) perfusion inflow concentrations in normoxic and hypoxic dogs during brain ventricular perfusions

Condition	K _O (μl/min)			J _g (nmoles/min)			J' _g (nmoles/min)		
	c ₁	c ₂	c ₃	c ₁	c ₂	c ₃	c ₁	c ₂	c ₃
A. Long Duration Normoxia									
	(6)	(4)	(5)	(6)	(4)	(5)	(6)	(4)	(5)
	138±14	84±1 [†]	87±16 [†]	-820±150	-650±310	510±100 [†]	-470±220	-340±220	750±110 [†]
	141±12	84±3 [†]	84±17 [†]	-650±40	-630±360	570±160 [†]	-410±130	-380±270	830±180 [†]
	3±5	0±2	-3±4	170±50*	20±50	60±120	60±40	-40±60	80±110
	c ₁	c ₂	c ₄	c ₁	c ₄	c ₁	c ₄		
B. Normoxia-Hypoxia									
	(9)	(3)	(3)	(9)	(3)	(3)	(9)	(3)	(3)
	149±12	53±9 [†]	70±20 [†]	-500±30	460±290 [†]	-220±50	110±50 [†]	520±240 [†]	410±230
	113±4	35±10 [†]	390±230	-630±140	460±290 [†]	-430±100	520±240 [†]	410±230	
	36±13*	18±3*	130±90	390±230	390±230	-210±70*	410±230		

Number of dogs in parentheses.

c_1 , c_2 , c_3 , c_4 = inflow D-glucose concentration referring to 0.0, 4.5 \pm 0.2, 16.9 \pm 1.0, and 11.1 \pm 0.1 mM, respectively.

* $p < 0.05$; $P_1 \neq P_2$.

$^\dagger p < 0.05$; K_O ; J_g , J'_g at $c_1 \neq c_2$, c_3 , or c_4 .

Table 6. L-lactate concentration in the inflow fluid (c_i), outflow fluid (c_o), and arterial plasma (c_p) in normoxic and hypoxic dogs during brain ventricular perfusion

Condition	L-Lactate Concentration mM					
	c_i	c_o	c_p	c_i	c_o	c_p
A. Long Duration Normoxia	P_1	(6)	(6)	(4)	(4)	(5)
	$\bar{X} \pm SE$	0.0	2.1 \pm 0.2	1.5 \pm 0.2	2.0 \pm 0.1	2.2 \pm 0.3
			3.9 \pm 0.6 [†]			5.2 \pm 0.4
P_2						(5)
	$\bar{X} \pm SE$	2.5 \pm 0.3	2.6 \pm 0.3 [†]	3.0 \pm 0.2	2.4 \pm 0.1	5.3 \pm 0.2
	$\Delta\bar{X} \pm SE$	0.4 \pm 0.1*	-1.3 \pm 0.6	1.0 \pm 0.2*	0.3 \pm 0.2	0.6 \pm 0.3
B. Normoxia- Hypoxia	P_1	(6)	(6)			(6)
	$\bar{X} \pm SE$	0.0	1.5 \pm 0.2			4.5 \pm 0.3
			3.5 \pm 0.5			4.2 \pm 0.3
P_2						(6)
	$\bar{X} \pm SE$	2.7 \pm 0.2	6.9 \pm 1.1			5.8 \pm 0.4
	$\Delta\bar{X} \pm SE$	1.2 \pm 0.1*	3.4 \pm 1.1*			1.6 \pm 0.2*
Number of dogs in parentheses						

* $p < 0.05$; $P_1 \neq P_2$.

[†] c_p elevated by iv infusion (see section 4.9.1.1).

Table 7. Lactate transepndymal outflux coefficient (K_O) and net flux rate (J_1 ; J_1') at low (c_1), normal (c_2), and elevated (c_3 ; c_4) perfusion inflow concentrations in normoxic and hypoxic dogs during brain ventricular perfusion

Condition	K_O ($\mu\text{l}/\text{min}$)			J_1 (nmoles/min)			J_1' (nmoles/min)		
	c_1	c_2	c_3	c_1	c_2	c_3	c_1	c_2	c_3
A. Long Duration Normoxia									
	(6)	(4)	(5)	(6)	(4)	(5)	(6)	(4)	(5)
	P_1	$\bar{X} \pm \text{SE}$	$\bar{X} \pm \text{SE}$	$\bar{X} \pm \text{SE}$	$\bar{X} \pm \text{SE}$	$\bar{X} \pm \text{SE}$	$\bar{X} \pm \text{SE}$	$\bar{X} \pm \text{SE}$	$\bar{X} \pm \text{SE}$
	74 \pm 9	48 \pm 6 †	48 \pm 8 †	-520 \pm 60	-220 \pm 10 †	-190 \pm 30 †	-320 \pm 60	-130 \pm 10 †	-80 \pm 20 †
	P_2	$\bar{X} \pm \text{SE}$	$\bar{X} \pm \text{SE}$	$\bar{X} \pm \text{SE}$	$\bar{X} \pm \text{SE}$	$\bar{X} \pm \text{SE}$	$\bar{X} \pm \text{SE}$	$\bar{X} \pm \text{SE}$	$\bar{X} \pm \text{SE}$
B. Normoxia- Hypoxia									
	(6)	(6)	(6)	(6)	(6)	(6)	(6)	(6)	(6)
	P_1	$\bar{X} \pm \text{SE}$	$\bar{X} \pm \text{SE}$	$\bar{X} \pm \text{SE}$	$\bar{X} \pm \text{SE}$	$\bar{X} \pm \text{SE}$	$\bar{X} \pm \text{SE}$	$\bar{X} \pm \text{SE}$	$\bar{X} \pm \text{SE}$
	78 \pm 3	32 \pm 4 †	32 \pm 4 †	-370 \pm 50	-160 \pm 50 †	-160 \pm 50 †	-220 \pm 30	-60 \pm 50 †	-60 \pm 50 †
	P_2	$\bar{X} \pm \text{SE}$	$\bar{X} \pm \text{SE}$	$\bar{X} \pm \text{SE}$	$\bar{X} \pm \text{SE}$	$\bar{X} \pm \text{SE}$	$\bar{X} \pm \text{SE}$	$\bar{X} \pm \text{SE}$	$\bar{X} \pm \text{SE}$
Number of dogs in parentheses									
	(6)	(6)	(6)	(6)	(6)	(6)	(6)	(6)	(6)
	P_1	$\bar{X} \pm \text{SE}$	$\bar{X} \pm \text{SE}$	$\bar{X} \pm \text{SE}$	$\bar{X} \pm \text{SE}$	$\bar{X} \pm \text{SE}$	$\bar{X} \pm \text{SE}$	$\bar{X} \pm \text{SE}$	$\bar{X} \pm \text{SE}$
	63 \pm 7	51 \pm 8	51 \pm 8	-650 \pm 80	-410 \pm 50 †	-410 \pm 50 †	-420 \pm 40	-230 \pm 50 †	-230 \pm 50 †
	$\Delta \bar{X} \pm \text{SE}$	$\Delta \bar{X} \pm \text{SE}$	$\Delta \bar{X} \pm \text{SE}$	$\Delta \bar{X} \pm \text{SE}$	$\Delta \bar{X} \pm \text{SE}$	$\Delta \bar{X} \pm \text{SE}$	$\Delta \bar{X} \pm \text{SE}$	$\Delta \bar{X} \pm \text{SE}$	$\Delta \bar{X} \pm \text{SE}$
Number of dogs in parentheses									
	(6)	(6)	(6)	(6)	(6)	(6)	(6)	(6)	(6)
	P_1	$\bar{X} \pm \text{SE}$	$\bar{X} \pm \text{SE}$	$\bar{X} \pm \text{SE}$	$\bar{X} \pm \text{SE}$	$\bar{X} \pm \text{SE}$	$\bar{X} \pm \text{SE}$	$\bar{X} \pm \text{SE}$	$\bar{X} \pm \text{SE}$
	78 \pm 3	32 \pm 4 †	32 \pm 4 †	-370 \pm 50	-160 \pm 50 †	-160 \pm 50 †	-220 \pm 30	-60 \pm 50 †	-60 \pm 50 †
	P_2	$\bar{X} \pm \text{SE}$	$\bar{X} \pm \text{SE}$	$\bar{X} \pm \text{SE}$	$\bar{X} \pm \text{SE}$	$\bar{X} \pm \text{SE}$	$\bar{X} \pm \text{SE}$	$\bar{X} \pm \text{SE}$	$\bar{X} \pm \text{SE}$
Number of dogs in parentheses									
	(6)	(6)	(6)	(6)	(6)	(6)	(6)	(6)	(6)
	P_1	$\bar{X} \pm \text{SE}$	$\bar{X} \pm \text{SE}$	$\bar{X} \pm \text{SE}$	$\bar{X} \pm \text{SE}$	$\bar{X} \pm \text{SE}$	$\bar{X} \pm \text{SE}$	$\bar{X} \pm \text{SE}$	$\bar{X} \pm \text{SE}$
	63 \pm 7	51 \pm 8	51 \pm 8	-650 \pm 80	-410 \pm 50 †	-410 \pm 50 †	-420 \pm 40	-230 \pm 50 †	-230 \pm 50 †
	$\Delta \bar{X} \pm \text{SE}$	$\Delta \bar{X} \pm \text{SE}$	$\Delta \bar{X} \pm \text{SE}$	$\Delta \bar{X} \pm \text{SE}$	$\Delta \bar{X} \pm \text{SE}$	$\Delta \bar{X} \pm \text{SE}$	$\Delta \bar{X} \pm \text{SE}$	$\Delta \bar{X} \pm \text{SE}$	$\Delta \bar{X} \pm \text{SE}$
Number of dogs in parentheses									
	(6)	(6)	(6)	(6)	(6)	(6)	(6)	(6)	(6)
	P_1	$\bar{X} \pm \text{SE}$	$\bar{X} \pm \text{SE}$	$\bar{X} \pm \text{SE}$	$\bar{X} \pm \text{SE}$	$\bar{X} \pm \text{SE}$	$\bar{X} \pm \text{SE}$	$\bar{X} \pm \text{SE}$	$\bar{X} \pm \text{SE}$
	78 \pm 3	32 \pm 4 †	32 \pm 4 †	-370 \pm 50	-160 \pm 50 †	-160 \pm 50 †	-220 \pm 30	-60 \pm 50 †	-60 \pm 50 †
	P_2	$\bar{X} \pm \text{SE}$	$\bar{X} \pm \text{SE}$	$\bar{X} \pm \text{SE}$	$\bar{X} \pm \text{SE}$	$\bar{X} \pm \text{SE}$	$\bar{X} \pm \text{SE}$	$\bar{X} \pm \text{SE}$	$\bar{X} \pm \text{SE}$
Number of dogs in parentheses									
	(6)	(6)	(6)	(6)	(6)	(6)	(6)	(6)	(6)
	P_1	$\bar{X} \pm \text{SE}$	$\bar{X} \pm \text{SE}$	$\bar{X} \pm \text{SE}$	$\bar{X} \pm \text{SE}$	$\bar{X} \pm \text{SE}$	$\bar{X} \pm \text{SE}$	$\bar{X} \pm \text{SE}$	$\bar{X} \pm \text{SE}$
	63 \pm 7	51 \pm 8	51 \pm 8	-650 \pm 80	-410 \pm 50 †	-410 \pm 50 †	-420 \pm 40	-230 \pm 50 †	-230 \pm 50 †
	$\Delta \bar{X} \pm \text{SE}$	$\Delta \bar{X} \pm \text{SE}$	$\Delta \bar{X} \pm \text{SE}$	$\Delta \bar{X} \pm \text{SE}$	$\Delta \bar{X} \pm \text{SE}$	$\Delta \bar{X} \pm \text{SE}$	$\Delta \bar{X} \pm \text{SE}$	$\Delta \bar{X} \pm \text{SE}$	$\Delta \bar{X} \pm \text{SE}$
Number of dogs in parentheses									
	(6)	(6)	(6)	(6)	(6)	(6)	(6)	(6)	(6)
	P_1	$\bar{X} \pm \text{SE}$	$\bar{X} \pm \text{SE}$	$\bar{X} \pm \text{SE}$	$\bar{X} \pm \text{SE}$	$\bar{X} \pm \text{SE}$	$\bar{X} \pm \text{SE}$	$\bar{X} \pm \text{SE}$	$\bar{X} \pm \text{SE}$
	78 \pm 3	32 \pm 4 †	32 \pm 4 †	-370 \pm 50	-160 \pm 50 †	-160 \pm 50 †	-220 \pm 30	-60 \pm 50 †	-60 \pm 50 †
	P_2	$\bar{X} \pm \text{SE}$	$\bar{X} \pm \text{SE}$	$\bar{X} \pm \text{SE}$	$\bar{X} \pm \text{SE}$	$\bar{X} \pm \text{SE}$	$\bar{X} \pm \text{SE}$	$\bar{X} \pm \text{SE}$	$\bar{X} \pm \text{SE}$
Number of dogs in parentheses									
	(6)	(6)	(6)	(6)	(6)	(6)	(6)	(6)	(6)
	P_1	$\bar{X} \pm \text{SE}$	$\bar{X} \pm \text{SE}$	$\bar{X} \pm \text{SE}$	$\bar{X} \pm \text{SE}$	$\bar{X} \pm \text{SE}$	$\bar{X} \pm \text{SE}$	$\bar{X} \pm \text{SE}$	$\bar{X} \pm \text{SE}$
	63 \pm 7	51 \pm 8	51 \pm 8	-650 \pm 80	-410 \pm 50 †	-410 \pm 50 †	-420 \pm 40	-230 \pm 50 †	-230 \pm 50 †
	$\Delta \bar{X} \pm \text{SE}$	$\Delta \bar{X} \pm \text{SE}$	$\Delta \bar{X} \pm \text{SE}$	$\Delta \bar{X} \pm \text{SE}$	$\Delta \bar{X} \pm \text{SE}$	$\Delta \bar{X} \pm \text{SE}$	$\Delta \bar{X} \pm \text{SE}$	$\Delta \bar{X} \pm \text{SE}$	$\Delta \bar{X} \pm \text{SE}$

Number of dogs in parentheses

c_1 , c_2 , c_3 , c_4 = inflow L-lactate concentration referring to 0.0, 1.5 \pm 0.2, 5.2 \pm 0.4, and 4.5 \pm 0.3 mM, respectively.

* $p < 0.05$; $P_1 \neq P_2$.

$^\dagger p < 0.05$; K_O ; J_1 ; J_1' at $c_1 \neq c_2$, c_3 , or c_4 .

Table 8. Mannitol transependymal outflux coefficient (K_o) at low (c_1) and elevated (c_2) perfusion inflow concentrations in normoxic and hypoxic dogs during brain ventricular perfusion

Condition	K_o ($\mu\text{l}/\text{min}$)	
	c_1	c_2
B. Normoxia-Hypoxia		
P_1 $\bar{X} \pm \text{SE}$	14 ± 2 (3)	18 ± 5 (3)
P_2 $\bar{X} \pm \text{SE}$	14 ± 1	16 ± 4
$\Delta\bar{X} \pm \text{SE}$	0 ± 2	1 ± 2

Number of dogs in parentheses.

c_1, c_2 = inflow mannitol concentration referring to 0.0 and 16.8 ± 0.2 mM, respectively.

Table 9. Mean pyruvate concentrations in the inflow fluid (c_i), outflow fluid (c_o), and arterial plasma (c_p) in normoxic and hypoxic dogs during brain ventricular perfusion

Condition	Pyruvate Concentration mM								
	c_i	c_o	c_p	c_i	c_o	c_p	c_i	c_o	c_p
A. Long Duration Normoxia									
$P_1 \bar{X} \pm SE$	(6) 0.0	(6) 0.21 \pm 0.02	(6) 0.24 \pm 0.02 [†]	(4) 0.12 \pm 0.02	(4) 0.15 \pm 0.04	(4) 0.08 \pm 0.01	(5) 0.29 \pm 0.01	(5) 0.28 \pm 0.01	(5) 0.11 \pm 0.02
$P_2 \bar{X} \pm SE$		0.22 \pm 0.02	0.22 \pm 0.01 [†]		0.15 \pm 0.03	0.08 \pm 0.01		0.29 \pm 0.01	0.12 \pm 0.02
$\Delta \bar{X} \pm SE$		0.01 \pm 0.01	-0.02 \pm 0.01		0.00 \pm 0.01	0.00 \pm 0.01		0.00 \pm 0.00	0.01 \pm 0.01
B. Normoxia-Hypoxia									
$P_1 \bar{X} \pm SE$	(6) 0.0	(6) 0.09 \pm 0.01	(6) 0.13 \pm 0.01				(6) 0.24 \pm 0.01	(6) 0.22 \pm 0.01	(6) 0.09 \pm 0.01
$P_2 \bar{X} \pm SE$		0.09 \pm 0.01	0.14 \pm 0.01					0.23 \pm 0.01	0.10 \pm 0.01
$\Delta \bar{X} \pm SE$		0.01 \pm 0.01	0.01 \pm 0.01					0.00 \pm 0.01	0.01 \pm 0.01

Number of dogs in parentheses.

[†] c_p elevated by iv infusion (see section 4.9.1.1).

Table 10. Pyruvate net flux (J_{py} , J'_{py}) at low (c_1), normal (c_2), and elevated (c_3 , c_4) perfusion inflow concentrations in normoxic and hypoxic dogs during brain ventricular perfusion

Condition	J _{py} (nmoles/min)			J' _{py} (nmoles/min)			
	c ₁	c ₂	c ₃	c ₁	c ₂	c ₃	
A. Long Duration Normoxia							
	P ₁ $\bar{X} \pm SE$	-50±2 (6)	-16±6 [†] (4)	-13±2 [†] (5)	-38±3 (6)	-9±5 [†] (4)	-8±2 [†] (5)
	P ₂ $\bar{X} \pm SE$	-50±3	-14±5 [†]	-12±2 [†]	-41±4	-9±4 [†]	-7±1 [†]
	$\Delta\bar{X} \pm SE$	-1±2	-2±2	1±2	-3±1	0±1	1±1
B. Normoxia-Hypoxia							
	P ₁ $\bar{X} \pm SE$	-23±4 (6)	-6±1 [†] (6)		-17±4 (6)		-1±2 [†] (6)
	P ₂ $\bar{X} \pm SE$	-22±4	-4±2 [†]		-15±5		-2±1 [†]
	$\Delta\bar{X} \pm SE$	-1±4	2±2		2±4		0±2

Number of dogs in parentheses.

c_1 , c_2 , c_3 , c_4 = inflow pyruvate concentration referring to 0.0, 0.12±0.02, 0.29±0.01, 0.24±0.01 mM, respectively.

[†] $p < 0.05$, J_{py} , J'_{py} at $c_1 \neq c_2$, c_3 , or c_4 .

VI. DISCUSSION

6.1. CSF bulk absorption and formation rates

Perfusion of the brain ventricles with artificial cerebrospinal fluid (CSF) containing test molecules permits the study of exchanges between this fluid and the blood or the brain. Molecular clearance is expressed as the volume of CSF from which a substance is removed per unit time. It is a function of the rate at which the test molecule enters and leaves the ventricles through a perfusion inflow and effluent, respectively, as well as its concentration in the ventricles.

Inulin, a large molecule, does not penetrate the ventricular ependyma, and its clearance reflects CSF bulk absorption rate (\dot{V}_a) (Rall *et al.*, 1962; Heisey *et al.*, 1962). Inulin clearance which is a direct, linear function of intraventricular pressure, was used to predict \dot{V}_a in the present study (Heisey *et al.*, 1962; Bering and Sato, 1963; Bierer, 1972). Intraventricular pressure was maintained at a steady level (section 4.2) so that \dot{V}_a was constant.

Data reported in Table 2 indicate that \dot{V}_a was unaffected by hypoxia. Increased \dot{V}_a in experiments testing the effects of hypoxia is attributable to a factor of time

since \dot{V}_a increased similarly in both normoxic and hypoxic animals. A similar judgment may be valid for analogous data reported earlier (Michael *et al.*, 1971) in which radioiodinated human serum albumin (RIHSA) was used as the test molecule for calculating \dot{V}_a .

The increase in \dot{V}_a with time (Table 2) may be attributed to preparation deterioration (Cserr, 1965). Data reported in Table 8 indicate that mannitol K_o did not change during hypoxia, implying that neither time nor hypoxia affect mannitol transepithelial permeability. Since inulin is a larger molecule than mannitol, it is presumed that its ventricular permeability would be similarly unaffected, and inulin clearance would remain an accurate estimation of \dot{V}_a in these experiments.

Changes in \dot{V}_a (Table 2) may be related to changes in sagittal sinus venous pressure (SSVP; unmeasured in this study), since both intraventricular pressure (IVP) and an IVP-SSVP pressure difference linearly and directly vary \dot{V}_a (Heisey *et al.*, 1962; Bering and Sato, 1963). Since IVP was maintained constant, SSVP appears an effective independent variable in these studies, and changes in \dot{V}_a may have occurred distal to the fourth ventricle at the arachnoid villi.

The mean CSF formation rate (\dot{V}_f) of 50 $\mu\text{l}/\text{min}$ (Table 2; A-P₁; B-P₁) is similar to that previously reported for the anesthetized dog (Bering and Sato, 1963; Oppelt *et*

al., 1964; Atkinson and Weiss, 1969). Similarly, the range of \dot{V}_f reported here (30-85 $\mu\text{l}/\text{min}$) is the same as that reported earlier (Oppelt *et al.*, 1964; Cserr, 1965).

\dot{V}_f is proposed to be an active transport system (Vates *et al.*, 1964; Cserr, 1965; Holloway *et al.*, 1972) and would be expected to vary with cerebral oxygen consumption and cerebral blood flow (CBF; Bering, 1959). \dot{V}_f decreased significantly during hypoxia (Table 2; B-P₂) as reported earlier (Holloway *et al.*, 1972; Michael *et al.*, 1972), possibly through an indirect effect on CBF (Kety and Schmidt, 1948; Fujishima *et al.*, 1971); it also decreased with time. Although total brain perfusion increases with hypoxia (Kety and Schmidt, 1948; Shapiro *et al.*, 1970), decreases in regional CBF may affect \dot{V}_f .

CSF formation may be reduced not only due to the direct and indirect effects of hypoxia but also due to the effects of the anesthetic. Barbiturates affect \dot{V}_f possibly by inhibiting active transport of ions (Lorenzo *et al.*, 1968; Bering, 1959) and may be implicated in the decrease in \dot{V}_f with time reported here, related to the anesthetization procedure (section 4.9).

6.2. Glucose flux from CSF

Carrier-mediated glucose transport has been reported for the membranes which separate the blood, brain and CSF compartments, and which moves glucose from blood into brain

tissue (Crone, 1965; Gilboe *et al.*, 1970), from blood into CSF (Fishman, 1964; Atkinson and Weiss, 1969; Welch *et al.*, 1970) and from the CSF into either blood or brain (Bradbury and Davson, 1964; Bronsted, 1970a and b). *In vitro* studies using the choroid plexus, further suggest active transport of glucose from the CSF (Csaky and Rigor, 1968). In brain ventricular perfusion studies, glucose can go from CSF into the cerebral capillary blood, the brain parenchyma (neurons and glial cells), or the epithelium of the choroid plexus, however the specific course is unidentifiable.

As glucose concentration in the perfusion inflow increased, its efflux (K_O ; Table 5) decreased, implying saturation of a carrier-mediated transport system, as reported earlier (Bradbury and Davson, 1964; Bronsted, 1970a and b). This occurred when the ventricular glucose concentration was nearly equal to that in normal CSF (5.0 mM; Table 3).

Since mannitol (which moves only by diffusion) and glucose show similar diffusion characteristics, the inhibition of glucose active transport should result in similar K_O 's for both molecules. Even with glucose transport saturated, its K_O (Table 5) remained 4 times greater than that for mannitol (Table 8), suggesting additional transport systems with a higher saturation point.

The decrease in glucose K_o during hypoxia (Table 5) suggests the inhibition of an aerobic process. Glucose accumulation by the choroid plexus (*in vitro*) is inhibited by DNP and anoxia suggesting an active transport mechanism (Csaky and Rigor, 1968). Intraventricular administration of ouabain, a $\text{Na}^+ - \text{K}^+$ ATPase inhibitor, reduces both glucose efflux and \dot{V}_f (Bronsted, 1970a), suggesting further that both are dependent on active transport. In the present study, hypoxia also may have inhibited the high capacity glucose transport system.

Consistent with the observation that glucose K_o decreased during hypoxia (Table 5) are data indicating net glucose influx during hypoxia increased when glucose concentration in the perfusion inflow was less than that in plasma. When perfusion inflow concentration was elevated above that of plasma, however, there was no change in net glucose outflux, even though glucose K_o decreased. However if the active transport component of glucose efflux makes a small contribution to its net flux, net glucose flux would reflect concentration differences among compartments. In the present study, net glucose flux during normoxia and hypoxia reflected glucose concentration differences between the CSF and plasma. This supports the concept of a low capacity active transport system for glucose in the choroid plexus (Csaky and Rigor, 1968).

6.3. Lactate flux from CSF

Lactate concentrations in the blood are independent of those in either brain or CSF (Klein and Olsen, 1947; Alexander *et al.*, 1962), whereas CSF lactate concentrations correlate with those in brain (Plum and Posner, 1967; Plum *et al.*, 1968; Kaasik *et al.*, 1970). Hydrogen ion activity (pH) influences the distribution of lactate among these fluids (Gurdjian *et al.*, 1944; Milne *et al.*, 1958). Lactate exists in brain, CSF and blood as an anion ($pK = 3.8$) but diffuses across compartment membranes only when non-ionized.

Net lactate flux rates were negative (Table 7) even at elevated lactate concentrations in the perfusion inflow, indicating a net lactate influx. Blood pH exceeds that of CSF during normocapnic normoxia (Davison, 1967), and would favor lactate diffusion from CSF. When lactate concentrations in the perfusion inflow exceeded those in plasma, net lactate influx must be either from brain or by an active process from blood. When perfusion inflow concentration was 0.0 mM net lactate influx (c_1 ; Table 7) was more when plasma glucose and pyruvate concentrations were elevated and further suggests that the increased lactate influx was due to increased lactate production by brain. The lack of a direct linear relationship between perfusion inflow concentrations of lactate and its net influx (net influx was same at normal and elevated perfusion inflow concentrations)

are consistent with the hypothesis of carrier-mediated lactate transport (Stein, 1967).

Net lactate influx increased with time, but increased more during hypoxia (Table 7). The increased lactate influx with time may be attributable to mitochondrial inhibition by a barbiturate anesthetic (Aldridge, 1962). Hypoxia results in an increased glycolytic rate and increased brain lactate concentration (Lowry *et al.*, 1964; Kaasik *et al.*, 1970), which would increase net lactate influx.

As lactate concentration in the perfusion inflow increased, its outflux coefficient (K_o ; Table 7) decreased, implying saturation of carrier-mediated transport. This conflicts with the hypothesis that lactate clearance from CSF is only by non-carrier mediated diffusion and bulk absorption (Prockop, 1968). Lactate transport was saturated when CSF lactate concentrations were normal (1.6 mM; Table 3) and explains the failure to identify a saturable carrier at CSF concentrations of 5-10 mM (Prockop, 1968). When the lactate carrier was saturated lactate K_o was approximately twice that of mannitol as previously reported (Prockop, 1968). Further, the inclusion of mannitol in lieu of glucose in the perfusion inflow (section 4.9.2) allows the inference that lactate efflux is independent of glucose flux (Prockop, 1968).

Lactate K_o (Table 7) was unaffected by time but at c_1 K_o decreased from normoxic values during hypoxia. The K_o decrease could be due either to inhibition of an active aerobic transport or to competition for the lactate carrier due to increased lactate influx from brain. Lactate K_o at elevated perfusion inflow concentrations of lactate did not change significantly with hypoxia, indicating no change in transependymal permeability to lactate.

6.4. Pyruvate flux from CSF

Klein and Olsen (1947) suggested that pyruvate moves rapidly from plasma into brain tissue and is rapidly converted to lactate. Data in Table 9 show that elevated plasma pyruvate concentrations may be reflected by those in CSF. Rapid equilibration of pyruvate ($pK = 2.5$) among the blood, CSF and brain would suggest some process other than simple diffusion.

There was always a net pyruvate flux into CSF (Table 10). Simple diffusion of pyruvate into CSF from plasma cannot explain the net influx at elevated perfusion inflow concentrations (c_3, c_4), since neither the pyruvate concentration gradient nor the pH of these fluids favor it. When plasma pyruvate concentrations were the same (Table 9), there was no direct linear relationship between net pyruvate flux and pyruvate concentrations at normal and elevated

concentration in the perfusion inflow fluid (Table 10) further implying a carrier-mediated pyruvate transport.

Data in Table 9 suggest pyruvate movement from CSF is not rapid and the failure of net pyruvate influx to change with either time or hypoxia (Table 10) would suggest that movement from CSF into brain may be slow.

VII. SUMMARY

1. Inulin clearance a measure of the bulk absorption rate of cerebrospinal fluid (CSF) increased with perfusion time.

2. Mean CSF formation rate (\dot{V}_f) in normoxic dogs was 50 $\mu\text{l}/\text{min}$. \dot{V}_f decreased both with perfusion time and hypoxia, and the latter decrease was greater.

3. Mannitol efflux from CSF was unaffected by time, hypoxia, or concentration, implying movement by non-carrier mediated diffusion.

4. Carrier-mediated glucose efflux from CSF may be by two types of carriers. The first, a low capacity-carrier, was saturated at normal CSF glucose concentrations. The second, a high capacity-carrier, accounted for an outflux coefficient which was significantly greater than that of mannitol.

5. The glucose outflux coefficient was unaffected by time but was significantly reduced during hypoxia, suggesting inhibition of an aerobic dependent glucose transport.

6. Net glucose flux during normoxia and hypoxia reflected glucose concentration differences between the CSF and plasma.

7. There was a net lactate flux into CSF at CSF lactate concentrations ranging from 0.0 to 5.0 mM. Net lactate influx increased with time, but increased more during hypoxia. Carrier-mediated lactate transport was indicated by the lack of a direct linear relationship of net lactate flux with perfusion inflow concentrations of lactate.

8. Carrier-mediated lactate flux from CSF was indicated by concentration dependent outflux coefficient (K_o). K_o was unaffected by perfusion time, but was decreased with hypoxia when lactate concentration in the perfusion inflow was 0.0 mM.

9. There was a net pyruvate flux into CSF at CSF pyruvate concentrations ranging from 0.00 to 0.30 mM. Carrier-mediated pyruvate transport was indicated by the lack of a direct linear relationship between net pyruvate flux and pyruvate concentrations in the CSF. Neither time nor hypoxia affected net pyruvate influx.

10. Net fluxes of glucose, lactate, and pyruvate were calculated assuming two different values for their concentration in newly formed CSF (c_f). The direction of their net flux was independent of c_f 's indicating minimal contribution of \dot{V}_f to exchange of metabolites.

APPENDICES

APPENDIX A

COMPOSITION AND PREPARATION OF ARTIFICIAL DOG CEREBROSPINAL FLUID (CSF)

Dog CSF contains: Na^+ , 150 mEq/l; K^+ , 3.0 mEq/l; Ca^{++} , 2.3 mEq/l; Mg^{++} , 0.8 mEq/l; Cl^- , 133.2 mEq/l; HCO_3^- , 25.0 mEq/l; PO_4^{-3} , 0.5 mEq/l (Cserr, 1965).

Reagents

1. $\text{Na}_2\text{HPO}_4 \cdot \text{H}_2\text{O}$, analytical reagent (A.R.)
2. KCl , A.R.
3. NaHCO_3 , A.R.
4. NaCl , A.R.
5. CaCl_2 , A.R.
6. $\text{MgCl}_2 \cdot 6\text{H}_2\text{O}$, A.R.

Solutions

- A. 34 mg of reagent 1; 224 mg of reagent 2; 2.1 g of reagent 3; 7.25 g of reagent 4 are dissolved in distilled H_2O ; q.s. to one liter.
- B. 12.76 g of reagent 5 is dissolved in distilled H_2O ; q.s. to 100 ml.
- C. 8.13 g of reagent 6 is dissolved in distilled H_2O ; q.s. to 100 ml.

CSF for ventricular perfusion was made by adding 0.1 ml of both solutions B and C to 100 ml of solution A. The resultant mixture is adjusted to approximately pH 7.3 by bubbling with 3-9% CO₂ at room temperature for one-half hour prior to use.

APPENDIX B

PREPARATION OF ANESTHETIC

The anesthetic, Dial and Urethane solution, was prepared from a commercial formula (CIBA Pharm. Co., Summit, N.J.). Each ml of anesthetic solution contained: 100 mg diallylbarbituric acid, 400 mg urethane, and 400 mg monoethyl urea.

Reagents

1. Diallylbarbituric acid (Dial; K & K Lab. Inc., Plainview, N.Y.).
2. Monoethyl urea (Pfaltz and Bauer, Inc., Flushing, N.Y.).
3. Disodium calcium ethylene diamine tetraacetate trihydrate (Pfaltz and Bauer, Inc.).
4. Ethyl carbamate (Urethane; Aldrich Chemical Co., Inc., Milwaukee, Wis.).

Procedure

To make 100 ml of anesthetic, place 10 g of reagent 1; 40 g of reagent 2; and 40 g of reagent 4 in a 250 ml beaker. Dissolve 50 mg of reagent 3 in one ml of distilled H₂O, and add solution to powders. Place beaker in water

bath (100°C) and stir occasionally until solution is complete. Cool to room temperature; q.s. to 100 ml with distilled H₂O. Place solution in dark bottle, cap, and store at room temperature.

APPENDIX C

DEPROTEINIZATION OF PLASMA AND CSF SAMPLES

Reagents

1. HClO_4 , 70-72%, w/v; Sp. Gr. 1.6; A.R.
2. K_2CO_3 , A.R.

Solutions

- A. HClO_4 , approx. 6%, w/v

Dilute 15.6 ml of reagent 1 to 300 ml with distilled H_2O .

- B. K_2CO_3 , 5M

Dissolve 69 g of reagent 2 in approximately 80 ml of distilled H_2O ; q.s. to 100 ml.

Deproteinization procedure

Frozen plasma and CSF samples were thawed in ice (0°C); 0.5 ml aliquots were added to 4.0 ml of ice-cold solution A, mixed, and centrifuged ($1000 \times g$ at 0°C) for 10 minutes to precipitate and remove protein from the sample. Three-tenths ml of solution B was added dropwise, with mixing, precipitating KClO_3 and neutralizing the solution to a pH of 6.8-7.2 (addition of solution B is done slowly to

prevent the loss of sample by rapid CO₂ evolution). The samples were centrifuged (1000 x g; 0°C; 10 min.) to remove KClO₃. The supernate was decanted and used for subsequent analyses. Total dilution of deproteinated sample was 9.6x.

APPENDIX D

SPECTROPHOTOMETRIC DETERMINATION OF D-GLUCOSE¹

Principle

The glucose oxidase method is a coupled enzyme system for the quantitative, colorimetric determination of D-glucose (Hugget and Nixon, 1957) based upon the following reactions:

1. $\text{D-glucose} + \text{O}_2 + \text{H}_2\text{O} \xrightarrow{\text{glucose oxidase}} \text{H}_2\text{O}_2 + \text{D-gluconic acid}$
2. $\text{H}_2\text{O}_2 + \text{reduced chromogen} \xrightarrow{\text{peroxidase}} \text{oxidized chromogen}$

Reaction 1 is specific for D-glucose. The amount of oxidized chromogen present in the assay mixture is determined by its absorbance at 400 mμ.

Reagents

1. Glucostat reagent kit (Worthington Biochemical Corp., Freehold, N.J.)
 - a. buffered glucose oxidase vial
 - b. chromogen vial
2. HCl, concentrated, A.R.

¹From H. U. Bergmeyer and E. Bernt (1965).

3. Glucose stock solution, 10 mg glucose/ml (55.6 mM) containing 0.25% benzoic acid (Fisher Scientific Co., Fairlawn, N.J.).

Solutions

- A. Glucostat reagent (for approximately 80 determinations)

Dissolve contents of two vials of reagents 1a and 1b in distilled H_2O ; q.s. to 160 ml.

- B. HCl, 4N

172 ml of reagent 2 diluted to 500 ml with distilled H_2O .

Glucose standard solutions

Glucose standards (2.78, 5.56, 8.34, and 11.1 mM) are made within 24 hours of the assay by diluting 0.5, 1.0, 1.5, and 2.0 ml of reagent 3 to 10 ml with distilled H_2O .

Procedure

To 0.5 ml duplicate aliquots of deproteinated samples, standards, and distilled H_2O (see Appendix C), add 2.0 ml of solution A, mix, and incubate at room temperature. After exactly 10 minutes incubation, add two drops of solution B, mix, and let stand for at least 5 minutes. Read absorbancy (O.D.) of standards and samples in spectrophotometer (Model DB, Beckman Instruments Inc., Fullerton, Cal.) against the distilled H_2O blank at 400 m μ .

Calculations

Plot absorbancy (O.D.₄₀₀) as a function of the concentration of the glucose standards. The plot should be linear through 11.1 mM. The concentration of glucose in the unknown samples is calculated using the following formula:

$$C_u = \frac{\Sigma (C_s / OD_s)}{n_s} \times OD_u$$

where:

OD = absorbancy

C = concentration

s = standard

u = unknown

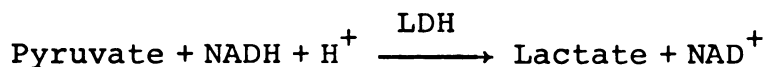
n = number of samples.

APPENDIX E

FLUOROMETRIC DETERMINATION OF PYRUVATE¹

Principle

Lactic dehydrogenase (LDH) catalyzes the reduction of pyruvate by reduced nicotine-adenine dinucleotide (NADH) to form lactate and nicotine-adenine dinucleotide (NAD).



The equilibrium of the reaction favors lactate formation at pH 7.5. With excess NADH in the mixture, the reaction proceeds to completion and pyruvate is quantitatively converted to lactate. When NADH is oxidized to NAD^+ , absorbancy and/or fluorescence decreases, and this decrease is measured.

Reagents

1. NaOH, A.R.
2. $(\text{NH}_4)_2\text{SO}_4$, A.R.
3. NaHCO_3 , A.R.
4. Triethanolamine-HCl, A.R. (Sigma Chemical Co., St. Louis, Mo.)

¹From J. R. Williamson and B. E. Cory (1969) and T. Buchner *et al.* (1965).

5. Ethylene-diamine-tetraacetic acid, EDTA-disodium salt, $\text{EDTA-Na}_2\text{H}_2\cdot 2\text{H}_2\text{O}$.
6. Reduced nicotine-adenine dinucleotide, NADH (Sigma Chemical Co.). Stable for at least a year when stored dessicated in dark at 0-4°C.
7. Lactic dehydrogenase suspension (LDH; Sigma Chemical Co.). Crystalline preparation from rabbit skeletal muscle which is suspended in 2.1 M ammonium sulfate; stable for periods up to a year if kept between 0-4°C. The concentration of LDH is 5 mg protein/ml with a specific activity of at least 600 units/ml.
8. Sodium pyruvate, A.R. (Calbiochemical Corp., Los Angeles, Cal.). Stored dessicated in dark at 0-4°C.

Solutions

A. NaOH, 18N

Dissolve 360 g of reagent 1 in distilled H_2O ; q.s. to 500 ml.

B. $(\text{NH}_4)_2\text{SO}_4$, 2.1 M

Dissolve 27.8 g of reagent 2 in distilled H_2O ; q.s. to 100 ml.

C. NaHCO_3 , 1%, w/v

Dissolve 1 g of reagent 3 in distilled H_2O ; q.s. to 100 ml.

D. Triethanolamine buffer (TEA), pH 7.5

Suspend 37.2 g of reagent 4 and 7.4 g of reagent 5 in 400 ml of distilled H_2O . Add solution A until

pH 7.5 is obtained; q.s. to 500 ml with distilled H_2O .

E. NADH

1. To 30 mg of reagent 6 add solution C; q.s. to 100 ml. This solution is for the spectrophotometric determination of the pyruvate standard concentration.
2. Dilute 0.1 ml of solution E-1 to 10 ml with solution C for use in fluorometric assay.

F. LDH (for approximately 50 determinations)

Dilute 0.1 ml of reagent 7 to 1.0 ml with solution B.

Pyruvate standard (approximately 0.1 mM)

Dissolve approximately 11 mg of reagent 8 in distilled H_2O ; q.s. to one liter. Prepare fresh solution just prior to assay.

Spectrophotometric determination of pyruvate standard concentration (External standard)

To three test tubes containing 4.0 ml of solution D, 2.0 ml of pyruvate standard, and 0.025 ml of solution E-1, add 0.020 ml of solution F and mix. To another test tube (reference blank) containing the above constituents add 0.020 ml of distilled H_2O in lieu of the LDH. Read in spectrophotometer (Model DB, Beckman Instruments Inc.) at a wavelength of 340 m μ . Since the absorbance of the sample (with LDH) is less than that of the blank (without LDH) the reference blank is inserted in the site normally used for samples.

Calculations

Calculate the concentration of the pyruvate standard from the following formula.

$$V_1/6.22 \times L/V_2 \times OD = C_s$$

where:

V_1 = total volume in test solution (6.045 ml)

V_2 = volume of standard added (2.0 ml)

L = length of light path (1 cm)

6.22 = molar extinction coefficient of NADH at 340 mμ
(cm²/μM)

OD = mean absorbancy of three pyruvate standard samples

C_s = pyruvate concentration of standard solution (mM).

Fluorometric assay for pyruvate

To obtain assay range prepare a test tube containing: 4.0 ml of solution D, 0.2 ml of deproteinized standard pyruvate solution, 0.010 ml of solution E-2, and 0.02 ml of distilled H₂O. Mix and read sample fluorescence against that of a distilled H₂O blank in Model 110 Fluorometer (G.K. Turner Assoc., Palo Alto, Cal.) with:

- a. UV light source, 4 watt, Cat. #110-850 (G.K. Turner Assoc.)
- b. Primary filter (360 mμ), Cat. #110-811 (G.K. Turner Assoc.)

- c. Secondary filter, 2A (415 m μ), Cat. #110-816
(G.K. Turner Assoc.)
- d. Neutral density filter (A.H. Thomas, Philadelphia, Pa.).

Use the appropriate neutral density filter such that the fluorescence reading for the assay range is between 80-100 scale units. Record this as R_r . This reading is the maximum fluorescence due to NADH.

For both deproteinated samples, and the pyruvate standard (the concentration of which has been determined spectrophotometrically) add to test tubes, in order, 4.0 ml of solution D, to one test tube 0.2 ml and to another 0.1 ml of sample (0.2 ml and 0.1 ml of sample will suffice as two readings per sample), and 0.020 ml of solution F, mix and read fluorescence. Record as R_1 . (This is the sample background fluorescence). Add 0.010 ml of solution E-2, mix, and incubate at room temperature, and measure fluorescence after exactly 15 minutes. Record fluorescence (R_2). R_2 of tubes containing 0.2 ml of sample should be one-half that containing 0.1 ml of sample. If 0.2 ml sample reads zero or R_1 , more NADH must be added or sample size decreased. Check reaction completeness by adding 0.010 ml of solution E-2 and fluorescence should increase by a value of R_r .

Calculations

The pyruvate concentration in the samples are determined from the following equation.

$$\frac{R_r - (R_{2,u} - R_{1,u})}{R_r - (R_{2,s} - R_{1,s})} \times C_s = C_u$$

where:

R = fluorometer reading

1 = background (i.e., no NADH)

2 = assay reading (i.e., after NADH added)

r = assay range (i.e., no LDH and full NADH deflection)

C = concentration

u,s = unknown and standard samples, respectively.

Special precautions

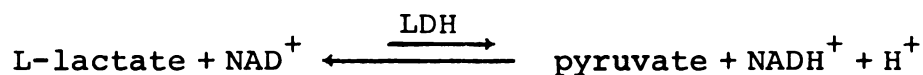
NADH fluorescent properties are temperature dependent, thus all assay mixtures must be read at the same temperature. All tubes used in the direct reading of fluorescence must be soaked in soapy water overnight and then rinsed a minimum of 6 times in hot tap water, followed by 6 rinses in distilled H₂O, and finally 2 rinses in deionized distilled H₂O to remove all trace of fluorescent compounds in the soap.

APPENDIX F

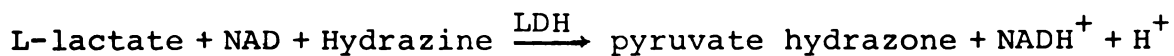
SPECTROPHOTOMETRIC DETERMINATION OF L-LACTATE¹

Principle

Lactate dehydrogenase (LDH) catalyses the oxidation of L-lactate with nicotine-adenine dinucleotide (NAD) to form pyruvate and reduced nicotine-adenine dinucleotide (NADH).



Since the equilibrium of the reaction lies far to the left, the reaction products must be removed from the mixture to obtain quantitative oxidation of L-lactate. Protons are bound by use of an alkaline reaction medium (pH = 9.5) and pyruvate is trapped as the hydrazone. The basic equation describing the reaction used in the spectrophotometric assay of L-lactate is:



The amount of NADH^+ formed is determined by its absorbancy at 340 mμ.

¹From J. P. Ellis *et al.* (1963).

Reagents

1. NaOH, A.R.
2. $(\text{NH}_4)_2\text{SO}_4$, A.R.
3. Hydrazine sulfate, A.R. (Sigma Chemical Co.)
4. Glycine, A.R. (Sigma Chemical Co.)
5. Ethylene-diamine-tetra-acetic acid, EDTA disodium salt, $\text{EDTA-Na}_2\text{H}_2\cdot 2\text{H}_2\text{O}$
6. Nicotine-adenine dinucleotide (NAD; Sigma Chemical Co.)

NAD is stable for periods up to a year when stored frozen and desicated.

7. Lactic dehydrogenase suspension (LDH; Sigma Chemical Co.)

Crystalline preparation from rabbit skeletal muscle which is suspended in 2.1 M ammonium sulfate and stable for periods up to a year if kept between 0-4°C. The concentration of LDH is 5 mg protein/ml with a specific activity of at least 600 units/ml.

8. L-lactic acid standard solution (4.4 mM; Sigma Chemical Co.).

Preparation of solutions

- A. NaOH, 18N

Dissolve 360 g of reagent 1 in distilled H_2O ; q.s. to 500 ml.

B. $(\text{NH}_4)_2\text{SO}_4$, 2.1 M

Dissolve 27.8 g of reagent 2 in distilled H_2O ;
q.s. to 100 ml.

C. Hydrazine-glycine buffer (0.4 M Hydrazine;

1 M glycine; pH 9.5). Suspend 7.5 g of reagent 4, 5.2 g of reagent 3, and 0.2 g of reagent 5 in approximately 30 ml of distilled H_2O . Add solution A until pH 9.5 is obtained and dilute mixture to 100 ml with distilled H_2O . Dilute 50 ml of this solution with equal volume of distilled H_2O for assay. Undiluted hydrazine-glycine buffer solution is stable for at least two weeks when stored at 0-4°C.

D. LDH

Dilute 0.4 ml of reagent 7 to 2 ml with solution B.

E. NAD

Dissolve 160 mg of reagent 6 in 100 ml of diluted solution C just prior to use.

Lactate standard solutions

Lactate standards (0.6, 1.1, 2.2, 3.3 mM) were prepared by diluting 1.25, 2.5, 5.0, and 7.5 ml of reagent 8 to 10 ml with distilled water. L-lactate standards are stable indefinitely, when stored at 0-4°C.

Procedure

To 0.3 ml duplicate aliquots of deproteinized samples, standards, and distilled H₂O (see Appendix B) add 2.0 ml of solution E and mix. Add 0.04 ml solution D and mix. Incubate at room temperature for exactly 35 minutes. Read absorbancy (O.D.) of standard and sample solutions in spectrophotometer (Model DB, Beckman Instruments, Inc.) at 340 mμ against the distilled H₂O blank. Read O.D. again after 45 minutes, and at 10 minute intervals thereafter until readings stabilize. A change in O.D. from the initial reading indicates the reaction was not complete. If the reaction does not reach a constant end point within 60 minutes, more enzyme or a fresh preparation of enzyme is needed because the activity of the LDH (solution D) was too low. All reactants must be at room temperature prior to adding solution D.

Calculations

Plot absorbancy (O.D.₃₄₀) as a function of lactate concentration in the lactate standard solutions. The plot should be linear through a concentration of 4.4 mM. Lactate concentration in the unknown samples can be calculated using the following equation:

$$C_u = \frac{\Sigma (C_s / OD_s)}{n_s} \times OD_u$$

where:

OD = absorbancy

C = concentration

s = standard

u = unknown

n = number of samples.

APPENDIX G

SPECTROPHOTOMETRIC DETERMINATION OF INULIN

(Direct Resorcinol Method Without Alkali Treatment)¹

Principle

Inulin, a polysaccharide, is hydrolyzed into its fructose moieties; fructose reacts stoichiometrically with resorcinol forming a colored complex with peak absorbancy at 490 mμ.

Reagents

1. Resorcinol, A.R.
2. Ethanol, 95%
3. HCl, concentrated, A.R.
4. Inulin, A.R. (Pfanstiehl Lab. Inc., Waukegan, Ill.)

Solutions

- A. Resorcinol (100 mg%)

Dissolve 100 mg of reagent 1 in reagent 2; q.s. to 100 ml. Prepare fresh just prior to assay.

- B. HCl, 10 N

Add 224 ml of distilled H₂O to 776 ml of reagent 3.

¹From H. W. Smith (1956).

Inulin standard solutions

Dissolve 200 mg of reagent 4 in distilled H₂O; q.s. to 100 ml. Pipette 7.5, 5.0, 4.0, 3.0, 2.0, and 1.0 ml of this solution (2 mg/ml) and dilute each to 10 ml with distilled H₂O obtaining 1.5, 1.0, 0.8, 0.6, 0.4, and 0.2 mg/ml standards, respectively. Store inulin standards at 0-4°C.

Procedure

To duplicate 0.05 ml CSF samples (nondeproteinated), inulin standards, and distilled H₂O, add 1.0 ml of solution A and mix. Add 2.5 ml of solution B (in fume hood) and mix. Place marbles on top of test tubes and heat at 80°C for 25 minutes. Cool tubes to room temperature in cold water and read O.D. of samples and standards at 490 mμ in spectrophotometer (Model DB, Beckman Instruments, Inc.) against distilled H₂O blank within one hour.

Calculations

Plot absorbancy (O.D.₄₉₀) as a function of the concentration of the inulin standards. The plot should be linear through a concentration of 2 mg/ml. The concentration of the unknown samples can be determined from the following formula:

$$C_u = \frac{\Sigma (C_s / OD_s)}{n_s} \times OD_u$$

where:

OD = absorbancy

C = concentration

s = standard

u = unknown

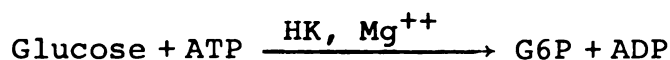
n = number of samples.

APPENDIX H

ISOLATION AND IDENTIFICATION OF RADIOACTIVELY LABELLED GLUCOSE¹

Principle

The sample containing various solutes is passed through an anion exchange resin removing the anions in the sample. The glucose, a neutral molecule, in the effluent is reacted with adenosine triphosphate (ATP) in the presence of hexokinase (HK) and Mg^{++} ion at a pH 8.0 forming glucose-6-phosphate (G6P) and adenosine diphosphate (ADP).



This reaction mixture is passed through another anion exchange resin and G6P is retained on the resin. This G6P is eluted with 3N HCl. Any radioactivity in the eluted sample will be due to radioactively labelled glucose in the initial sample.

Reagents

1. $MgCl_2 \cdot 6H_2O$, A.R.
2. $(NH_4)_2SO_4$, A.R.

¹From H. J. Horhost (1965) and S. England and K. R. Hanson (1969).

3. HCl, concentrated, A.R.
4. KOH, A.R.
5. Tris-hydroxymethyl-aminomethane (Trizma base; Sigma Chemical Co.)
6. Adenosine Triphosphate (ATP; Sigma Chemical Co.) disodium salt, $\text{ATP-Na}_2\text{H}_2\cdot 3\text{H}_2\text{O}$. When stored desiccated and frozen it is stable for at least one year.
7. Hexokinase (HK; Sigma Chemical Co.)
Crystalline preparation from yeast which is suspended in 3.2 M $(\text{NH}_4)_2\text{SO}_4$ and stable for at least one year when stored at 0-4°C. HK concentration is at least 410 mg protein/ml with a specific activity of 2000 units/ml.
8. Dowex 1-8x, Anion Exchange Resin (Cl^- ; Sigma Chemical Co.)
100-200 mesh; 8% crosslinked.

Solutions

- A. MgCl_2 , 0.1 M
Dissolve 2.0 g of reagent 1 in distilled H_2O ; q.s. to 100 ml.
- B. $(\text{NH}_4)_2\text{SO}_4$, 2.1 M
Dissolve 27.8 g of reagent 2 in distilled H_2O ; q.s. to 100 ml.

C. HCl, 3 N

Add 258 ml of reagent 3 to approximately 500 ml of distilled H₂O; q.s. to one liter.

D. Tris buffer, approximately 0.1 M, pH 8.0

To 1.21 g of reagent 5 add approximately 30 ml of distilled H₂O. Adjust to pH 8.0 with solution C; q.s. to 100 ml with distilled H₂O. Tris buffer solution is stable for at least 6 months at 0-4°C.

E. ATP, approximately 0.01 M

Dissolve 30 mg of reagent 6 and dilute to 5 ml with solution D. ATP dissolved in Tris buffer is not stable and must be prepared just prior to use.

F. Hexokinase, HK

Dilute 0.02 ml of reagent 7 to 1.0 ml with solution B. Diluted HK is stable for at least 6 months at 0-4°C.

G. KOH, 5%, w/v.

Dissolve 50 g of reagent 4 in distilled H₂O; q.s. to one liter.

H. Dowex-18X (Cl⁻)

Reagent 8 is washed with distilled H₂O, removing excess acid, and adjusted to pH 6.8 with solution G. The resin is stored at 0-4°C as a slurry and must be rewashed every month.

Procedure

- a. 1.0 ml of deproteinated sample (dilution factor 9.6, see Appendix C) is passed through a Dowex-1 resin (solution G) column (0.5 x 4.0 cm) followed by 1.0 ml of distilled H₂O. The total effluent is adjusted to 2 ml with distilled water.
- b. To convert glucose to glucose-6-phosphate in the 2.0 ml of effluent from part a, add 0.04 ml of solution A, 0.2 ml of solution E, and 0.02 ml of solution F (total volume = 2.26 ml; dilution factor = 21.7). Mix and incubate 10 minutes at room temperature.
- c. Add 2.0 ml of incubation mixture (part b) to another Dowex-1 resin (Cl⁻) column (see part a). Collect effluent (total volume 2.0 ml; dilution factor = 21.7).
- d. Elute glucose-6-phosphate by adding 1.0 ml of solution C and collect 1.0 ml of eluate (dilution factor 10.8).
- e. Repeat steps a-d, substituting distilled H₂O for Hexokinase (solution F) in step b. The radioactivity in this eluate is due to any anions passed through the resin column in step a and must be subtracted from the radioactivity measured in the glucose-6-phosphate eluate (procedure d).

Recovery profile of ^3H -glucose isolation

The recovery of ^3H -activity is shown in Table H for two CSF inflow samples (R_1 , R_2) and for six CSF outflow samples (2, 3, 4, 6, 7, and 8) in dog Sc-1. Duplicate 0.1 ml aliquots of each fluid sample were counted using standard liquid scintillation procedures (Appendix J) on: (1) nondeproteinized sample; (2) following deproteinization; (3) following conversion to glucose-6-phosphate; (4) effluent containing cations and neutral compounds passed through the second Dowex column; and (5) the fluid eluted from the second column with HCl. The deproteinization procedure resulted in a 2-6% loss of ^3H activity; an additional 8-9% of ^3H activity was retained on the first resin column (procedure b). Less than 1% of the ^3H activity was due to conversion to cations or nonglucose neutral molecules (procedure c). Only 1-2% of ^3H activity was lost due to either glucose conversion to anions which passed through column 1 (procedure a) or retention by column 2 (procedure e). In dog Sc-1 only 75% of the original inflow fluid ^3H activity was due to ^3H -glucose; of this 75% there averaged a 92% recovery in the outflow fluid. The relative lack of interconversion of isotopically labelled glucose to other molecules during the perfusion of the brain ventricular spaces has been reported previously (Bronsted, 1970b) and is supported by Table H-1. Similar recoveries were obtained

in all dogs; the amount of ^3H -glucose activity in the perfusion inflow fluid ranged from 79-84% of the original ^3H activity.

Table H-1. Isolation and recovery of ^3H -glucose in the inflow (R_1 ; R_2) and outflow (2, ..., 8) fluids in dog Sc1 (11/17/71)

Step	Dilution Factor	Sample Number						
		R_1	R_2	2	3	4	6	7 8
Original sample Concentration	1	139640	141702	73980	74154	75954	73035	73540 72251
Deproteinization (Appendix C)	9.6							
Concentration		13746	14244	7359	7562	7690	7501	7254 7187
% recovery		94.5	96.5	95.5	97.9	97.2	98.6	94.7 95.5
Column 1 Effluent (Procedure b)	21.7							
Concentration		5546	5710	2956	3016	3096	3010	2920 2898
% recovery		86.2	87.4	86.7	88.3	88.5	89.4	86.2 87.0
Column 2 Effluent (Procedure c)	21.7							
Concentration		63	48	19	3	9	2	6 22
% recovery		1.0	0.7	0.5	0.0	0.1	0.0	0.0 0.5
Column 2 Eluate (Procedure d)	10.8							
Concentration (A)		9650	10317	5009	5452	4868	5028	5004 4629
(Procedure e)	10.8							
Concentration (B)		125	127	298	205	159	278	263 261
Concentration (A-B)		9525	10090	4711	5147	4609	4750	4741 4368
% recovery		73.7	76.9	68.8	75.0	65.5	70.2	69.6 65.3

^aConcentration = $^3\text{dpm}/0.1\text{ ml.}$

^b% recovery = $\frac{\text{Conc'n sample} \times \text{dilution factor} \times 100}{\text{Conc'n original sample}}$.

APPENDIX I

ISOLATION OF LABELLED LACTATE ¹

Principle

Ion-exchange chromatography utilizes the differential affinity of charged molecules in solution for inert, immobile oppositely charged substances on the resin bed. L-lactate, an anion, is bound to an anion (Cl^-) exchange resin. Elution of lactate from the resin bed is accomplished by using a progressively more acid (HCl) eluent. The Cl^- of the acid displaces the weaker anions (such as lactate) bound to the resin bed.

Reagents

1. HCl , concentrated, A.R.
2. Dowex 1-8X Anion Exchange Resin (Cl^- ; Sigma Chemical Co.)
100-200 mesh; 8% crosslinked.
3. KOH , A.R.

¹From R. W. VonKorf (1969).

Solutions

A. KOH, 5%, w/v.

Dissolve 50 g of reagent 3 in distilled H₂O;
q.s. to one liter.

B. HCl, 0.01 N

Add 0.8 ml of reagent 1 to distilled H₂O;
q.s. to one liter.

C. HCl, 0.05 N

Add 4.2 ml of reagent 1 to distilled H₂O;
q.s. to one liter.

D. HCl, 0.1 N

Add 8.4 ml of reagent 1 to distilled H₂O;
q.s. to one liter.

Preparation of resin column

Reagent 2 is washed with distilled H₂O to remove impurities and acid. After washings reach approximately pH 4.5, the resin suspension in water is adjusted to pH 6.8 with solution A and stored as a slurry at 0-4°C.

A resin column (1 X 17 cm) is formed by pouring water-suspended resin into a 50 ml burette. Packing of the column is aided if the tip of the burette is attached to an aspirator. The packed resin column should have about 2 mm of water remaining above the resin at all times.

Procedure

- a. A 2 ml aliquot of the deproteinated sample (pH 6.8-7.2; Appendix C) is added to the resin column and allowed to drain into the resin bed. The burette stopcock is closed until sample is to be eluted.
- b. Begin elution with distilled H₂O via gravity flow from an eluant flask into a reservoir flask (continuously stirred). Fluid from reservoir flask passes via siphon to the resin column. Elute and collect ten 5 ml fractions using an automatic fraction collector (Model 1205 DE, Warner-Chilcott Lab., Richmond, Cal.).
- c. After 10 fractions have been collected, empty eluant flask, add 0.01 N HCl (solution B) and continue elution. Collect ten 5 ml fractions.
- d. Again empty eluant flask, refill with solution C and collect twenty 5 ml fractions.
- e. Repeat step d refilling with solution D and collecting twenty 5 ml fractions.
- f. Radioactivity of labelled material in each fraction is counted using 0.1 ml duplicate aliquots from each 5 ml sample tube (see Appendix J). The eluted fractions containing L-lactate (lactate peak) are identified by chemical methods (Appendix F).

L-lactate elution profile

The results from eluting a single CSF sample (vial 8; dog Sc-1) are shown in Figure I-1. There is a single peak corresponding to ^3H activity (fractions 2-6) and a single peak corresponding to ^{14}C activity (fractions 29-33). ^3H -glucose, a neutral molecule, is eluted first since it is not bound by the anion exchange resin. The total ^{14}C activity (dpm) in fractions 29-33 (Table I-1) corresponds to 95% of the total ^{14}C activity in the sample. The specific activity (dpm/mg) (Table I-1) is the same in fractions 30-32 as in the initial CSF sample (collected after 4 hours of ventricular perfusion) suggesting that ^{14}C activity remains on L-lactate during perfusion. Similar recoveries and specific activities were obtained from single samples for seven dogs.

Figure I-1. Elution profile of CSF outflow sample (vial 8; Dog Sc-1) containing ^3H -glucose and ^{14}C -lactate. The ordinate on the left corresponds to radioactivity ($\text{dpm} \times 10^3$); the ordinate on the right to the concentration of L-lactate (mg/ml). The abscissa corresponds to the fraction tube number (5 ml).

● ^3H dpm
 ▲ ^{14}C dpm
 ■ mg/ml L-lactate

Mixing chamber contained 100 ml of eluant fluid. Arrows (from left to right) indicate when eluant was changed from distilled H_2O to 0.01 N, 0.05 N, and 0.1 N HCl, respectively.

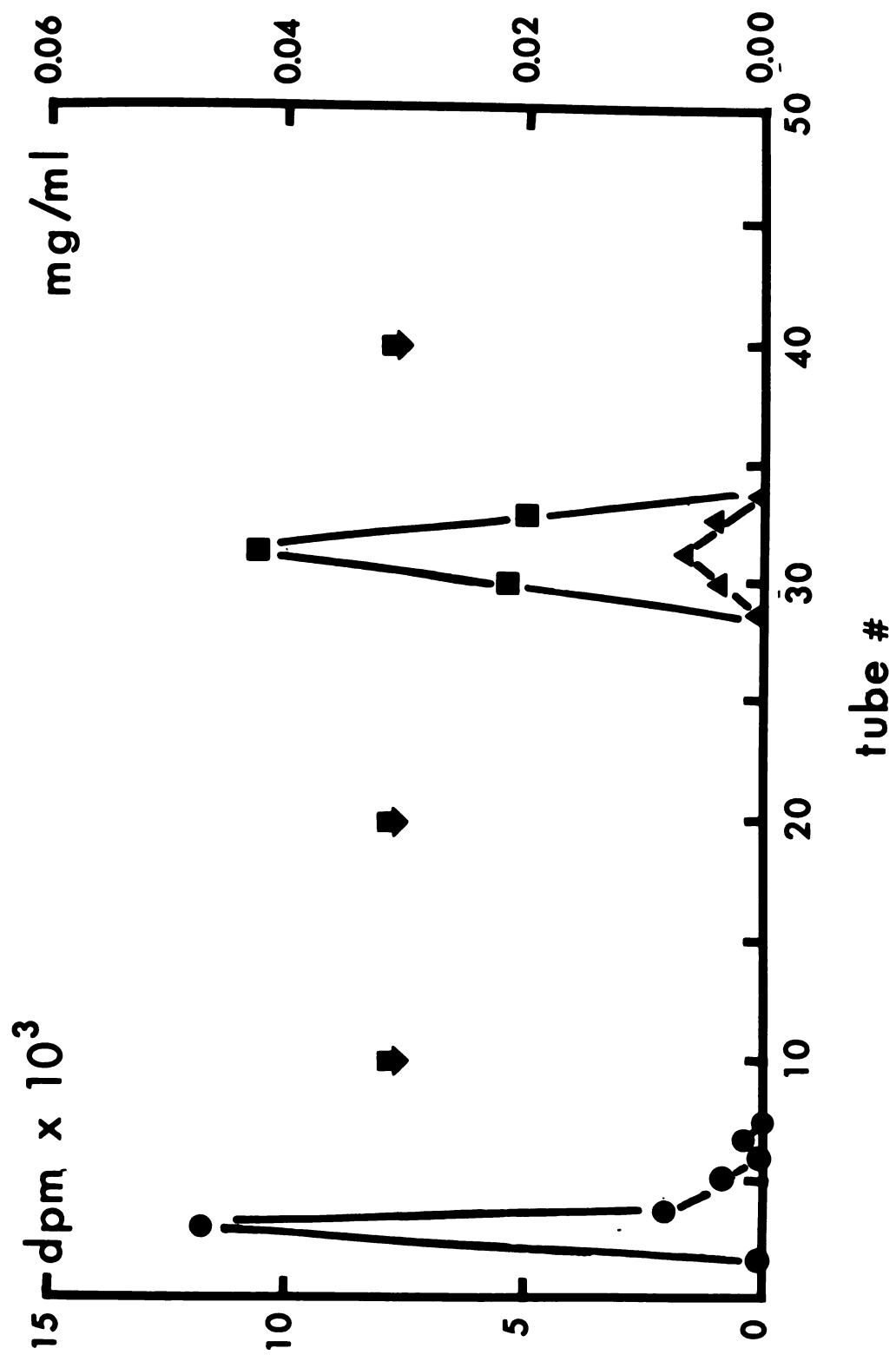


Figure I-1

Table I-1. Isolation of ^{14}C -lactate in ventricular perfusion effluent (Vial #8; Dog Sc-1; 11/17/71)

Sample	Volume (ml)	^{14}C activity			Specific activity (dpm/mg)
		dpm/0.1 ml	Total dpm	dpm/ml	
Vial 8	2.0	9,133	182,660	91,330	409,551
Fraction #					
29	5.0	7	350	70	0
30	5.0	957	48,750	9,570	416,087
31	5.0	1,687	84,350	16,870	411,463
32	5.0	802	40,100	8,020	401,000
33	5.0	2	100	20	0

APPENDIX J

LIQUID SCINTILLATION COUNTING¹

Principle

Liquid scintillation counting is a method of detecting radioactivity. The radioactive substance is dissolved in or completely wetted by the scintillation solution. The scintillation solution converts the energy of the primary particle emitted by the radioactive sample to light energy. The light quanta entering the multiplier phototube are amplified and counted by a scaling circuit.

The widest application of liquid scintillation counting has been in the counting of low energy beta emitters such as ^3H and ^{14}C . In any radiation detection method, the counting efficiency (ratio of observed counting rate to the actual rate of radioactive disintegrations in the sample) is greatest when the maximum number of emitted particles reaches and interacts with the multiplier phototube. Absorption along their paths within the sample and between the sample and the detector is most severe for low energy beta emissions; such losses are reduced and counting

¹From Instruction Manual, Mark I liquid scintillation computer, Model 6860, Nuclear-Chicago Corp., Des Plaines, Ill.

efficiency is increased by dissolving the radioactive sample directly in the scintillation solution.

Scintillation counting is a proportional counting method, i.e., the magnitude of the output signal from the detector is proportional to the energy given up to the detector by the primary particle. This signal is amplified and fed into a pulse height analyzer which compares the signal to reference voltages. A discriminator circuit passes the signal if it falls between two selected voltage levels. Counting between two finite discriminator levels is referred to as differential counting.

The energy spectra of ^3H and ^{14}C overlap, and when both beta emitters are present in the same sample they are counted simultaneously on two separate analyzer channels. Channel A amplifiers were adjusted to give high efficiency of counting ^3H with minimal interference of ^{14}C ; the amplifiers of channel C were set so that counting efficiency of ^3H was insignificant while efficiency for ^{14}C was maximal. Channel B amplifiers were set to maximize energy pulses from an external standard of known disintegration rate (^{133}Ba).

Quench correction curve

Any nonfluorescent solute or solvent will absorb or quench energy emitted from the primary particle and reduce the efficiency of counting the radioactivity. A set of ^3H and ^{14}C standards (Nuclear-Chicago Corp.) containing

known amounts of isotope (492,000 dpm and 255,000 dpm, respectively) and varying degrees of quenching for each isotope over the range used in these experiments were used to determine:

1. ^3H counting efficiency in channel A
2. ^{14}C counting efficiency in channel A
3. ^{14}C counting efficiency in channel C.

The external standard, ^{133}Ba , is used to determine the amount of quenching present in each sample. The channels ratio relates the net ^{133}Ba count rate in the channel (B) (i.e., preset to maximum ^{133}Ba efficiency) to the net ^{133}Ba count rate in channel A. Since the sample will quench energy emitted by the gamma source, ^{133}Ba , the channels ratio ($B/A = (\text{cpm}) \text{ channel B} / (\text{cpm}) \text{ channel A}$) increases as the amount of quenching decreases.

The quench correction curve (Figure J-1) is a plot of the efficiencies of ^3H and ^{14}C standards as a function of the standards' channels ratio (B/A). Counting efficiency of each isotope in an unknown sample can be read directly from the quench correction curve corresponding to the unknown sample's channels ratio (B/A).

Calculation of disintegration rates of ^3H and ^{14}C

The disintegration rates of unknown samples can be calculated from the net count rate of ^3H and ^{14}C and the efficiencies of counting each isotope in channels A and C from the following equations:

$$D_H = \frac{N_1 c_2 - N_2 c_1}{h_1 c_1}$$

$$D_C = \frac{N_2}{c_2}$$

where:

D_H = disintegration rate (dpm) of ^3H

D_C = disintegration rate (dpm) of ^{14}C

N_1 = count rate (cpm) in channel A

N_2 = count rate (cpm) in channel C

h_1 = counting efficiency (%) for ^3H in channel A

c_1 = counting efficiency (%) for ^{14}C in channel A

c_2 = counting efficiency (%) for ^{14}C in channel C.

Figure J-1. ^{133}Ba Barium external standard quench correction curves for differential counting of ^3H and ^{14}C samples. Efficiencies are calculated as net cpm on scaler A or C divided by dpm of ^3H or ^{14}C standards, respectively; multiplied by 100. ^{14}C quench correction curve for ^{14}C efficiency in channel C (squares); ^3H quench correction curve for ^3H efficiency in channel A (circles); ^{14}C quench correction curve for ^{14}C efficiency in channel A (triangles) are plotted as a function of channels ratio (B/A) of ^{133}Ba .

Discriminator settings:

<u>Channel</u>	<u>Window</u>	<u>Attenuation</u>
A	0.0-2.5	B524
B	0.0-9.9	F670
C	1.5-9.9	E738

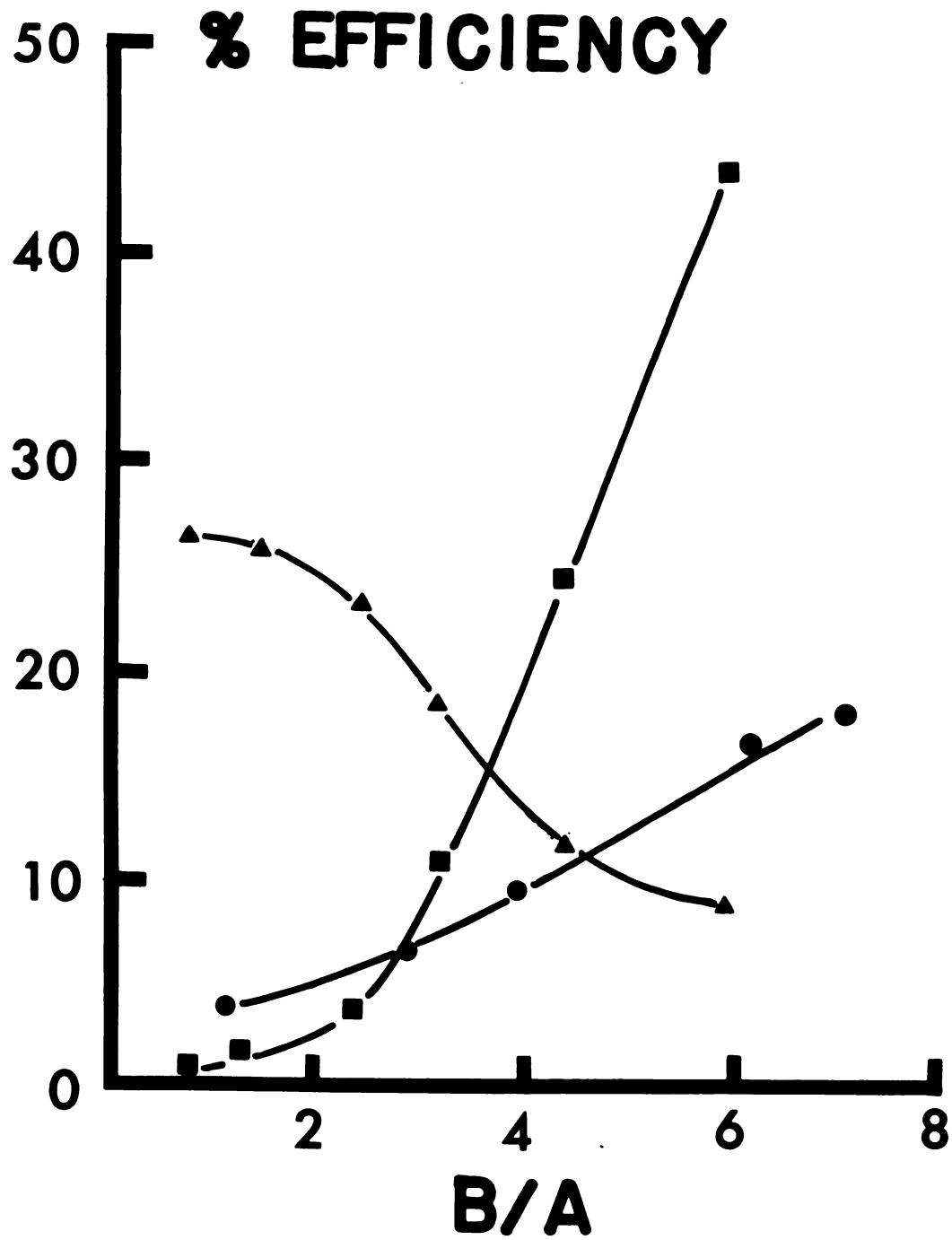


Figure J-1

APPENDIX K

STATISTICAL FORMULAE

Grand Mean: $\bar{\bar{X}} = \frac{\sum \bar{x}}{n}$

where:

$\sum \bar{x}$ = sum of individual means

n = number of individual means.

Standard error of grand mean (SE).

$$SE = \sqrt{\frac{\sum \bar{x}^2 - (\sum \bar{x})^2/n}{n(n-1)}}$$

Split plot design (Steel and Torrie, 1960)

The split plot analysis of variance (AOV) was employed since the experimental design incorporated the inclusion of two variable factors: perfusion time and metabolite concentration. The statistical formulae employed in the calculation of the sums of squares (SS) and the evaluation of the F statistics (Table K-2) are given below and illustrated from data in Table K-1.

X_{ijk} is the kth observation on the ith concentration in the jth period, and $X_{...}$ is the sum of all observations at all concentrations in all periods. Then n_{ij} = number of observations at the ith concentration; jth period.

$$n_i = \sum_{j=1}^{j=2} n_{ij} \quad n_j = \sum_{i=1}^{i=3} n_{ij} \quad n = \sum_{ij} n_{ij}$$

$$(I) \text{ Total sum of squares (SS)} = \sum X_{ijk}^2 - C = 100^2 + \dots + 90^2 - C$$

$$= 43,019.37$$

$$(II) \text{ Where } C = \frac{X^2 \dots}{n} = 3197^2/30 = 340,693.63$$

$$(III) \text{ Concentration SS} = \frac{X_{i..}^2}{n_i} - C = \frac{215^2 + \dots + 352^2}{12} + \dots - C$$

$$= 21,598.08$$

$$(IV) \text{ Dogs within Concentration SS} = \sum X_{i.k}^2 - C - (III) = \frac{1673^2 + 669^2 + 855^2}{2} - C - (III)$$

$$= 20,790.79$$

$$(V) \text{ Period SS} = \frac{\sum X_{.j.}^2}{n_j} - C = \frac{1596^2}{15} + \frac{1601^2}{15} - C$$

$$= 0.87$$

$$(VI) \text{ Interaction SS} = \frac{\sum X_{ij.}^2}{n_{ij}} - C - (III) - (V) = \frac{825^2 + 848^2}{6} + \dots - C - (III) - (V)$$

$$= 73.24$$

$$(VII) \text{ Error b SS} = (I) - (II) - (IV) - (V) - (VI)$$

$$= 1135.10$$

Analysis of mean differences employed Student's t distribution and was calculated by the following formulae.

$$\text{Test statistic } t_s = \frac{\bar{d}}{s_{\bar{d}}}$$

where:

\bar{d} = mean difference

$s_{\bar{d}}$ = standard error of the difference.

A. If there was no significant interaction between concentration and test periods.

1. To compare the difference between individual period means (j).

$$\bar{d} = \frac{\sum (\bar{x}_{.1} - \bar{x}_{.2})}{n_{ij}} = \frac{(100-115) + \dots + (175-177)}{6} = -7$$

$$s_{\bar{d}} = \sqrt{2(\text{Error b})/n_j} = \sqrt{\frac{2(1,135.10)}{12}} = 13.8$$

2. To compare the difference between grand means of any two concentrations within a period.

$$\bar{d} = x_{ij\cdot} - x'_{ij\cdot} = 825 - 335 = 490$$

$$s_{\bar{d}} = \sqrt{\text{Error a} \left[\frac{n_{ij} + n'_{ij}}{n_{ij} n'_{ij}} \right]} = \sqrt{20,790.79 \left[\frac{12 + 8}{96} \right]} = 65.8$$

B. If there was a significant interaction between concentration and the test period. (This situation was not evident in the present example, nor was it evident for any of the other molecules analyzed in this manner.) To analyze differences between two j means at the same concentration (i), or between i means in the same period.

$$s_{\bar{d}} = \sqrt{\left[(b-1) \text{ Error b} + \text{Error a} \right] \left(\frac{n_{ij} + n'_{ij}}{n_{ij} n'_{ij}} \right)}$$

where

b = number of different concentrations.

Table K-1. Statistic block of glucose K_0 data from 15 normoxic anesthetized dogs at different inflow concentrations (A, B, and C) during two experimental brain ventricular perfusion periods

Concentration (i)	Period (j)		Concentration Total	n_i
	x_{i1k}	x_{i2k}		
x_{1jk} (A)	100	115	215	12
	177	161	338	
	126	139	265	
	145	157	302	
	102	99	201	
	<u>175</u>	<u>177</u>	<u>352</u>	
Period total	825	848	1673	
x_{2jk} (B)	80	83	163	8
	83	78	161	
	86	91	177	
	<u>86</u>	<u>82</u>	<u>168</u>	
	335	334	669	
x_{3jk} (C)	146	145	291	10
	64	69	133	
	81	76	157	
	57	39	96	
	<u>88</u>	<u>90</u>	<u>178</u>	
	436	419	855	
Grand total	1596	1601	3197	
n_j	15	15		$n=30$

Table K-2. AOV table

Source	df	SS	MS	F
Concentration (III)	2	21,598.08	10,799.04	6.23*
Error a (IV)	12	20,790.79	1,732.56	
Period (V)	1	0.87	0.87	< 1.0
Interaction (VI)	2	73.24	36.62	< 1.0
Error b (VII)	12	1,135.10	94.59	

*p < 0.05.

df = degrees of freedom

MS = mean square = SS/df

Test statistic F (AOV)

To test variances between concentrations:

$$F = MS_{III}/MS_{IV}$$

To test variances between periods:

$$F = MS_V/MS_{VII}$$

To test interaction between concentrations and periods:

$$F = MS_{VI}/MS_{VII}.$$

LIST OF REFERENCES

LIST OF REFERENCES

- Alexander, S. C., R. D. Workman, and J. C. Lambertsen. 1962. Hyperthermia, lactic acid infusion, and composition of arterial blood and cerebrospinal fluid. *Amer. J. Physiol.* 202:1049-1054.
- Aldridge, W. N. 1962. *Enzymes and Drug Action*. CIBA Found. Sympos., London, 1961. ed. by A.V.S. DeReuck. Boston: Little, Brown & Co., pp. 155-169.
- Ames, A., K. Higaski, and F. B. Nesbett. 1965a. Relation of potassium concentration in choroid plexus fluid to that in plasma. *J. Physiol.* 181:506-515.
- Ames, A., K. Higashi, and F. B. Nesbett. 1965b. Effects of PCO₂, acetazolamide and ouabain on volume and composition of choroid plexus fluid. *J. Physiol.* 181:516-524.
- Arey, L. B. 1962. *Developmental Anatomy*. 6th ed. Philadelphia: W. B. Saunders Co., pp. 472-506.
- Atkinson, A. J., Jr., and M. F. Weiss. 1970. Kinetics of blood-cerebrospinal fluid glucose transfer in the normal dog. *Amer. J. Physiol.* 216:1120-1126.
- Baethmann, A., U. Steude, S. Horsch, and W. Brendel. 1970. The thiosulphate (³⁵S) space in the CNS of rats after ventriculo-cisternal perfusion. *Pflugers Arch* 316:51-63.
- Baky, L., and J. C. Lee. 1968. The effect of acute hypoxia and hypercapnia on the ultrastructure of the central nervous system. *Brain* 91:697-706.
- Barlow, C. F., M. S. Domek, M. A. Goldberg, and L. J. Roth. 1961. Extracellular brain space measured by ³⁵S-sulphate. *Arch. Neurol.* 5:102-110.
- Bergmeyer, H. U., and E. Bernt. 1965. *Methods of Enzymatic Analysis*. ed. by H. U. Bergmeyer. New York: Academic Press, pp. 123-130.

- Bering, E. A. 1959. Cerebrospinal fluid production and its relationship to cerebral metabolism and cerebral blood flow. *Amer. J. Physiol.* 197:825-828.
- Bering, E. A., and O. Sato. 1963. Hydrocephalus: Changes in formation and absorption of cerebrospinal fluid within the cerebral ventricles. *J. Neurosurg.* 20:1050-1063.
- Bidder, T. G. 1968. Hexose translocation across the blood brain interface: configurational aspects. *J. Neurochem.* 15:867-874.
- Bierer, D. W. 1972. Active transport of organic anions from the brain ventricles of the dog. (Master's thesis), Michigan State University. East Lansing, Michigan.
- Bito, L. Z., and H. Davson. 1966. Local variations in cerebrospinal fluid composition and its relationship to the composition of the extracellular fluid of the cortex. *Exp. Neurol.* 14:264-280.
- Bondareff, W., R. E. Myers, and A. W. Brann. 1970. Brain extracellular space in monkey fetuses subjected to prolonged partial asphyxia. *Exp. Neurol.* 28:167-178.
- Bradbury, M. W. B., and H. Davson. 1964. The transport of urea, creatinine, and certain monosaccharides between blood and fluid perfusing the cerebral ventricular system of rabbits. *J. Physiol.* 170:195-211.
- Bronsted, H. E. 1970a. Ouabain-sensitive carrier-mediated transport of glucose from the cerebral ventricles and surrounding tissues in the cat. *J. Physiol.* 208:187-201.
- Bronsted, H. E. 1970b. Transport of glucose, sodium, chloride, and potassium between the cerebral ventricle and surrounding tissues in cats. *Acta Physiol. Scand.* 79:523-532.
- Brooks, G. F., A. Koch, and J. Wong. 1970. Kinetics of sodium transfer from blood to brain of the dog. *Amer. J. Physiol.* 218:693-702.
- Bucher, T., R. Csok, W. Lamprecht, and E. Latzo. 1965. *Methods of Enzymatic Analysis*. ed. by H. U. Bergmeyer. New York: Academic Press, pp. 253-259.
- Buschiazzo, P. M., E. B. Terrell, and D. M. Regen. 1970. Sugar transport across the blood-brain barrier. *Amer. J. Physiol.* 219:1505-1513.

- Cain, S. 1965. Appearance of excess lactate in anesthetized dogs during anemic and hypoxic hypoxia. *Amer. J. Physiol.* 209:604-610.
- Crone, C. 1965. Facilitated transport of glucose from blood into brain tissue. *J. Physiol.* 181:103-113.
- Csaky, T. Z., and B. M. Rigor. 1968. The choroid plexus as a glucose barrier. *Prog. in Brain Res.* 29:147-154.
- Cserr, H. 1965. Potassium exchange between cerebrospinal fluid, plasma, and brain. *Amer. J. Physiol.* 209:1219-1226.
- Cutler, R. W. P., R. J. Robinson, and A. V. Lorenzo. 1968. Cerebrospinal fluid transport of sulfate in the cat. *Amer. J. Physiol.* 214:448-454.
- Dahl, N. A., and W. M. Balfour. 1964. Prolonged anoxic survival due to anoxia pre-exposure: brain ATP, lactate, and pyruvate. *Amer. J. Physiol.* 207:452-456.
- Dandy, W. E. 1919. Experimental hydrocephalus. *Ann. Surg.* 70:129-142.
- Dandy, W. E., and K. D. Blackfan. 1914. Internal hydrocephalus. An experimental clinical and pathological study. *Amer. J. Dis. Child.* 8:406-482.
- Davson, H. 1967. *Physiology of Cerebrospinal Fluid*. 1st ed. London: J. & A. Churchill Ltd.
- Davson, H., and J. F. Danielli. 1952. *The Permeability of Natural Membranes*. 2nd ed. Cambridge, England: Cambridge University Press.
- Davson, H., C. R. Kleeman, and E. Levin. 1961. Blood-brain barrier and extracellular space. *J. Physiol.* 159:67-86.
- Davson, H., C. R. Kleeman, and E. Levin. 1962. Quantitative studies of the passage of different substances out of the cerebrospinal fluid. *J. Physiol.* 161:126-142.
- Davson, H., and M. Pollay. 1963. Influence of various drugs on the transport of ^{131}I and PAH across the cerebrospinal fluid-blood barrier. *J. Physiol.* 167:239-246.
- Davson, H., and M. B. Segal. 1970. The effect of some inhibitors and accelerators of sodium transport on the turnover of ^{22}Na in the cerebrospinal fluid and the brain. *J. Physiol.* 209:131-153.

- Davson, H., and E. Spaziani. 1959. The blood-brain barrier and the extracellular space of brain. *J. Physiol.* 149: 135-143.
- Dunn, R. B., and F. Liroy. 1971. Lactate and pyruvate levels in brain and skeletal muscle during hyperthermia in dogs. *Can. J. Physiol. Pharmacol.* 49:520-524.
- Ellis, J. P., S. M. Cain, and E. W. Williams. 1963. Rapid accurate analysis of blood lactate. Tech. Doc. Report No. SAM-TDR-63-49. USAF School of Aerospace Medicine, Aerospace Medical Div. (AFSC) Brooks Air Force Base, Texas.
- Englard, S., and K. R. Hanson. *Methods in Enzymology*. XIII. ed. by J. W. Lowenstein. New York: Academic Press, pp. 573-574.
- Eich, J., and K. Wiemers. 1959. Cited by Davson, 1967.
- Ferguson, R. K., and D. M. Woodbury. 1969. Penetration of ^{14}C -inulin and ^{14}C -sucrose into brain, cerebrospinal fluid, and skeletal muscle of developing rats. *Exp. Brain Res.* 7:181-194.
- Fishman, R. A. 1964. Carrier transport of glucose between blood and cerebrospinal fluid. *Amer. J. Physiol.* 206: 836-844.
- Fleischhauer, K. 1957. Untersuchungen am Ependym des Zwischen-und Mittel-hirns der Landschildkröte. *Z. Zellforsch.* 46:729-769.
- Flexner, L. B. 1933. A note on the rate of circulation of cerebrospinal fluid. *Amer. J. Physiol.* 106:201-203.
- Folbergrova, J., O. H. Lowry, and J. Passoneau. 1970. Changes in metabolites of the energy reserves in individual layers of mouse cerebral cortex and subjacent white matter during ischaemia and anaesthesia. *J. Neurochem.* 17:1155-1162.
- Forbes, H. S. 1928. Observation and measurement of pial vessels. *Arch. Neurol. Psychiat.* 19:751-761.
- Frazier, C. H., and M. M. Peet. 1914. Factors of influence in the origin and circulation of the cerebrospinal fluid. *Amer. J. Physiol.* 35:268-282.

- Friedman, S. B., W. G. Austin, R. E. Rieselbach, J. B. Block, and D. P. Rall. 1963. Effect of hypochloremia on cerebrospinal fluid chloride concentration in a patient with anorexia nervosa and in dogs. *Proc. Soc. Exp. Biol. N. Y.* 114:801-805.
- Fujishima, M., P. Scheinberg, and R. Busto. 1971. Cerebral cortical blood flow. Variable effects of hypoxia in the dog. *Arch. Neurol.* 25:160-167.
- Gatfield, D. P., O. H. Lowry, D. W. Schulz, and J. Passonneau. 1966. Regional energy reserves in mouse brain and changes with ischaemia and anesthesia. *J. Neurochem.* 13:185-195.
- Geiger, A. 1958. Correlation of brain metabolism and function by use of a brain perfusion method in situ. *Physiol. Reviews* 38:1-20.
- Geiger, A., J. Magnes, R. M. Taylor, and M. Veralli. 1954. Effect of blood constituents on uptake of glucose and metabolic rate in brain perfusion experiments. *Amer. J. Physiol.* 177:138-149.
- Gibbs, E. L., W. G. Lennox, L. F. Nims, and F. A. Gibbs. 1942. Arterial and cerebral venous blood. Arterial-venous differences in man. *J. Biol. Chem.* 144:325-332.
- Gilboe, D. D., R. L. Andrews, and G. Dardenne. 1970. Factors affecting glucose uptake by the isolated dog brain. *Amer. J. Physiol.* 219:767-773.
- Goodale, R. L., B. Goetzman, and M. B. Visscher. 1970. Hypoxia and iodoacetic acid and alveolocapillary barrier permeability to albumin. *Amer. J. Physiol.* 219:1226-1230.
- Granholm, L., A. E. Kassik, L. Nilsson, and B. K. Siesjo. 1968. The lactate/pyruvate ratios of cerebrospinal fluid of rats and cats related to the lactate/pyruvate, the ATP/ADP, and the phosphocreatine/creatine ratios of brain tissue. *Acta Physiol. Scand.* 74:398-409.
- Granholm, L., and B. K. Siesjo. 1967. Lactate and pyruvate concentrations in blood, cerebrospinal fluid, and brain tissue of the cat. *Acta Physiol. Scand.* 70:255-256.
- Granholm, L., and B. K. Siesjo. 1969. The effects of hypercapnia and hypocapnia upon the cerebrospinal fluid lactate and pyruvate concentrations and upon the lactate, pyruvate, ATP, ADP, phosphocreatine, and creatine concentrations of cat brain tissue. *Acta Physiol Scand.* 75:257-266.

- Gurdjian, E. S., W. E. Stone, and J. E. Webster. 1944. Cerebral metabolism in hypoxia. *Arch. Neurol. Psychiat.* 51:472-477.
- Hasegawa, T., J. R. Ravens, and J. F. Toole. 1967. Pre-capillary arteriovenous anastomoses "thoroughfare channels" in the brain. *Arch. Neurol.* 16:217-224.
- Hassin, G. B. 1948. The morphology of the pial blood vessels and its bearing on the formation and absorption of the cerebrospinal fluid. *J. Neuropath.* 7:432-438.
- Heisey, S. R., D. Held, and J. R. Pappenheimer. 1962. Bulk flow and diffusion in the cerebrospinal fluid system of the goat. *Amer. J. Physiol.* 203:775-781.
- Hodgkin, A. L., and R. D. Keynes. 1955. Active transport of cations in giant axons from *Sepia* and *Loligo*. *J. Physiol.* 128:28-60.
- Holloway, L. S., S. Cassin, and I. Weinstein. 1972. The effect of hypoxia, acetazolamide and ouabain on CSF production rate in the newborn dog. *Fed. Proc.* 31:223.
- Horhost, H. J. 1965. *Methods of Enzymatic Analysis*. ed by H. U. Bergmeyer. New York: Academic Press, pp. 117-123.
- Horstman, E. 1954. Die Faserghlia des Selachiergehins. *Z. Zellforsch.* 39:588-617.
- Huckabee, W. E. 1958a. Relations of pyruvate and lactate during anaerobic metabolism. I. Effects of infusion of pyruvate or glucose and of hyperventilation. *J. Clin. Invest.* 37:244-254.
- Huckabee, W. E. 1958b. Relationships of pyruvate and lactate during anaerobic metabolism. III. Effect of breathing low oxygen gases. *J. Clin. Invest.* 37:264-271.
- Huggett, A. G., and D. A. Nixon. 1957. Use of glucose oxidase, peroxidase, and o-dianisidine in determination of blood and urinary glucose. *Lancet* 273:368-370.
- Kaasik, A. E., L. Nilsson, and B. K. Siesjo. 1970. The effect of asphyxia upon lactate, pyruvate, and bicarbonate concentrations of brain tissue and cisternal CSF, and upon the tissue concentrations of phosphocreatine and adenine nucleotides in anesthetized rats. *Acta Physiol. Scand.* 78:433-477.

- Kemeny, A., H. Boldizsar, and G. Pethes. 1961. The distributions of cations in plasma and cerebrospinal fluid following infusion of solutions of salts of sodium, potassium, magnesium, and calcium. *J. Neurochem.* 7:218-227.
- Kerr, S. E., and M. Ghantus. 1936. The carbohydrate metabolism of brain. II. The effect of varying the carbohydrate and insulin supply on the glycogen, free sugar, and lactic acid in mammalian brain. *J. Biol. Chem.* 116:9-20.
- Kety, S. S. 1950. Circulation and metabolism of the human brain in health and disease. *Amer. J. Med.* 8:205-217.
- Kety, S. S., and C. F. Schmidt. 1948. The effects of altered arterial tensions of carbon dioxide and oxygen on cerebral blood flow and cerebral oxygen consumption of normal young men. *J. Clin. Invest.* 27:484-492.
- Klein, J. R., and N. G. Olsen. 1947. Distribution of intravenously injected glutamate, lactate, pyruvate, and succinate between blood and brain. *J. Biol. Chem.* 167:1-5.
- LeFevre, P. G., and A. A. Peters. 1966. Evidence of mediated transfer of monosaccharides from blood to brain in rodents. *J. Neurochem.* 13:35-46.
- Lending, M., L. B. Slobody, and J. Mestern. 1961. Effect of hyperoxia, hypercapnia, and hypoxia on blood-cerebrospinal fluid barrier. *Amer. J. Physiol.* 200:959-962.
- Leusen, I. 1948. Influences des modifications simultanées de la concentration en ions K et Ca du liquide cephalorachidien sur le système vasomoteur. *Experientia* 4:154-155.
- Levin, V. A., J. D. Fenstermacher, and C. S. Patlak. 1970. Sucrose and inulin space measurements of cerebral cortex in four mammalian species. *Amer. J. Physiol.* 219:1528-1533.
- Lorenzo, A. V., J. P. Hammerstad, and R. W. P. Cutler. 1968. The effect of anaesthetic agents on the cerebrospinal fluid clearance of ^{35}S -sulfate and ^{125}I -iodide. *Biochem. Pharmacol.* 17:1279-1283.

- Lowry, O. H., J. V. Passonneau, F. X. Hasselberger, and D. W. Schultz. 1964. Effect of ischemia on known substrates and cofactors of the glycolytic pathway in brain. *J. Biol. Chem.* 239:18-30.
- Macri, F., A. Politoff, R. Rubin, R. Dixon, and D. Rall. 1966. Preferential vasoconstriction properties of acetazolamide on the arteries of the choroid plexus. *Int. J. Neuropharmacol.* 5:109-115.
- Maddock, S., J. E. Hawkins, and E. Holmes. 1939. The adequacy of substances of the glucose cycle for the maintenance of normal cortical potentials during hypoglycemia produced by hepatectomy with abdominal evisceration. *Amer. J. Physiol.* 125:551-565.
- Mayman, C. I., P. D. Gatfield, and B. McL. Breckenridge. 1964. The glucose content of the brain in anesthesia. *J. Neurochem.* 11:483-487.
- Merlis, J. K. 1940. The effect of changes in the calcium content of the cerebrospinal fluid on spinal reflex activity in the dog. *Amer. J. Physiol.* 131:67-72.
- Michael, D. K., D. W. Bierer, and S. R. Heisey. 1971. Hypoxia-induced changes in clearance from cerebrospinal fluid. *Fed. Proc.* 30:215.
- Michael, D. K., D. W. Bierer, and S. R. Heisey. 1972. Effects of anesthesia and hypoxia on cerebrospinal fluid production in the adult dog. *Fed. Proc.* 31:395.
- Millen, J. W., and D. H. M. Woollman. 1961. On the nature of the pia mater. *Brain* 84:514-520.
- Milne, M. D., B. H. Scribner, and M. A. Crawford. 1958. Non-ionic diffusion and the excretion of weak acids and bases. *Amer. J. Med.* 24:709-725.
- Myers, R. E., R. Beard, and K. Adamsons. 1969. Brain swelling in the newborn rhesus monkey following prolonged partial asphyxia. *Neurol.* 19:1012-1018.
- McGinty, D. A. 1929. The regulation of respiration. XXV. Variations in the lactic acid metabolism in the intact brain. *Amer. J. Physiol.* 88:312-325.
- Olsen, N. S., and G. G. Rudolph. 1955. Transfer of sodium and bromide ions between blood, cerebrospinal fluid, and brain tissue. *Amer. J. Physiol.* 183:427-432.

- Oppelt, W. W., T. H. Maren, E. S. Owens, and D. P. Rall. 1963a. Effects of acid-base alterations on cerebrospinal fluid production. *Proc. Soc. Exp. Biol. N. Y.* 114:86-89.
- Oppelt, W. W., E. S. Owens, and D. P. Rall. 1963b. Calcium exchange between blood and cerebrospinal fluid. *Life Sci.* 8:599-605.
- Oppelt, W. W., C. S. Patlak, and D. P. Rall. 1964. Effect of certain drugs on cerebrospinal fluid production in the dog. *Amer. J. Physiol.* 206:247-250.
- Pappenheimer, J. R., V. Fencel, S. R. Heisey, and D. Held. 1965. Role of cerebral fluids in control of respiration as studied in unanesthetized goats. *Amer. J. Physiol.* 208:436-450.
- Pappenheimer, J. R., S. R. Heisey, and E. F. Jordan. 1961. Active transport of diodrast and phenosulfonphthalein from cerebrospinal fluid to blood. *Amer. J. Physiol.* 200:1-10.
- Plum, F., and J. B. Posner. 1967. Blood and cerebrospinal fluid lactate during hyperventilation. *Amer. J. Physiol.* 212:864-870.
- Plum, F., J. B. Posner, and W. W. Smith. 1968. Effect of hyperbaric-hyperoxic hyperventilation on blood, brain, and CSF lactate. *Amer. J. Physiol.* 215:1240-1244.
- Pollay, M., and R. Curl. 1967. Secretion of cerebrospinal fluid by the ventricular ependyma of the rabbit. *Amer. J. Physiol.* 213:1031-1038.
- Pollay, M., and H. Davson. 1963. The passage of certain substances out of the cerebrospinal fluid. *Brain* 86: 137-150.
- Prockop, L. D. 1968. Cerebrospinal fluid lactic acid: Clearance and effect on facilitated diffusion of a glucose analogue. *Neurol.* 18:189-196.
- Raichle, M. E., J. B. Posner, and F. Plum. 1970. Cerebral blood flow during and after hyperventilation. *Arch. Neurol.* 23:394-403.
- Rall, D. P., W. W. Oppelt, and C. S. Patlak. 1962. Extracellular space of brain as determined by diffusion of inulin from the ventricular system. *Life Sci.* 2:43-48.

- Reed, D. J., and D. M. Woodbury. 1963. Kinetics of movement of iodine, sucrose, inulin, and radio-iodinated serum albumin in the central nervous system and cerebrospinal fluid in the rat. *J. Physiol.* 169: 816-850.
- Rossen, R., H. Kabat, and J. P. Anderson. 1943. Acute arrest of cerebral circulation in man. *A. M. A. Arch. Neurol. & Psychiat.* 50:510-528.
- Rothman, A. R., E. J. Freireich, J. R. Gaskins, C. S. Patlak, and D. P. Rall. 1961. Exchange of inulin and dextran between blood and cerebrospinal fluid. *Amer. J. Physiol.* 201:1145-1148.
- Shapiro, W., A. J. Wasserman, J. P. Baker, and J. L. Patterson, Jr. 1970. Cerebrovascular response to acute hypocapnic and eucapnic hypoxia in normal man. *J. Clin. Invest.* 49:2362-2368.
- Shimojyo, S., P. Scheinberg, K. Kogure, and O. M. Reinmuth. 1968. The effects of graded hypoxia upon transient cerebral blood flow and oxygen consumption. *Neurol.* 18:127-133.
- Siesjo, B. K., L. Granholm, and A. Kjallquist. 1968. Regulation of lactate and pyruvate levels in the cerebrospinal fluid. *Scand. J. Clin. Lab. Invest.* 22:Suppl. 102:1:F.
- Slobody, L. B., D. C. Yang, M. Lending, F. J. Borrelli, and M. Tyree. 1957. Effect of severe hypoxia on blood-cerebrospinal fluid barrier. *Amer. J. Physiol.* 190:365-370.
- Smith, H. W. 1956. *Principles of Renal Physiology*. New York: Oxford University Press, p. 206.
- Sokoloff, L. *Handbook of Physiology*, III, ed. by J. A. Field. Chap. 77. Washington, D.C.: American Physiological Society, pp. 1841-1864.
- Steel, R. G. D., and J. H. Torrie. 1960. *Principles and Procedures of Statistics*. New York: McGraw-Hill.
- Stein, W. D. 1967. *The Movement of Molecules Across Cell Membranes*. VI. New York: Academic Press.
- Truex, R. C., and M. B. Carpenter. 1969. *Human Neuroanatomy*. 6th ed. Baltimore: Williams and Wilkins Co.

- Valenca, L. M., D. C. Shannon, and H. Kazemi. 1971. Clearance of lactate from the cerebrospinal fluid. *Neurol.* 21:615-620.
- VanHarreveld, A., J. Cromwell, and S. K. Malhotra. 1965. A study of extracellular space in central nervous tissue by freeze substitution. *J. Cell. Biol.* 25: 117-137.
- Vates, T. S., S. L. Bonting, and W. W. Oppelt. 1964. Na-K activated adenosine triphosphatase and formation of cerebrospinal fluid in the cat. *Amer. J. Physiol.* 206:1165-1172.
- VonKorff, R. W. 1969. *Methods in Enzymology*. XIII. ed. by J. W. Lowenstein. New York: Academic Press, pp. 425-430.
- Wallace, G. B., and B. B. Brodie. 1937. The distribution of iodide, thiocyanate, bromide, and chloride in the central nervous system and spinal fluid. *J. Pharmacol. & Exper. Therap.* 61:397-411.
- Wallace, G. B., and B. B. Brodie. 1939. The distribution of administered bromide in comparison with chloride and its relations to body fluid. *J. Pharmacol & Exper. Therap.* 65:214-219.
- Weed, L. H. 1923. The absorption of cerebrospinal fluid into the venous system. *Amer. J. Anat.* 31:191-221.
- Welch, K. 1963. Secretion of cerebrospinal fluid by choroid plexus of the rabbit. *Amer. J. Physiol.* 205:617-624.
- Welch, K., and V. Friedman. 1960. The cerebrospinal fluid valves. *Brain* 83:454-468.
- Welch, K., K. Sadler, and R. Hendee. 1970. Cooperative phenomena in the permeation of sugars through the lining epithelium of choroid plexus. *Brain Res.* 19:465-482.
- White, A., P. Handler, and E. L. Smith. 1964. *Principles of Biochemistry*. 3rd ed. New York: McGraw-Hill.
- Williamson, J. R., and B. E. Corey. 1969. *Methods of Enzymology*. XIII. ed. by J. W. Lowenstein. New York: Academic Press, pp. 435-444.

- Wolff, P. H., and R. D. Tschirgi. 1956. Inability of cerebrospinal fluid to nourish the spinal cord. Amer. J. Physiol. 184:220-222.
- Woodward, D. L., D. J. Reed, and D. M. Woodbury. 1967. Extracellular space of rat cerebral cortex. Amer. J. Physiol. 212:367-370.

MICHIGAN STATE UNIVERSITY LIBRARIES



3 1293 03177 4452